Production and utilisation of prebiotic oligosaccharides

Applied bioinformatics of glycoside hydrolases

Månberger, Anna

2019

Document Version:
Publisher's PDF, also known as Version of record

Production and utilisation of prebiotic oligosaccharides

Applied bioinformatics of glycoside hydrolases

ANNA MÅNBERGER | BIOTECHNOLOGY | LUND UNIVERSITY

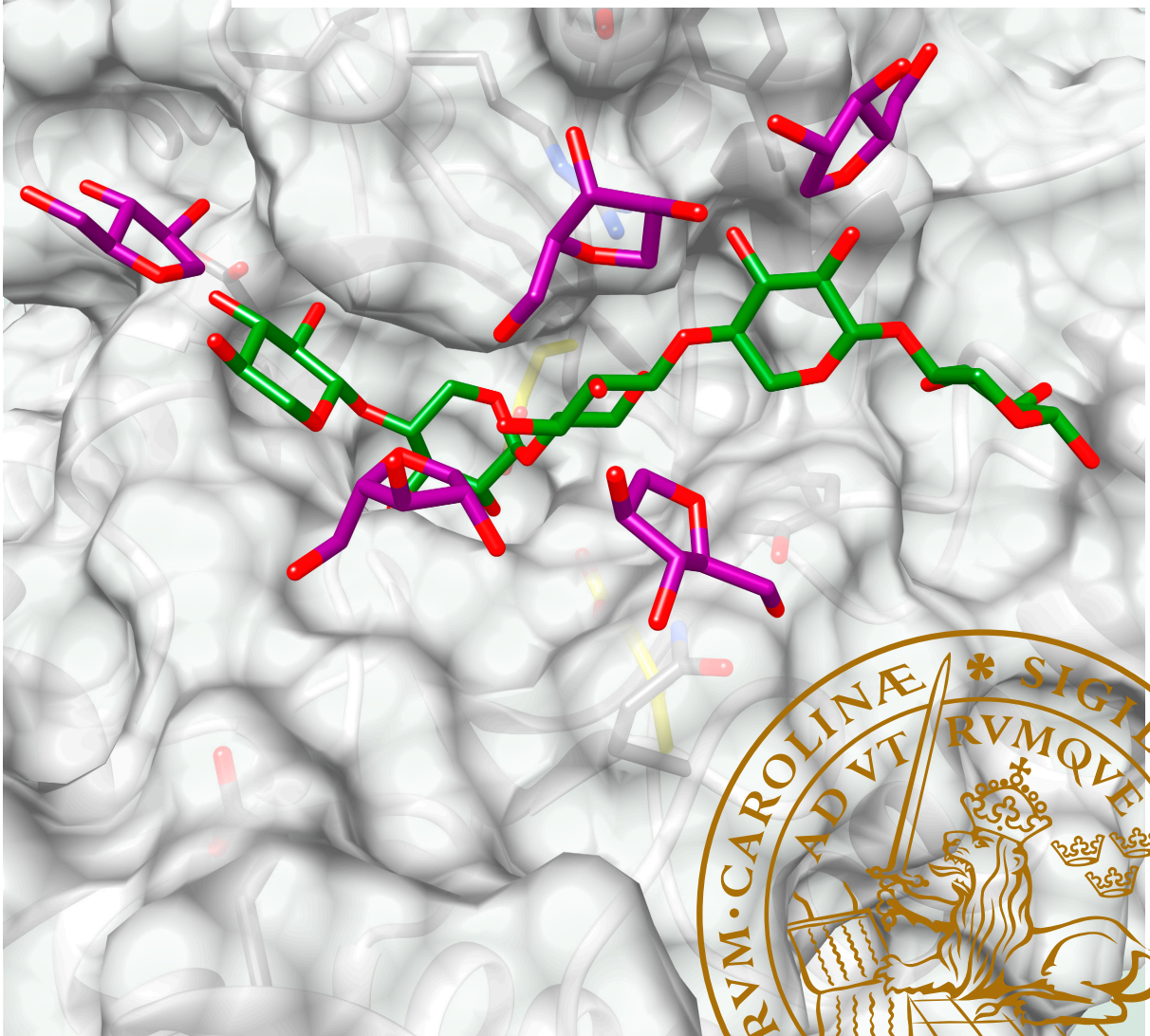

Production and utilisation of prebiotic oligosaccharides

Applied bioinformatics of glycoside hydrolases

by Anna Månberger

LUND
UNIVERSITY

DOCTORAL DISSERTATION
by due permission of the Faculty of Engineering, Lund University, Sweden.
To be defended at Kemicentrum lecture hall A the 15th of November 2019 at 09:30.

Faculty opponent
Professor Leila Lo Leggio
University of Copenhagen, Denmark

Organization
LUND UNIVERSITY
Division of Biotechnology
Box 124
SE-221 00 Lund
Sweden

Document name
DOCTORAL DISSERTATION

Date of disputation
2019-11-15

Sponsoring organization
The Swedish Research Council (VR) - 2014-05038. Anti-Diabetic Food Centre (a VINNOVA Excellence Centre)

Author(s)
Anna Månberger

Title and subtitle
Production and utilisation of prebiotic oligosaccharides: Applied bioinformatics of glycoside hydrolases

Abstract
Arabinoxylan-oligosaccharides ((A)XOS) are prebiotic candidates and stimulate health-promoting bacteria in the human gut including spp. of *Bifidobacterium* and strains of *Lactobacillus brevis*. (A)XOS can be produced from the polysaccharide arabinoxylan (AX). AX is found in e.g. cereal bran, a by-product from the production of flour. AX is mainly composed of a backbone of β-1,4-linked xylopyranosyl units (Xyl*p*) decorated with α-1,3 and/or α-1,2-linked arabinofuranosyl units (Ara*f*). Production of (A)XOS from cereal bran rich in AX by the environmentally-friendly extraction method autohydrolysis and enzymatic hydrolysis of AX by endo-β-xylanases was found to be a promising method to valorise the bran. Washing the bran, enzymatic degradation of protein and starch and ethanol precipitation increased purity of the extracted AX and eliminated by-products formed during autohydrolysis. Endo-β-xylanases hydrolyse the linkage between Xyl*p* of the AX backbone with different specificities. Factors such as solubility and ratio of Ara*f* to Xyl*p* was found having an impact on the (A)XOS yield between the two main glycoside hydrolase (GH) families, GH10 and GH11. A higher yield was found with GH10 on soluble AX but with GH11 on insoluble AX. GH11 was found to be more hampered by Ara*f* substitutions. To understand the hydrolysis profiles of individual endo-β-xylanases, the structure-function relationship is vital and it was studied for two GH10 and two GH11 endo-β-xylanases. The two GH10 endo-β-xylanases, *Rm*Xyn10A and *Gs*Xyn10A, revealed different tolerance for Ara*f* substitution at subsite +2 due to differences in loops surrounding the aglycone subsites. Different hydrolysis profiles for the two GH11 endo-β-xylanases Pentopan derived from *Ta*Xyn11A and *Np*Xyn11A was found to be a result of different interactions to Xyl*p* and steric hindrance to Ara*f* substitutions in subsites -3 and +3. The fine structure of (A)XOS produced, described in degree of polymerisation and average degree of Ara*f* substitutions, affects the selectivity of fermentation in the colon. Ara*f* substituted xylooligosaccharides (AXOS) selectively stimulate *Bifidobacterium* while unsubstituted xylooligosaccharides (XOS) are also fermented by *Lactobacillus* and certain other strains of lactic acid bacteria which are interesting probiotic candidates. One of them, *Weissella* sp. strain 92 isolated from fermented food was genome-sequenced and classified into *W. cibaria* by whole-genome phylogeny. The genome was used to map utilisation of XOS and arabinobiose, as well as production of lactate and acetate. The utilisation of another potential prebiotic, laminaribiose, was identified and coupled with upregulation of two 6-phospho-β-glucosidases, one in proximity to a phosphotransferase system.

Key words
arabinoxylan, arabinoxylan-oligosaccharides, bioinformatics, endo-β-xylanases, prebiotics, probiotics, *Weissella*

Classification system and/or index terms (if any)

Supplementary bibliographical information

Language
English

ISSN and key title

ISBN
978-91-7422-690-4 (print)
978-91-7422-691-1 (pdf)

Recipient's notes

Number of pages
206

Price

Security classification

Production and utilisation of prebiotic oligosaccharides

Applied bioinformatics of glycoside hydrolases

by Anna Månberger

LUND
UNIVERSITY

Front cover illustration: Active site of *Rm*Xyn10A_CM docked with X_5 (green) in subsite -2 to +3 and several Ara*f* (purple). The picture is produced by the software USCF Chimera.

Back cover illustration: The 20 standard amino acids (at *p*H 7.0). The chemical structures are produced in the software Accelrys Draw.

Faculty of Engineering, Division of Biotechnology

ISBN: 978-91-7422-690-4 (print)
ISBN: 978-91-7422-691-1 (pdf)
ISRN: LUTKDH/TKBT-19/1176-SE

Printed in Sweden by Media-Tryck, Lund University, Lund 2019

NORDIC SWAN ECOLABEL
Printed matter
3041 0903

Media-Tryck is an environmentally certified and ISO 14001:2015 certified provider of printed material.
Read more about our environmental work at www.mediatryck.lu.se

MADE IN SWEDEN

Acknowledgements

A lot of people have supported me during my time as a PhD student and to those, I would like to show my appreciation.

To my main supervisor *Eva Nordberg Karlsson* for creating the opportunity for me to proceed my PhD studies within the field of bioinformatics under her supervision and for fruitful discussions resulting in progression in my research projects.

To my co-supervisor *Javier Linares-Pastén* for his patience and guidance in bioinformatics as well as in the lab.

The research presented in this thesis would not be possible without the work and competence of others. For constructive collaborations, I thank (in order of appearance): *Patrick Adlercreutz*, *Peter Falck*, *Carl Grey*, *Henrik Stålbrand*, *Sindhu Mathew*, *Fatma Güler*, *Zubaida Gulshan Ara* and *Phebe Verbrugghe*. I also thank *Susan Crennell*, *Dmitri Svergun*, *Maxim Petoukhov* and *Sara Santesson*, and for sharing their work and together creating more comprehensive and interesting papers.

A special thanks to *Elisabet Eik Guðmundsdóttir* and *Guðmundur Óli Hreggviðsson* for not only a nice collaboration but also for hosting me at Matís, Reykjavík.

To *Björn Stenqvist* for his generous help in programming and for extending his lunch breaks to teach me electrostatic interactions in molecular dynamic simulations.

Besides the scientific collaborations I would like to show my appreciation to the always kind and helpful *Christina Wennerberg*, *Frans-Peder Nilsson* and *Emma Poaches* at the division of Biotechnology for practical, technical and administrative support, and to *Paula Leckius* for putting emphasis on the details during the printing process.

Time at work would not be enjoyable without the company of great colleges. Therefore, I would like to show my thankfulness to all the present and former members of the fermentation group as well as the entire division of Biotechnology for creating a nice atmosphere during coffee- and lunch breaks, and especially to *Emanuel*

for interesting and challenging discussions spanning from research to pregnancy. Moreover, I want to show my warmest gratitude to *Evelina*, *Viktoria*, *Sumitha*, *Johan*, *Nick*, *David*, *Anna* and *Samuel* for friendliness, encouragement and great company at conferences.

Jag vill ta tillfället i akt att visa uppskattning för mina vänner utanför universitet och speciellt till *Maria*, *Kajsa*, *Sara*, *Madde*, *Sarah* och *Gabbie* vilka alltid finns där trots avståndet emellan oss.

Tack till *Anna*, *Ronny*, *Erik*, *Silvia*, *Ammie* och *Moje* för hur ni välkomnat mig till eran familj.

Tack till *Mamma*, *Pappa*, *Johan*, *Edvin*, *Selma*, *Mormor* och *Farfar* för att ni finns där för mig.

Till sist vill jag tacka de två viktigaste personerna is mitt liv. Tack *André* för att du stöttar, tror på mig och alltid har en kram nära till hands. Tack *Vilma* för att just du kom till oss med en enorm livsglädje och gav mig en välbehövlig paus i mina doktorsstudier.

Abstract

Arabinoxylan-oligosaccharides ((A)XOS) are prebiotic candidates and stimulate health-promoting bacteria in the human gut including spp. of *Bifidobacterium* and strains of *Lactobacillus brevis*. (A)XOS can be produced from the polysaccharide arabinoxylan (AX). AX is found in e.g. cereal bran, a by-product from the production of flour. AX is mainly composed of a backbone of β-1,4-linked xylopyranosyl units (Xyl*p*) decorated with α-1,3 and/or α-1,2-linked arabinofuranosyl units (Ara*f*). Production of (A)XOS from cereal bran rich in AX by the environmentally-friendly extraction method autohydrolysis and enzymatic hydrolysis of AX by endo-β-xylanases was found to be a promising method to valorise the bran. Washing the bran, enzymatic degradation of protein and starch and ethanol precipitation increased purity of the extracted AX and eliminated by-products formed during autohydrolysis. Endo-β-xylanases hydrolyse the linkage between Xyl*p* of the AX backbone with different specificities. Factors such as solubility and ratio of Ara*f* to Xyl*p* was found having an impact on the (A)XOS yield between the two main glycoside hydrolase (GH) families, GH10 and GH11. A higher yield was found with GH10 on soluble AX but with GH11 on insoluble AX. GH11 was found to be more hampered by Ara*f* substitutions. To understand the hydrolysis profiles of individual endo-β-xylanases, the structure-function relationship is vital and it was studied for two GH10 and two GH11 endo-β-xylanases. The two GH10 endo-β-xylanases, *Rm*Xyn10A and *Gs*Xyn10A, revealed different tolerance for Ara*f* substitution at subsite +2 due to differences in loops surrounding the aglycone subsites. Different hydrolysis profiles for the two GH11 endo-β-xylanases Pentopan derived from *Ta*Xyn11A and *Np*Xyn11A was found to be a result of different interactions to Xyl*p* and steric hindrance to Ara*f* substitutions in subsites -3 and +3. The fine structure of (A)XOS produced, described in degree of polymerisation and average degree of Ara*f* substitutions, affects the selectivity of fermentation in the colon. Ara*f* substituted xylooligosaccharides (AXOS) selectively stimulate *Bifidobacterium* while unsubstituted xylooligosaccharides (XOS) are also fermented by *Lactobacillus* and certain other strains of lactic acid bacteria which are interesting probiotic candidates.

One of them, *Weissella* sp. strain 92 isolated from fermented food was genome-sequenced and classified into *W. cibaria* by whole-genome phylogeny. The genome was used to map utilisation of XOS and arabinobiose, as well as production of lactate and acetate. The utilisation of another potential prebiotic, laminaribiose, was identified and coupled with upregulation of two 6-phospho-β-glucosidases, one in proximity to a phosphotransferase system.

Populärvetenskaplig sammanfattning

I människans tjocktarm finns tarmfloran, ett ekosystem utav mikroorganismer med stor påverkan på människans hälsa. De senaste decennierna har forskningen visat att en välbalanserad tarmflora ger upphov till bland annat stärkt immunförsvar, sänkt kolesterolhalt samt minskad risk för hjärt- och kärlsjukdomar och cancer. Tarmfloran har även länkats till fetma, diabetes, ångest och depression. Till stor del består tarmfloran av bakterier, vilka ofta lite slarvigt beskrivs som onda eller goda. Inom vetenskapen beskrivs ofta bakterierna som kommensala, probiotiska eller patogena. Kommensala bakterier varken påverkar eller påverkas av människan. Probiotiska bakterier har en dokumenterad positiv effekt för hälsan, dessa grupper av bakterier vill vi ska växa och frodas inom oss.

Tarmfloran påverkas av vår diet. De kolhydrater som människan själv inte kan spjälka utan passerar vidare i mag- och tarmsystemet till tjocktarmens bakterier betecknas fibrer och utgör den främsta energikällan för tarmflorans bakterier. Fibrerna har stor variation och olika bakterier kan tillgodogöra sig olika fibrer. De fibrer som har bevisats selektivt gynna tillväxten av de probiotiska bakterierna på ett sådant sätt att det ger positiva hälsoeffekter för människan kallas prebiotika. Intag av pro- och/eller prebiotika är en strategi för att modulera tarmfloran på ett hälsostimulerande sätt. En del livsmedel innehåller det naturligt, exempelvis finns probiotiska bakterier i yoghurt, fil och inlagda grönsaker, och prebiotika kan hittas i lök, jordärtskocka och bönor. Genom berikning utav livsmedel kan utbudet och tillgängligheten av pro- och prebiotika öka ytterligare.

Arabinoxylanoligosackarider, förkortat (A)XOS, är en grupp av små fibrer som är kandidater till att klassificerats som prebiotika. De har visats öka tillväxten av bakterier från *Bifidobacterium* och *Lactobacillus*, de två mest välstuderade släktena av probiotiska bakterier. Vid fermentering utav (A)XOS i dessa bakterier produceras kortkedjade fettsyror vilka ger upphov till flera positiva effekter såsom hämmad tillväxt av pa-

togena bakterier, ökat upptag av mineraler och minskad förstoppning. (A)XOS är uppbyggda av sockerarterna xylos och arabinos; xylosenheter länkade till varandra i en kedja och enskilda arabinosenheter länkade till enskilda xylosenheter. Finns inga arabinosenheter, betecknas dessa XOS. Två egenskaper som påverkar den prebiotiska effekten är hur många xylosenheter som sitter länkade samt arabinostätheten. (A)XOS finns endast i mindre mängder i vår diet, i processade produkter baserade på säd, som exempelvis öl och bröd.

(A)XOS kan produceras från förnyelsebar biomassa innehållandes arabinoxylan i en miljövänlig process. För framställning utav (A)XOS bryter man ned fibern arabinoxylan till kortare fragment, oligosackarider, med enzymet xylanas. Arabinoxylan hittar man exempelvis i de klassiska sädesslagen, med högst koncentration i skalet runt kärnan. Vid framställning av vanligt mjöl används endast kärnan, skalresterna separeras bort och utgör en billig och hållbar källa för arabinoxylan. Arabinoxylanet i skalet är inte lösligt i vatten utan sammantvinnat med cellulosa, stärkelse, proteiner, träämnet lignin och andra mindre näringsämnen. Separation och upprening utav arabinoxylanet från övriga komponenter i skalet är nödvändigt innan den enzymatiska nedbrytningen till (A)XOS kan ske. Skalrester från råg och vete har i den här avhandlingen använts som ett förnyelsebart startmaterial för att producera (A)XOS där olika processalternativ för isolering studerades. Genom att kombinera tryckkokning, enzymatisk nedbrytning utav stärkelse och proteiner samt etanolfällning uppnåddes bäst resultat för isolering utav arabinoxylanet med avseende på utbyte och renhet. Det isolerade arabinoxylanet används vidare för enzymatisk nedbrytning till (A)XOS.

Det är viktigt att välja rätt xylanas till sin process. Från vilken källa och vilken typ av xylanas som används spelar stor roll för vilka produkter, med avseende på antal xylosenheter och arabinostäthet, som bildas vid nedbrytningen. Även hur effektivt arabinoxylanet kan brytas ned beroende på egenskaper såsom löslighet och arabinostäthet påverkas av valet av xylanas. Xylanasets funktion är en direkt följd utav dess tredimensionella (3D)-struktur, denna information är därför nödvändig för att förstå vilka produkter som bildas. Xylanaser, liksom andra kolhydrat-nedbrytande enzymer delas in i familjer baserad på evolutionärt släktskap. Fyra xylanaser från de två mest välstuderade familjerna för arabinoxylan-nedbrytande xylanaser användes och jämfördes. Generella skillnader i produktprofilen observerades mellan familjerna, samt mindre skillnader inom familjerna. För tre av de studerade xylanaserna fanns en experimentellt bestämd 3D-struktur tillgänglig, i det fjärde fallet skapades en modell av xylanaset genom homologimodellering. Genom datasimuleringar studerades vilka produkter som skulle kunna bildas från alla xylanaserna och vilka strukturella delar som var viktiga för de olika funktionerna.

Förutom bakterier från *Lactobacillus* och *Bifidobacterium* är få tarmbakterier ansedda som probiotiska eller ”goda”. Detta beror snarare på bristande kunskap än att det

inte finns fler som är viktiga för människans hälsa. Ett första steg för att förstå hela tarmfloran och en möjlighet att hitta individuella bakterier som genom berikning ökar människans hälsa är att studera de enskilda bakterierna. I förlängningen är det dock mycket viktigt att även titta på hur de individuella bakterierna samspelar med varandra och människans fysiologiska system för att förstå dess mekanismer. Troligtvis kommer den svart-vita synen på ”onda” och ”goda” bakterier suddas ut, flera av de som idag anses som onda har kanske en viktig roll som vi är omedvetna om idag.

En mindre välstuderad bakterie som har probiotisk potential är *Weissella* stam 92. Dessa är mjölksyrabakterier som hittats och isolerats från fermenterad indisk mat och som därför även förekommer i vår tarmflora. Bakterierna tros vara probiotiska då de visats kunna växa på XOS och producera kortkedjade fettsyror. För att kunna bryta ned och utnyttja fiber behöver bakterien olika protein, dels kolhydrat-nedbrytande enzymer, men även transportsystem och metabola enzymer för den specifika sockerarten. Koden för alla proteiner en bakterie kan producera finns i genomet. Genomet för *Weissella* stam 92 sekvenserades och däri hittades ett enzym för att byta ned XOS till xylos, transportproteiner och enzymer för vidare metabolisering av xylos. Även motsvarande proteiner som tyder på att bakterien även kan bryta ned andra prebiotika såsom arabinooligosackarider (AOS) och glukosbaserade korta fibrer. Odlingsförsök visade att bakterien kan växa på disackariderna arabinobios och laminaribios. Tillväxten på laminaribios, som är uppbyggd utav glukosenheter, kopplades till uttryck utav enzymer som byter ned glukosbaserade disackarider. Att bakterien kan växa på flera typer utav fibrer ökar dess överlevnadschanser i tjocktarmen och gör den mer intressent ur ett probiotiskt perspektiv. Genomet användes också för att klassificera stammen till en utav två arter vilket tidigare metoder inte klarat.

Den här avhandlingen bidrar till ökad kunskap kring hur xylanasers 3D-struktur påverkar utbyte och produktbildningen vid nedbrytning av arabinoxylan. Dessa studier möjliggör bättre underbyggda val av xylanas vid (A)XOS framställning med hänsyn till startmaterial, process och önskade produkter. Avhandlingen har också bidragit med ökad kunskap kring kolhydratsupptag i stam mjölksyrabakterier som har potential att användas som probiotika. Denna avhandling är en del i utvecklingen av pro- och prebiotika för framtagning av nya hälsofrämjande produkter.

List of papers

This thesis is based on the following papers, referred to by their Roman numerals:

I **Production of arabinoxylan-oligosaccharide mixtures of varying composition from rye bran by combination of process conditions and type of xylanase**
P. Falck, A. Aronsson*, C. Grey, H. Stålbrand, E. Nordberg Karlsson and P. Adlercreutz
2014, Bioresource Technology 174: 118-125

II **Structural Considerations on the Use of Endo-Xylanases for the Production of prebiotic Xylooligosaccharides from Biomass**
J.A. Linares-Pastén, A. Aronsson* and E. Nordberg Karlsson
2017, Current Protein and Peptide Science 18: 1-20

III **Structural insights of *Rm*Xyn10A - A prebiotic-producing GH10 xylanase with a non-conserved aglycone binding region**
A. Aronsson*, F. Güler, M.V. Petoukhov, S.J. Crennell, D.I. Svergun, J.A. Linares-Pastén and E. Nordberg Karlsson
2018, Biochimica et Biophysica (BBA) - Proteins and Proteomics 1866: 292-306

IV **Xylo- and arabinoxylooligosaccharides from wheat bran by endoxylanases, utilisation by probiotic bacteria, and structural studies of the enzymes**
S. Mathew, A. Aronsson*, E. Nordberg Karlsson and P. Adlercreutz
2018, Applied Microbiology and Biotechnology 102: 3105-3120

V **Genomic analysis of *Weissella cibaria* strain 92 focusing on utilisation of oligosaccharides derived from dietary fibres**
A. Månberger, P. Verbrugghe, E.E. Guðmundsdóttir, S. Santesson, G.Ó. Hreggviðsson, J.A. Linares-Pastén, and E. Nordberg Karlsson
Manuscript

*Previous surname.

My contributions to the papers

All work described in this thesis was performed under the supervision of Prof. Eva Nordberg Karlsson and Dr. Javier Linares-Pastén.

I I took an active part in designing the experiments and analysing the results, and I performed a major part of the experimental work (excluding small scale heat treatment and characterisation of products after xylanase treatment). I took part in writing and revising the manuscript.

II I have performed the literature review about structures of GH10, GH11 and GH30 (subfamily 8) xylanases and written the corresponding part of the manuscript. I had an active part in the revision of the manuscript.

III With the exception of the SAXS experiments, I had a major part in planning the study, I have designed the computational experiments and performed the computational work. I designed the mutants and the primers for the mutants, planned and designed the experiments of enzyme activity and hydrolysis of arabinoxylan extracted from rye bran and analysed the results. I wrote the vast majority of the first draft of the manuscript and coordinated the editing and revision of the manuscript with co-authors. Corresponding author

IV I have planned, designed and performed the bioinformatic work, and written the corresponding part of the manuscript. I took an active part in discussions about comparing the biochemical and bioinformatic data in order to draw the conclusions.

V I took part in the genome sequencing and performed the following bioinformatic work. I designed and performed the phylogenetic analysis and the analysis of genes involved in oligosaccharide degradation, uptake and metabolism. I cultivated the bacteria for the growth curves and the RNA extraction, and took part in the RT-qPCR experiments. I have analysed all data, wrote the vast majority of the first draft of the manuscript and coordinated the editing of the manuscript with co-authors.

List of Abbreviations

(A)XOS	arabinoxylan-oligosaccharides
A/X ratio	arabinose to xylose ratio
AOS	arabinooligosaccharides
Ara*f*	arabinofuranosyl unit(s)
avDS	average degree of substitution
AX	arabinoxylan
AXOS	arabinoxylooligosaccharides
CAZy	Carbohydrate-Active enZymes
CM	catalytic module
DP	degree of polymerisation
EM	energy minimisation
gDNA	genomic DNA
GH	glycoside hydrolase
GH#	glycoside hydrolase family #
*Gs*Xyn10A	extracellular GH10 xylanase from *Geobacillus stearothermophilus*
HM	homology modeling
HPAEC-PAD	high-performance anionic exchange chromatography coupled with pulsed amperiometric detection
MD	molecular dynamics
*Np*Xyn11A	catalytic module of GH11 xylanase A from *Neocallimastix patriciarum*
PDB	protein data bank

Pentopan	Pentopan Mono BG, GH11 endo-β-xylanase derived from *Thermomyces langinosus*
PTS	phosphotransferase system
RMSD	root mean square deviation
*Rm*Xyn10A	GH10 xylanase A from *Rhodothermus marinus*
SCFA	short-chain fatty acid
*Tl*Xyn11A	GH11 xylanase A from *Thermomyces langinosus*
w/w	weight per weight
XOS	xylooligosaccharides
Xyl*p*	xylopyranosyl unit(s)
A_2	arabinobiose
A_3	arabinotriose
X_2	xylobiose
X_3	xylotriose
X_4	xylotetraose
X_5	xylopentaose
X_6	xylohexaose
A^3X	α-1,3-Ara*f*-β-1,4-Xyl*p*-β-1,4-Xyl*p*
XA^3X	β-1,4-Xyl*p*-(α-1,3-Ara*f*)-β-1,4-Xyl*p*-β-1,4-Xyl*p*
XA^3XX	β-1,4-Xyl*p*-(α-1,3-Ara*f*)-β-1,4-Xyl*p*-β-1,4-Xyl*p*-β-1,4-Xyl*p*
XXA^3XX	β-1,4-Xyl*p*-β-1,4-Xyl*p*-(α-1,3-Ara*f*)-β-1,4-Xyl*p*-β-1,4-Xyl*p*-β-1,4-Xyl*p*
A^2XX	α-1,2-Ara*f*-β-1,4-Xyl*p*-β-1,4-Xyl*p*-β-1,4-Xyl*p*
XA^2XX	β-1,4-Xyl*p*-(α-1,2-Ara*f*)-β-1,4-Xyl*p*-β-1,4-Xyl*p*-β-1,4-Xyl*p*
XXA^2XX	β-1,4-Xyl*p*-β-1,4-Xyl*p*-(α-1,2-Ara*f*)-β-1,4-Xyl*p*-β-1,4-Xyl*p*-β-1,4-Xyl*p*
$A^{2+3}XX$	α-1,2-Ara*f*-(α-1,3-Ara*f*)-β-1,4-Xyl*p*-β-1,4-Xyl*p*-β-1,4-Xyl*p*
$XA^{2+3}XX$	β-1,4-Xyl*p*-(α-1,2-Ara*f*)-(α-1,3-Ara*f*)-β-1,4-Xyl*p*-β-1,4-Xyl*p*-β-1,4-Xyl*p*

Contents

1 Introduction

The human gut hosts an ecosystem of microbes, the gut microbiota, which is an integrated part of the human physiology. The gut microbiota is mainly composed of bacteria but also archaea, unicellular eukaryotes and viruses, and the number of microbial cells is of the same magnitude as the number of human cells in the whole body [1]. These microbes are responsible for beneficial functions that include strengthening gut integrity, harvesting energy, protecting against pathogens and regulating host immunity [2]. In recent years, the understanding of the gut microbiota in human health has expanded and connections to other systems of the body have been demonstrated, e.g. influence on stress-related behaviours and activation of neural pathways and the central nervous system [3], and association with obesity and glucose intolerance [4]. Hence, having a well-functioning gut microbiota is important to stay healthy. The functionality of the gut microbiota depends upon its composition and activity. Besides disruption of important functions, alterations in the gut microbiota can result in the production of harmful metabolites and induction of disease.

The importance of the gut microbes has led to the development of strategies to maintain a well-balanced gut microbiota and enhance its beneficial effect. Probiotics are live microorganisms that are beneficial for human health upon ingestion in adequate amounts [5]. Known probiotic bacteria today are mainly found within the genera *Lactobacillus* and *Bifidobacterium*. These bacteria produce short-chain fatty acids (SCFAs) and lactate from various oligosaccharides. The SCFAs have several beneficial properties, including creating a hostile environment for pathogens by lowering the *p*H, improving mineral adsorption, stimulating the immune system, and being an energy source in the host glucose, cholesterol and lipid metabolism [6–9]. Lately, other bacteria from the gut microbiota and fermented food have gained interest as potential probiotics, one such example is the genus *Weissella*, a lactic acid producer isolated from human faeces and fermented food [10].

Prebiotics are compounds that, when eaten, resist the gastric acidity and degradation by host enzymes, and selectively stimulate the probiotic bacteria, which in turn

improve the health of their host [11]. Well-established prebiotics are mainly different types of oligosaccharides. Arabinoxylan-oligosaccharides ((A)XOS) are derived from the polysaccharide arabinoxylan (AX). (A)XOS are prebiotic candidates, they have been shown to stimulate *Bifidobacterium* in general [12], and individual strains of *Lactobacillus*, the latter only by xylooligosaccharides (XOS) [13]. Other not so well-studied lactic acid bacteria, such as a few strains of *Weissella* sp. (strains 85, 92, 145 and AV1) [14] and strain of *Leuconostoc lactis* (SHO-47 and SHO-54) [15], have been shown to utilise XOS and produce SCFAs and lactate.

(A)XOS in the diet is limited, however, production from agricultural side streams containing AX is possible [12]. Cereal bran is rich in AX [16], where the polysaccharide is present in the cell wall, associated with cellulose, lignin, proteins and other hemicelluloses [17]. After isolation of AX, breakdown into oligosaccharides can be done enzymatically by endo-β-xylanases which randomly cleave the xylose-based backbone by hydrolysis. The choice of enzyme for the process is important to obtain a high yield and desired products [18].

One interesting candidate for hydrolysis of AX is the endo-β-xylanase *Rm*Xyn10A from *Rhodothermus marinus*. *R. marinus* are thermophilic bacteria with optimal growth at 65 °C isolated from shallow-water submarine hot springs northwest of Iceland which harbours a plethora of glycoside hydrolases for degradation of several types of carbohydrates, including xylan [19–21]. *Rm*Xyn10A is a thermostable endo-β-xylanase efficient in hydrolysing internal glycosidic linkages in the xylan backbone of AX from various sources, including wheat bran, rye bran and flour, birchwood, quinoa stalk and Brewer's spent grain [22–26].

Endo-β-xylanases belong to class of enzymes called glycoside hydrolases (GHs). GHs catalyse the breakdown of polysaccharides mainly through hydrolysis. Due to the complexity of polysaccharides in terms of monosaccharide composition, different linkages, branching and presence of side groups, the glycoside hydrolases have a broad range of activities and varied substrate specificities. GHs are classified into families based on amino acid sequences [27] where the majority of characterised endo-β-xylanases hydrolysing AX can be found within GH family 10 (GH10) and GH11. The overall three-dimensional (3D) fold is conserved within each family. However, activity and substrate specificities are not conserved, the same activity can be found in different families, and within one family the specificity can vary. These parameters can be studied by biochemical means, but to fully understand the mechanisms of substrate binding and hydrolysis, the 3D structure needs to be determined [28].

Structural information on endo-β-xylanases is scarce. For the well-studied GH10, around four thousand sequences are available in the Carbohydrate-Active EnZyme (CAZy) database (www.cazy.org), but only 360 are characterised and 45 structure-

determined [29, 30]. Besides the protein structure, the structure of a complex where a ligand is bound in the active site of the enzyme is valuable. Ligands in complex with GH10 enzymes are often XOS, while arabinoxylooligosaccharides (AXOS) only can be found in a handful where they are bound in the glycone subsites with the arabinose substitution at subsite -2 [31–34]. To fully understand the hydrolysis of AX, structural information including AXOS bound in both the aglycone as well as the glycone part of the active site is needed. The lack of structure-determined complexes with desired ligands is due to the elaborative and complex process of protein crystallisation where the right conditions need to be found and applied. Bioinformatic tools offer a possibility to study enzyme-complexes that are difficult to crystallise. 3D structures can be modelled by homology modeling and ligand interaction can be studied by docking including molecular dynamic simulations. Accuracy is a trade-off in the bioinformatic approach, however, the flexibility in ligand docking is an advantage.

1.1 Aim of thesis

In light of the promising health-promoting effects of prebiotic oligosaccharides, the aim of this thesis is to increase the knowledge and understanding about the hydrolytic enzymes, GHs, essential for the production of prebiotic oligosaccharides and utilisation of these in health-promoting bacteria. The first part of the thesis focuses on revealing structure-function relationships in different GH families as well as individual enzymes including *Rm*Xyn10A and commercially available enzymes with the potential to be effective in producing (A)XOS. The last part of the thesis focuses on exploring and understand the mechanisms of oligosaccharide utilisation in *Weissella* sp. strain 92.

1.2 Scope of thesis

To achieve the above-mentioned aim of the thesis, five studies have been conducted; one study with the aim to produce different (A)XOS from rye bran including endo-β-xylanases from GH10 and GH11 (Paper **I**), one review on the current research on structure-function relationship of endo-β-xylanases from GH10 and GH11 (Paper **II**), one study of *Rm*Xyn10A with the aim to understand the structural basis of its specificity (Paper **III**), one study with the aim to find the structural basis of different product profiles of endo-β-xylanases from GH10 and GH11 (Paper **IV**) and finally, one study of the genome of *Weissella* sp. strain 92 in order to find possible mechanisms of degradation, uptake and metabolism of oligosaccharides derived from dietary fibres by this strain (Paper **V**).

2 Arabinoxylan

Biomass constitute a huge renewable resource with the possibility to substitute fossil based alternatives of energy and chemicals. Polysaccharides are major components in plant-based biomass and have either a role in nutrition storage such as starch, or a structural role like cellulose, hemicelluloses and pectins. Together with lignin and proteins, these structural polysaccharides forms a recalcitrant matrix in the plant cells walls allowing the plant to stand up and provide a barrier for environmental factors and microbial attacks [35].

Hemicellulose is a diverse class of polysaccharides composed of a β-1,4-linked backbone of monosaccharides [35]. The backbone can be decorated with saccharides and non-saccharide side groups. The dominating type of monosaccharide in the backbone determines the type, e.g. xylan, glucan and mannan where the dominating monosaccharides are xylose, glucose and mannose respectively. Presence of other monosaccharides, as decorations or in the backbone, adds a prefix to the name, e.g. arabinoxylan, xyloglucan and galactoglucomannan, where arabinose, xylose and galactose are decorations in the three hemicelluloses, respectively, and glucose are present in the backbone of galactoglucomannan.

Xylan is the second most abundant polysaccharide on earth after cellulose, and the most common hemicellulose [36]. Xylan is found as the main hemicellulose in grasses, e.g. the cereals wheat and rye, the second most abundant in dicots, e.g. the hardwoods birch and beech, and in minor amounts in softwoods, e.g. spruce and pine [35]. The main decorations of xylan are the monosaccharides arabinose and/or glucuronic acid depending on its origin and these are subsequently named arabinoxylan (AX), glucuronoarabinoxylan and glucuronoxylan. This thesis will cover AX from the cereals wheat (*Triticum* spp.) and rye (*Secale cereale*).

2.1 Structure and occurrence

Cereal AX is made up of a xylan backbone of 1,4-linked β-D-xylopyranosyl units (Xyl*p*) to which α-L-arabinofuranosyl units (Ara*f*) are liked through 1,3- and/or 1,2-bonds. Ferulic acids, linked via ester linkages to O5 of Ara*f*, and units of glucuronopyranosyl and its 4-methyl ether are among those substituents of AX that has been reported, see Figure 2.1 [37, 38]. The ratio of total Ara*f* and Xyl*p* in AX is usually expressed as the A/X ratio. Ara*f* O3-linked to Xyl*p* are present in a higher ratio than O2-linked Ara*f* or double-substituted Xyl*p*.

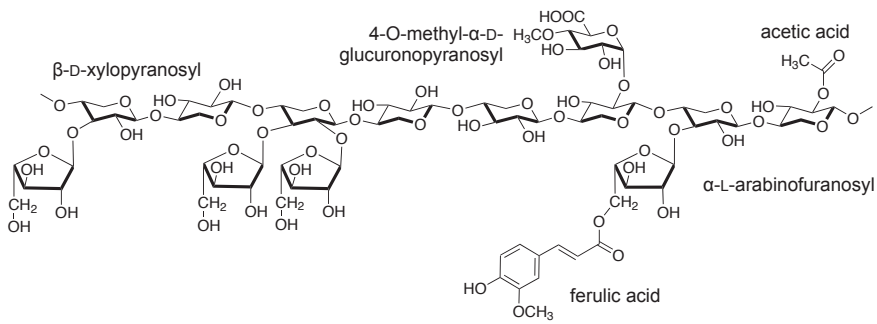

Figure 2.1: Structure of cereal arabinoxylan including some possible substituents (Adapted from Paper **II**).

Cross-linking in AX occurs by diferulic acid bridges. Linkages to other components in the cell wall occurs by covalent bonds to lignin and non-covalent bonds to cellulose and the xylan chain when the A/X ratio is low [39]. These linkages contribute to the recalcitrance of the cell wall and the water-extractability of AX. Part of the AX is water-extractable (WE) whereas the other water-unextractable (WU) part needs pretreatment, e.g. as alkali, to be extracted, this will be more discussed in Chapter 3.

The content and structure of AX in cereals vary with the source, both between species, but also from different components of the plant [16, 37, 39, 40]. Conditions where the crop is grown and time of harvest have also effect on content and structure. For rye and wheat, there is more AX in the bran and it has a lower A/X ratio compared to AX in the endosperm. The bran itself contains several fractions which have different A/X ratio. In WE-AX from both rye and wheat bran, it has been suggested that several polymers or regions of the same polymer display different A/X ratios, presence of mono- and disubstituted Xyl*p* and substitution patterns [39, 40]. In Paper **I** and **IV**, rye bran and wheat bran was used as raw material, respectively. The AX content was found to be 21 % for rye bran and 18 % for wheat bran with A/X ratios of 0.47 and 0.57 (Paper **I**), [41]. These results are in line with previous reports [16, 40, 42–44].

2.2 Applications

Plant-based non-starch polysaccharides are a renewable resource that can be used for various applications, without competing with food production [36]. The xylan-derived product with the largest market is xylitol, a low-calorie sweetener associated with better tooth health used in many products including tooth paste, chewing gums and diabetic products. Another application is the production of bioethanol. Xylitol and ethanol can be produced by fermentation which first requires saccharification of the polysaccharide. Other applications of xylan includes novel, non-fossil based packaging films, foams, gels and surfactants [36].

Production of putative prebiotic oligosaccharides by enzymatic hydrolysis of AX, arabinoxylan-oligosaccharides ((A)XOS), is an application which has received great interest in the last years. (A)XOS are prebiotic candidates associated with an increased gut health by stimulation of the probiotic bacteria from *Bifidobacterium* [12]. (A)XOS can be produced by extraction and isolation of AX from plant material following enzymatic hydrolysis of AX into shorter fragments. Naturally present (A)XOS in food items are limited but can be found in e.g. beer and processed cereal-based food products due to hydrolysis of endo-β-xylanases either present in the cereal, produced by microorganisms in the food or added to the food product [12].

For the production of cereal flour, only the starch-rich endosperm is used. The remaining fractions of the grains, which are rich in AX, are mostly used as animal feed. However, there is an interest from the industry to convert the AX-rich fractions into value-added products. Hence, production of (A)XOS constitute an opportunity for the agricultural industry to valorise their cultivated biomass. The main focus on the rest of this thesis is on the application of (A)XOS as prebiotic candidates and their production from wheat and rye bran.

2.3 Enzymatic degradation

AX and other plant cell wall polysaccharides are naturally degraded by microbes by the aid of enzymes. Enzymatic degradation occurs e.g. in the soil and in the human gut, the latter described more in details in Chapter 5 [45, 46]. Enzyme activities for the complete degradation of AX into monosaccharides are illustrated in Figure 2.2. The xylan backbone is degraded by endo-β-xylanases (EC 3.2.1.1.8). Xyl*p* from the non-reducing end is cleaved by β-xylosidases (EC 3.2.1.37). Ara*f* are released by α-L-arabinofuranosidases (EC 3.2.1.55) which are divided into two types; AXH-d3 cleaves the O3-bound Ara*f* on a double-substituted Xyl*p* and AXH-m cleaves Ara*f* from monosubstituted Xyl*p* [47]. Any glucuronopyranosyl unit can be cleaved by α-

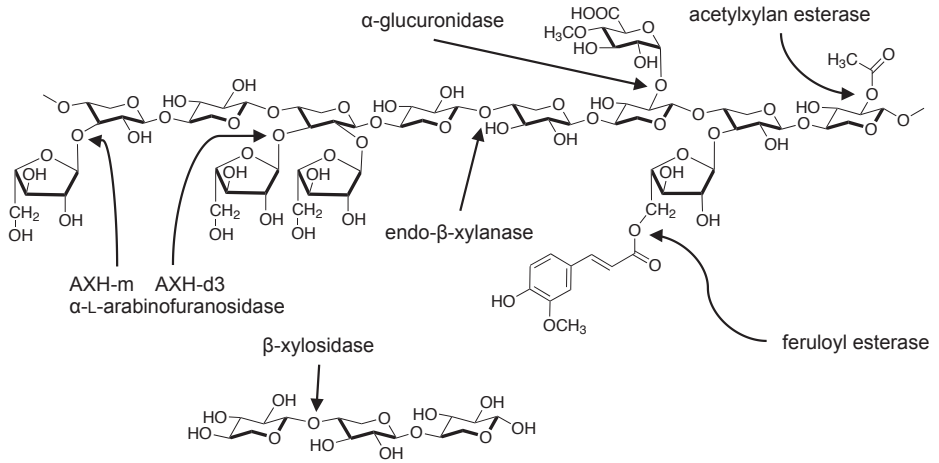

Figure 2.2: Enzyme activities required for complete degradation of cereal arabinoxylan to monosaccharides (Adapted from Paper II).

glucuronidases (EC 3.2.1.139). Acetyl groups are cleaved by acetylxylan esterases (EC 3.1.1.72) and ferulic acids by feruloyl esterases (EC 3.1.1.73).

Degradation of cereal AX by endo-β-xylanases produces (A)XOS (Paper **I** and **IV**). (A)XOS can be divided into two main groups; unsubstituted oligosaccharides, named xylooligosaccharides (XOS), and Ara*f* substituted xylooligosaccharides, named arabinoxylooligosaccharides (AXOS). XOS are abbreviated X_n where n is the number of Xyl*p* or degree of polymerisation (DP). AXOS are abbreviated based on each unit in the backbone chain starting from the non-reducing end, where X is an unsubstituted Xyl*p*, A^n is a Xyl*p* substituted with an Ara*f* at position n, A^{5fn} is a Xyl*p* substituted with a ferulated Ara*f* at position n and A^{2+3} is a doubly substituted Xyl*p* [48]. Some examples of (A)XOS are illustrated in Figure 2.3

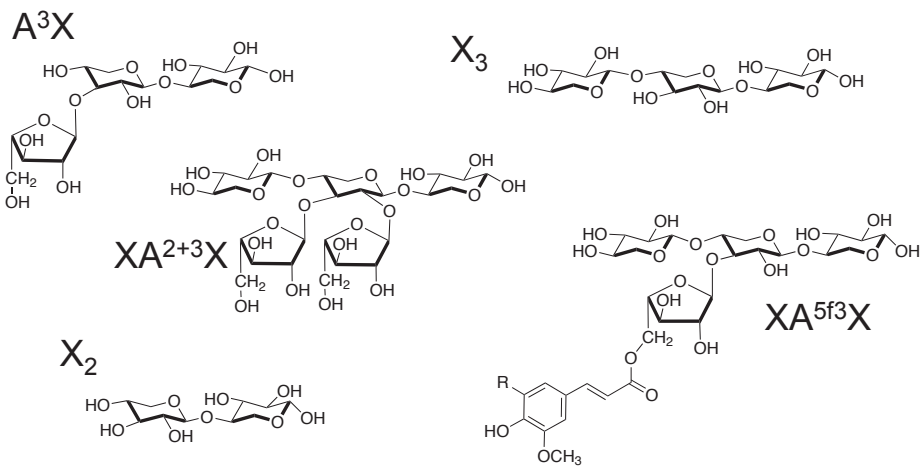

Figure 2.3: Examples of arabinoxylan-oligosaccharides derived from hydrolysis of cereal arabinoxylan by endo-β-xylanases (Adapted from Paper **II**).

3 Production of arabinoxylan-oligosaccharides

Arabinoxylan-oligosaccharides ((A)XOS) can be produced from renewable resources rich in arabinoxylan (AX) and subsequently added to food products. The production can be included within a biorefinery. A biorefinery fractionates biomaterial and refines the different fractions into marketable chemicals, material, food, feed and energy in a sustainable way [46, 49]. Today, it is desired that a biorefinery is able to process several different raw materials, in different processes to obtain several products, as a comparison to the first biorefineries that could refine one type of raw material into one product. It is also desired that waste fractions or by-products can be recirculated and utilised in the biorefinery, e.g. as an energy carrier.

Cereals such as wheat and rye are yearly cultivated in large quantities. The starch-rich endosperm is used to produce regular flour, leaving the fibre-rich non-endosperm parts of the cereal unused. This materials are mostly used as animal feed, but there is a growing interest from the agricultural industry to valorise these fibre-rich fractions. Prebiotic (A)XOS to be used in food products can be produced from these fractions due to the high content of AX. Production of (A)XOS in parallel with regular flour production would generate value-added products from the cultivated cereals, in line with the biorefinery concept.

3.1 Extraction of arabinoxylan

The first step in a biorefinery is fractionation of the raw material. In a carbohydrate-rich raw material, the fractionation aims to untangle the material matrix, get access to its individual components, and separate the material into fractions enriched in starch, hemicellulose, cellulose or lignin. The extracted fraction will be further refined, often by enzymes acting on the enriched component and by purification. The main tech-

niques used for solubilising AX for the production of (A)XOS are extraction using an alkaline solution followed by neutralisation (chemical), aqueous extraction under high pressure and high temperature (thermophysical) and aqueous extraction and hydrolysis in the presence of high doses of an endo-β-xylanase (enzymatic) [12, 50, 51].

There are advantages and disadvantages with the different methods. Alkali pretreatment is efficient in dissociate lignin from lignocellulose material and solubilise the hemicellulose fraction [52]. The alkali breaks ester bonds, both within lignin which is the mechanism of dissociation, but also between hemicellulose and ferulic acid [51], which is a disadvantage due to the antioxidant capacity of ferulic acid [12]. Process conditions are important, severe conditions will increase yield but also remove arabinofuranosyl (Ara*f*) substitutions. The process requires a neutralisation step, not required in other process alternatives, and also a purification step to get rid of the added salts. These extra processing step will increase the cost of the process. A relatively high arabinose to xylose (A/X) ratio has been observed in the extracted AX from wheat bran by alkali pretreatment compared to other methods [53].

Autohydrolysis is an environmentally-friendly pretreatment. Under elevated temperature and pressure, hydronium ions are generated from water which release acetic acid by breaking acetyl groups from hemicellulose [54]. The acetic acid decreases the *p*H and generates more hydronium ions which further break glycosidic bonds leading to solubilisation of the hemicellulose fraction. Advantage of this method is that no chemicals besides water is used. The pretreatment can be used to directly produce (A)XOS without an additional enzymatic treatment. However, this requires severe conditions which can produce both monosaccharides, furfural and hydroxymethylfurfural which are not desired and require purification for their removal [55, 56]. Severe conditions also removes Ara*f* substitutions and ferulic acid [22, 55, 57].

Enzymatic degradation by high doses of an endo-β-xylanase is also an environmentally-friendly method as it does not require any chemicals. Another advantage is that no by-products are formed and Ara*f* substitutions and ferulic acid are not removed. However, depending on the raw material, the yield is relatively low due to limited access of the endo-β-xylanase to AX. This has been the case for rye bran which is the raw material in Paper **I** [58] and wheat bran which is used in Paper **IV** [53]. Direct enzymatic treatment is more efficient with endo-β-xylanases from glycoside hydrolase family 11 (GH11) than from GH10, as they are better at solubilising AX in the lignocellulosic matrix [59, 60]. GH10 endo-β-xylanases which are larger in size can only solubilise and degrade a sub-fraction with higher A/X ratio of the AX which can be solubilised by GH11. Thus, simultaneous hydrolysis with the two GH families will not improve the yield. Enzymes are expensive, high enzyme concentration necessary in this treatment will result in a high production cost. Another important consideration in a direct enzymatic treatment is inhibitors

present in the untreated raw material. Wheat and rye contains proteinaceous inhibitors for endo-β-xylanases from both GH10 and GH11 originating from both microbial and fungal sources [61, 62].

In Paper **I**, a combination of a mild pretreatment of autohydrolysis followed by enzymatic hydrolysis of the AX enriched fraction have been applied on rye bran to overcome the disadvantages of by-product formation in a severe pretreatment, low yield and inhibition by direct enzymatic treatment of the raw material. Direct autohydrolysis resulted in an AX yield of 45 % with a purity of 17 % and an A/X ratio of 0.42 where the AX content was 21 % and A/X ratio 0.47 in the raw material. Before the enzymatic treatment, improvement of the AX purity was further investigated by different purification steps in the process.

3.2 Purification of arabinoxylan

Purification is an important aspect in a biorefinery and several aspects needs to be considered. One aspect is the application of the products which determines the level of purity needed. Another aspect is the raw material and the process which determine what impurities and by-products are present in the product. Purification adds extra cost to the process and should therefore be optimised in a cost-effective manner. Purification steps can be added at different stages during the process which will influence the process and product. Like all other steps in a process, upscaling from lab scale, to pilot scale and to full production factory scales needs to be considered.

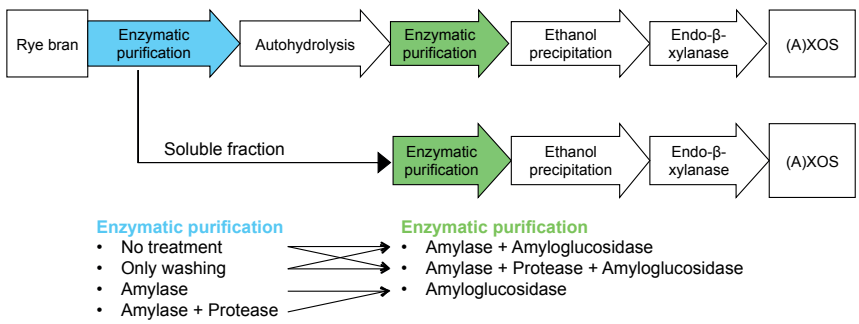

Figure 3.1: Process alternatives for extracting and purifying AX from rye bran applied in Paper I.

In Paper **I**, purification by washing of raw material, enzymatic treatment with amylase, protease and amyloglucosidase, as well as ethanol precipitation were applied in different combinations, see Figure 3.1. Direct autohydrolysis resulted in a dark col-

Table 3.1: Isolation of AX from rye bran by the combination by autohydrolysis and different purification steps, according to Figure 3.1 (Paper I).

Process		Mass (%)	Arabinoxylan		
			Yield (%)	Content (%)	A/X ratio
Raw material		100	100	21	0.47
Extract after ethanol precipitation					
Direct autohydrolysis	Amylase + AMG[1]	17	33	41	0.38
	Amylase + Protease + AMG	13	33	53	0.34
Washing	Amylase + AMG	11	23	45	0.38
	Amylase + Protease + AMG	8	25	60	0.30
Amylase	AMG	11	26	48	0.39
Amylase + Protease	AMG	8	21	58	0.39
Side stream after ethanol precipitation					
Washing	Amylase + AMG	22	12	11	0.62
	Amylase + Protease + AMG	20	10	11	0.47
Amylase	AMG	23	10	9	0.63
Amylase + Protease	AMG	23	11	10	0.52

[1] AMG - Amyloglucosidase

oured material, possibly because of Maillard reaction between sugar and proteins. This was reduced when amylase and protease treatment were applied before the autohydrolysis but also when only washing was applied. By applying amylase and protease treatment after the autohydrolysis, the AX purity was improved compared to when these enzymatic treatment was applied before autohydrolysis, see Table 3.1. Ethanol precipitation was applied to purify the AX, by getting rid of e.g. salts and monosaccharides. However, ethanol precipitation is not a good purification technique for an upscaled process, due to the high amounts of ethanol needed. In addition, the ethanol precipitation decreases the A/X ratio which is a disadvantage. An alternative purification method should be applied, e.g. membrane filtration, adsorption or a chromatographic technique [50].

3.3 Enzymatic hydrolysis of isolated arabinoxylan

Hydrolysis of AX by endo-β-xylanases into (A)XOS is a mild and environmentally-friendly method. Enzymes in general can offer high efficiency and selectivity. Drawbacks are a high cost, low stability and low availability of commercial enzymes. The challenge is to find or develop the right enzyme. The choice of enzyme is highly dependent of the raw material, the process and the desired product outcome.

3.3.1 Raw material and process

The raw material and the extraction process affect the performance of endo-β-xylanase degradation. In case of a direct endo-β-xylanase treatment, GH11 are more efficient and can hydrolyse AX to a greater extent [59, 60]. This has been ascribed to their relatively smaller size than GH10 endo-β-xylanases, which enables them to penetrate the cell wall matrix and dissociate the AX from the other components.

The A/X ratio has a high impact on the extractability of AX. Fractions of rye bran AX with an A/X ratio of 0.5 to 0.6 were directly solubilised in water and fractions with an A/X ratio of 0.3 to 0.5 was water-extracted by autohydrolysis (Paper **I**). For wheat bran AX, soluble fractions have shown an A/X ratio of 0.45-0.60 [41], while the insoluble fraction used in Paper **IV** had an A/X ratio of 0.42. Insoluble and water-unextractable (WU) AX have either a lower or a higher A/X ratio than WE-AX [39, 40]. Depending on which process is applied and which fraction is used, WE-AX or WU-AX, GH10 or GH11 is in general better at degrading the substrate as illustrated for rye bran in Paper **I** and for wheat bran in Paper **IV** and [41], see Table 3.2. It can be concluded that the (A)XOS yield by GH11 is negatively associated with the A/X ratio and that insoluble AX is not hampering the catalytic efficiency. For GH10, there seems to be an optimum A/X ratio and that WU-AX is a big hindrance for GH10 endo-β-xylanases. These findings is in line with previous observations [60, 63].

Table 3.2: (A)XOS yields of hydrolysis by the catalytic module (CM) of *Rm*Xyn10A from GH10 and Pentopan from GH11 on fractions from rye and wheat bran. The enzymatic treatment of rye bran and wheat bran has been performed with different enzyme loadings and hydrolysis times and should not be directly compared.

Raw material and process	A/X ratio	(A)XOS yield (%)[1]		Reference
		*Rm*Xyn10A_CM	Pentopan	
Rye bran	0.47			Paper **I**
Soluble fraction after autohydrolysis[2]	0.30	51	28	Paper **I**
Soluble fraction after autohydrolysis[3]	0.39	41	19	Paper **I**, unpubl. data
Soluble fraction before autohydrolysis[4]	0.62	15	5	Paper **I**, unpubl. data
Wheat bran	0.57			Paper **IV**
Soluble fraction after autohydrolysis[5]	0.45	37	21	[41]
Insoluble fraction after autohydrolysis[6]	0.42	19	24	Paper **IV**

[1] The (A)XOS yield is calculated based on (A)XOS with available standards: X_2-X_6, A^3X and A^2XX and in the case of soluble fraction of wheat bran AX after autohydrolysis also XA^3XX, XA^2XX and $A^{2+3}XX$.

[2] Washing step before autohydrolysis and amylase, amyloglucosidase and protease treatment after hydrolysis followed by ethanol precipitation after autohydrolysis.

[3] Amylase and protease treatment before autohydrolysis and amyloglucosidase treatment followed by ethanol precipitation after autohydrolysis.

[4] Amylase treatment before separation of soluble fraction followed by amyloglucosidase treatment and ethanol precipitation.

[5] Amylase and protease treatment before autohydrolysis.

[6] Amylase and protease treatment before autohydrolysis and ethanol precipitation after autohydrolysis.

3.3.2 Product profile

Hydrolysis of AX will generate different product profiles depending on which endo-β-xylanase is used. There are general differences in specificity between GH families and smaller difference between enzymes within one family. Aspects like degree of polymerisation (DP), average degree of substitution (avDS), type of branching and presence of ferulic acids and monosaccharides will vary, and these are factors influencing the prebiotic properties of (A)XOS [12, 64, 65]. In this work, three commercially available endo-β-xylanases, *Gs*Xyn10A from *Geobacillus stearothermophilus* (GH10), Pentopan derived from *Thermomyces lanuginosus* (GH11), and *Np*Xyn10A from *Neocallimastix patriciarum* represented by the catalytic module (CM) only (GH11), and *Rm*Xyn10A_CM, the catalytic module of the in-house GH10 endo-β-xylanase from *Rhodothermus marinus*, were used for hydrolysis of AX. Comparisons will be made between the two GH families, while difference in specificities within the families are discussed in Chapter 4.

DP has a large impact on fermentability. (A)XOS with a high DP (> 60) are more slowly fermented and these prebiotics can therefore reach the distal colon where *Bifidobacterium* are present [64]. It is important to feed carbohydrates to the bacteria in the distal part of the colon to avoid proteolytic fermentation resulting in toxic metabolites. On the other hand, short xylooligosaccharides (XOS) are easily fermented by *Lactobacillus* which are present in the proximal colon. In addition (A)XOS with a high DP need to be further hydrolysed by other non-probiotic gut bacteria before they can be fermented by *Lactobacillus* or *Bifidobacterium*. DP can to some extent be controlled by time and temperature of the enzymatic hydrolysis. Figure 3.2 illustrated how some intermediate products are produced and degraded during time of hydrolysis. After extended incubation, product accumulation of the final products will occur according to each endo-β-xylanase's product profile. In general, GH10

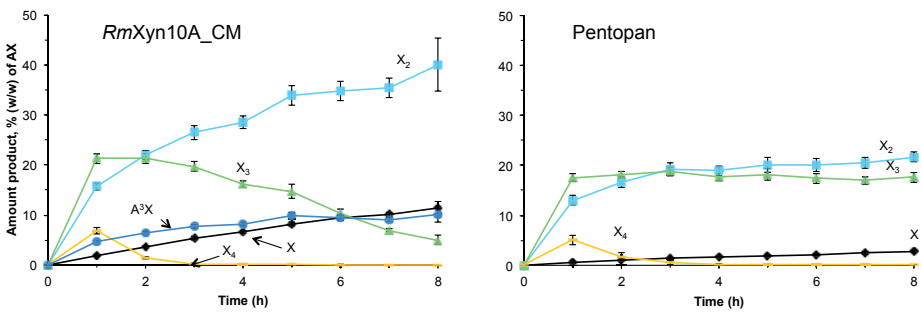

Figure 3.2: Hydrolysis profiles over time for high concentrations of *Rm*Xyn10A_CM from GH10 and Pentopan from GH11 acting on WE-AX from rye bran (Paper I). (A)XOS products representing > 1.5 % (w/w) of initial AX has been excluded for a clearer picture.

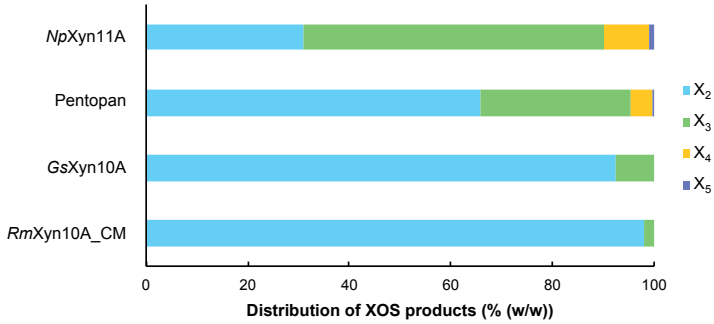

Figure 3.3: Distribution of XOS (X_2 - X_5) in the hydrolysates from two GH10 (bottom two) and two GH11 (top two) endo-β-xylanases acting on WU-AX from wheat bran for 28 h (Paper **IV**). XOS products representing > 0.1 % of initial AX has been excluded for a clearer picture.

endo-β-xylanases accumulate small (A)XOS with a DP of 2 or 3 and GH11 somewhat longer, mainly DP 3 and above [66]. This general difference was observed for the two GH10 endo-β-xylanases *Rm*Xyn10A_CM and *Gs*Xyn10A and the two GH11 endo-β-xylanases Pentopan and *Np*Xyn11A, see Figure 3.3 (Paper **I** and **IV**). By comparing Figure 3.2 and Figure 3.3, it can be seen that *Rm*Xyn10A_CM and Pentopan accumulates similar ratio of end products during hydrolysis of high enzyme loadings, regardless of the different start material, WE-AX from rye bran and WU-AX from wheat bran.

Important, for the production of (A)XOS to be used as prebiotic in food products, any monosaccharides, like xylose and arabinose, are not desired as they are not prebiotic but widely utilised by the gut bacteria. In this aspect, GH11 endo-β-xylanases are more suitable due to their general hydrolysis pattern where X_2 is the smallest product compared to GH10 endo-β-xylanases which accumulate xylose.

A desired outcome of hydrolysis of AX is a high amount of arabinoxylooligosaccharides (AXOS), as they selectively stimulates *Bifidobacterium*. GH10 endo-β-xylanases are in general better at accepting Ara*f* substitutions in the active site and thus produce (A)XOS with a higher avDS than GH11 endo-β-xylanases. The structural basis for tolerance to Ara*f* substitution in GH10 and GH11 endo-β-xylanases are discussed in Chapter 4.

Besides endo-β-xylanases from GH10 and GH11 which is the subject for this thesis, candidates from other families are interesting for hydrolysis of AX. In particular, some endo-β-xylanases from GH5 subfamily 34 have been characterised and showed to be arabinoxylan-specific. One example is *Ct*Xyl5A from *Ruminiclostridium thermocellum* (former *Clostridium thermocellum*) which acts only on AX and not unsubstituted xylan [67]. It needs an O3-bound Ara*f* at subsite -1 and thus, produces only significant

amounts of AXOS. Furthermore, the enzyme does not produce xylose. Combining GH10 or GH11 endo-β-xylanases with an arabinoxylan-specific endo-β-xylanases from GH5 can be a strategy to improve the (A)XOS yield by degradation of highly substituted regions of AX.

3.3.3 Thermostability

Thermostable GHs with activities at high temperatures are an attractive choice for hydrolysis of pretreated raw material. In the choice of enzyme to use in the production of (A)XOS, besides a hydrolytic action resulting in a desired yield and product profile, the operating conditions need to be considered. Extraction of AX by heat pretreatments such as autohydrolysis requires elevated temperatures. In a following enzymatic treatment, it is advantageous to add the enzyme directly without a cooling step to decrease the production time and cost. Depending on the raw material, enzymatic degradation at elevated temperatures is also advantageous due to better solubility of substrates and lower viscosity [46]. High-DP oligomers solubilised by autohydrolysis from oat spelt and birchwood xylan has been shown to precipitate upon cooling from 80 to 26 °C [68]. Enzymes with a high temperature optimum are a good choice to use for these application, either at the optimum temperature or at a sub-optimal temperature, the latter will increase the stability of the enzyme which can be used for a longer time and a more comprehensive hydrolysis. In addition, thermostable enzymes operating at high temperatures often have higher specific activities than enzymes operating at lower temperatures, and a lower dose of enzymes can be applied which lowers the costs [69].

Enzymes are adapted for the environment in which they have evolved, making most enzymes inactive over 50 °C. One strategy to acquire thermostable enzymes is to isolate organisms in environments where the temperature is naturally high. Thermophilic organisms harbour genes for thermostable enzymes with high temperature optimum. Extracellular proteins, exported from the cell to the surrounding environment, are generally more thermostable than intracellular proteins, reflecting the more fluctuating environment outside the cell [70]. This has been the case for *Rm*Xyn10A used in Paper **I**, **III** and **IV**. The source organism, *R. marinus*, are thermophilic bacteria isolated from shallow-water submarine hot springs northwest of Iceland. *R. marinus* have optimal growth at 65 °C [19], while *Rm*Xyn10A is most efficient at 80 °C and is stable in 70 °C for 24 hours [71].

Another strategy to acquire thermostable enzymes is using forced protein evolution on mesophilic enzymes, selecting for desired activity and thermostability. This has been done for several GH10 endo-β-xylanases, where mutation of a few amino acids resulted in increased thermostability while the activity remained [34, 72, 73].

4 Structure-function relations in endo-β-xylanases

4.1 Glycoside hydrolases

Glycoside hydrolases (GHs) is a class of enzymes that hydrolyses the glycosidic linkage between monosaccharide units within carbohydrates. Carbohydrates is a very diverse class of compounds, they differ in terms of monosaccharide composition, linkages, branching and presence of side groups. All these factors are reflected in the enzymes that act on them. Thus, GHs is a diverse class of enzymes.

4.1.1 Mechanism

GHs work either through a retaining or an inverting mechanism. In the retaining mechanism the configuration of the anomeric carbon is restored after hydrolysis while in the reverting mechanism the sugar is shifted, from α- to β-configuration or the reverse. Only retaining GHs will be discussed in this thesis. Retaining GHs have two amino acid residues vital for hydrolysis, the nucleophile and the acid/base. The mechanism consist of two steps, see Figure 4.1. In the first step, the nucleophile performs an attack on the anomeric carbon, releases the aglycone and forms a covalent glycosyl-enzyme intermediate. This is facilitated by the acid/base, which in this step acts as an acid and donates a proton to the glycosidic oxygen. In the second step, the deprotonated acid/base now acts as a base and deprotonates a water molecule which performs a nucleophilic attack on the intermediate which releases the glycone from the enzyme [28, 74]. During the two transition states, the glycone saccharide next to the cleavage adopts a distorted conformation, from chair- to boat- or shewboat-conformation, to facilitate the nucleophilic attack of the anomeric carbon.

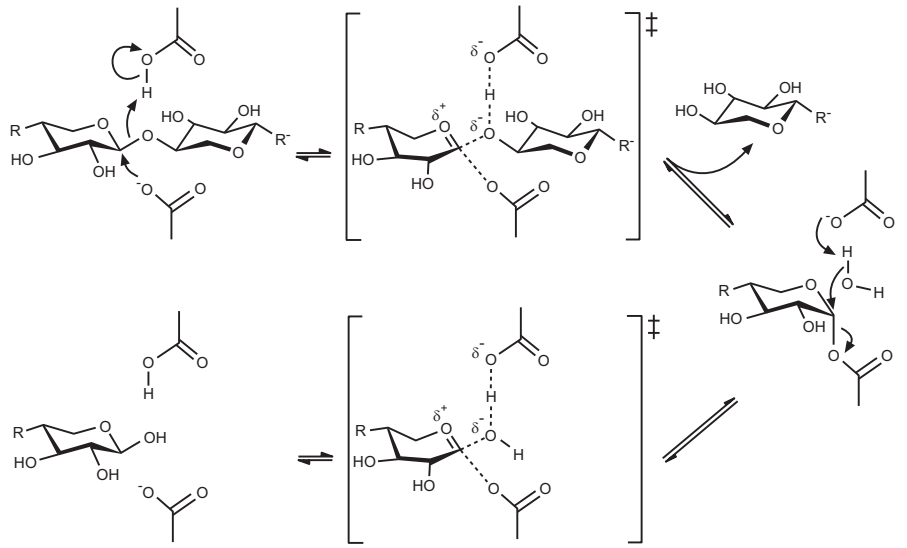

Figure 4.1: Representation of the chemical reaction of hydrolysis by the retaining mechanism of glycoside hydrolases (Adapted from Paper II).

4.1.2 Structure

GHs are, like all other enzymes, composed of a chain of 20 amino acids (primary sequence) which is further folded into a three-dimensional (3D) structure (tertiary structure) composed partly of highly ordered structures like β-sheets and α-helices (secondary structures). Some protein exist as oligomers where two or more protein chains together form an ordered structure (quaternary structure). Some proteins contains several domains, where each domain have an independent fold.

The 3D structure, including domain organisation and any oligomerisation, is important for the functionality of the enzyme. The reaction which the enzyme catalyses takes part in the active site of the enzyme, which can be a surface, groove, or tunnel on the outer part of the 3D structure. The active site is build up of amino acids spread along the primary sequence. The 3D structure enables the amino acids of the active site to be positioned for the catalysis to take place. The integrity and stability of the 3D structure is thus of high importance for the functionality of the enzyme.

The overall fold, which is the arrangement of secondary structure relative to each other in space, are highly conserved in nature. Only seven folds has been reported for glycoside hydrolases, the most common one being the TIM-barrel fold. The overall fold of an enzyme is more conserved than the primary sequence. This enables the prediction of the 3D structure by homology modeling. As catalysis is the result of interaction between a limited number of amino acids in position, very few mutations

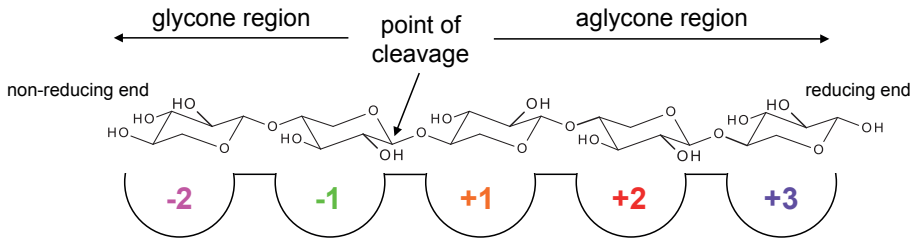

Figure 4.2: Schematic illustration and nomenclature of the active site in glycoside hydrolases, here exemplified with X_5 in subsites -2 to +3.

in the sequence can have a large effect on the activity and specificity of the reaction. However, too large change in the sequence, resulting in change in the overall fold will destroy all activity and likely denature the protein. These mutations are not selected during evolution. Selected mutations are much more likely in loop regions than in secondary structure, as these are not as involved in the integrity of the structure.

4.1.3 Active site

The active site of GHs contains several subsites to where the saccharide units of the substrate bind. The subsites are labelled from -n to +n where n is a positive integer, with -n towards the non-reducing end and +n towards the reducing end of the polysaccharide, see Figure 4.2. Cleavage of the glycosidic bond occurs between the saccharide units bound at the -1 and +1 subsites [75].

4.1.4 Classification

GHs are classified into different families based on amino acid sequence similarities in the Carbohydrate Active enZyme (CAZy) database [27, 29, 30], which today covers 165 families. Each family has a conserved overall fold, but a fold can be found in several families. GH families sharing the same fold, catalytic residues and mechanism has been grouped into clans and each clan is believed to share a common ancestor. Some large GH families are further divided into subfamilies in order to improve the prediction of activities, this has been done for e.g. GH5 [76], GH30 [77] and GH43 [78].

4.2 Endo-β-xylanases

Endo-β-xylanases, activity EC. 3.2.1.8, cleaves internal glycosidic bonds though hydrolysis between two xylopyranosyl units (Xyl*p*) within xylan. The activity can be found in GH5, GH8, GH10, GH11, GH30, GH43, GH51, GH98 and GH141 [29]. GH5, GH10 and GH30 belongs to clan A, they possess a TIM-barrel fold, uses the retaining mechanism and possess two glutamates as catalytic nucleophile and acid/base. GH11 shares the same mechanism and catalytic residues as clan A, however, they have a β-jelly roll fold and belongs to clan C. GH8 and GH43 uses the inverting mechanism and belong to clan M and F, respectively. GH98 and GH141 have not yet been classified into any clan. GH10 and GH11 are well-studied GH families that are known to act on arabinoxylan (AX), and GH30 subfamily 8 (GH30_8) contains several structure-determined enzymes acting on glucuronoxylan and glucuronoarabinoxylan (Paper **II**). Endo-β-xylanases from the other GH families are less explored.

4.3 GH10

GH10 endo-β-xylanases belong to clan A which shares the TIM barrel $(\alpha/\beta)_8$ fold consisting of eight alternating α-helices and β-strands. The eight parallel β-strands form a core of a barrel flanked which is flanked by the eight α-helices, see Figure 4.3. One end of the barrel is wider than the other, the active site is situated at this surface.

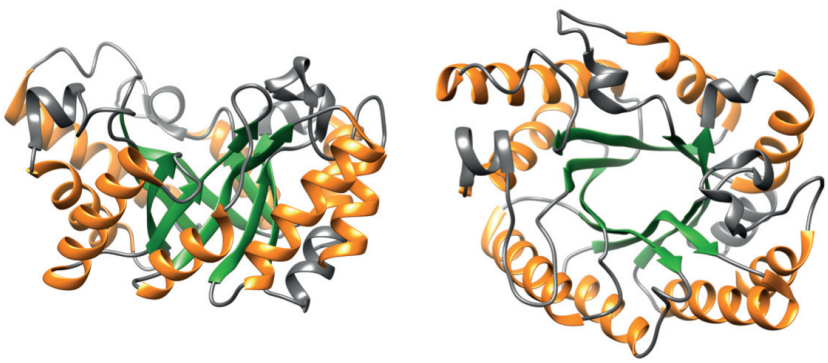

Figure 4.3: Typical 3D structure of GH10. Xys1Δ from *Streptomyces halstedii* (PDB: 1NQ6) [79] illustrating a TIM-barrel with α-helices in orange and β-strands in green (Paper **II**).

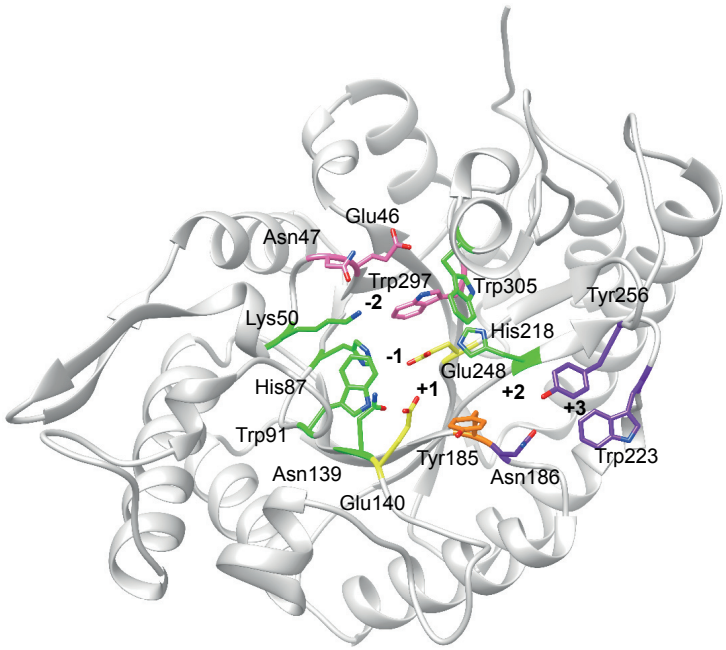

Figure 4.4: A typical active site of GH10 endo-β-xylanases, here illustrated by *Cb*Xyn10C from *Caldicellulosiruptor bescii* (PDB: 5OFK) [80]. The amino acid are coloured in accordance with subsite numbering; -2: pink, -1: green, +1: orange and +3: purple. The catalytic residues are coloured in yellow. Lys50 is also a part of subsite -2, Trp297 is also a part of subsite -1 and Trp305 is also a part of subsite +1.

4.3.1 Active site

The catalytic nucleophile is situated on β-strand 7 and the catalytic acid/base on β-strand 4. Two glycone subsites are well-conserved (Paper **II**). Conserved residues interacting with the Xyl*p* in subsite -1 are, according to numbering in *Cb*Xyn10C from *Caldicellulosiruptor bescii* [80], see Figure 4.4, Asn127, Lys50 and His87, as well as the nucleophile Glu248, and Trp305 and Trp91 contributing with stacking interactions [32, 80–83]. Conserved residues interacting with the Xyl*p* in subsite -2 are Trp297, Asn47 and Lys40, while Glu46 is semi-conserved. A third subsite is uncommon but has been observed in *Cj*Xyn10C from *Cellvibrio japonicus* with a non-conserved tyrosine stacking against Xyl*p* in subsite -3 [82]. The same tyrosine is seen in *Cj*Xyn10A from the same organism, both enzymes produce mainly X_3 from X_6 [84].

Substitution of the Xyl*p* at O3 in subsite -2 with an arabinofuranosyl unit (Ara*f*) has been seen in several structure-determined complexes and is regarded as a conserved feature of GH10 endo-β-xylanases [31–34]. In all complexes, the Ara*f* makes one hydrogen bond to Glu46. In the crystal complexes of *So*Xyn10A from *Streptomyces*

olivaceoviridis and *Cm*Xyn10B from *C. mixtus*, the Ara*f* were more rigid if the -3 subsite was occupied by a Xyl*p*, due to sandwiching of the Ara*f* [31, 32]. Substitutions in subsite -1 are highly unlikely since the hydroxyl groups at position 2 and 3 are directed towards the interior of the protein and any substitution would clash with the amino acids of the protein.

The aglycone subsites are less conserved and dominated by aromatic residues. Binding in this region is also weaker than the glycone region, and not as important for hydrolysis [81, 84]. This weaker binding is reflected in fewer structure-determined complexes with xylooligosaccharides (XOS) bound in the aglycone region. Nevertheless, the aglycone region is interesting since it plays an important role for the product profile. Less conservation in this region provides a broader substrate specificity among the members of the family. The Xyl*p* in subsite +1 is sandwiched between the conserved residues Tyr185 and Trp305, see Figure 4.4 [81, 84, 85]. An addition phenylalanine on loop $\beta_8\alpha_8$ next to Trp305 is common but not conserved [31, 82], also seen in intracellular XynA2 from *Geobacillus stearothermophilus*. The number of aglycone subsite varies, up to subsite +4 has been captured in structure-determined complexes [80, 84]. In subsite +3, Asn186 is semi-conserved making a hydrogen bond to O2. The length of loop $\beta_7\alpha_7$ varies, in case of a long loop, it is bended over the active site and provides most often one stacking interaction (Tyr256 in Figure 4.4) with the Xyl*p* in subsite +2 or +3 [31, 80, 84, 86, 87]. In the few cases where a subsite +4 is seen in a complex, an aromatic residue on loop $\beta_6\alpha_6$ is making stacking interaction with the Xyl*p* (Trp223 in Figure 4.4) [80, 84]. The same residue also provides stacking interaction with the Xyl*p* in subsite +3 [86, 87].

4.3.2 *Rm*Xyn10A_CM from *Rhodothermus marinus*

The structure of the catalytic module (CM) of *Rm*Xyn10A from *Rhodothermus marinus* was studied in Paper **III** by homology modeling, molecular dynamics (MD) simulations, docking and a mutational study. Two well-conserved glycone subsites were identified. However, the aglycone region was not conserved and contained an interesting feature. An α-helix on loop $\beta_6\alpha_6$ including Phe754 blocks the active site cleft in the position of subsite +2. This structural feature have only been seen in XynB from *Xanthomonas axonopodis* [88], the crystal structure on which the homology model was based upon. No complex with XOS bound in the aglycone region in XynB is available despite efforts of docking.

Two possible aglycone binding regions were identified in *Rm*Xyn10A_CM by MD simulations, one on each site of the mentioned α-helix on loop $\beta_6\alpha_6$, see Figure 4.5. Both binding regions provide several hydrogen bonds. The first region is similar to what is seen in other GH10 endo-β-xylanases but the xylan chain is positioned some-

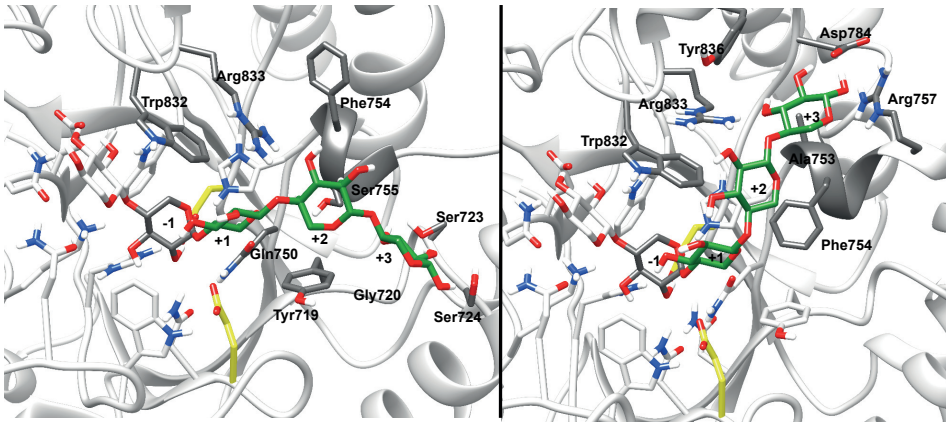

Figure 4.5: Illustrations of the *Rm*Xyn10A_CM aglycone binding region (Paper III). First binding region to the left, and second binding region to the right. The catalytic residues are coloured in yellow and the non-conserved α-helix on loop $\beta_6\alpha_6$ as well as interacting residues are marked in dark grey.

what lower and the Xyl*p* in subsite +2 is tilted. The second region forces the xylan chain to bend towards loops $\beta_7\alpha_7$ and $\beta_8\alpha_8$. In the first region, the glycosidic angles of the xylan chain are closer to what is energetic favourable and the binding energy is slightly lower than in the second cleft. Mutations in the first cleft also alters the hydrolysis profile while the activity is remained suggesting that binding do occur in this cleft. However, binding in the second cleft cannot be excluded. The second binding cleft is hypothesised to provide binding of xylan substituted with Ara*f*.

R. marinus are marine bacteria isolated outside Iceland [19]. In the marine environment, xylans including β-1,3-linkages can be found in seaweeds. Due to the difficulties during docking of XOS in the aglycone region, curiosity whether *Rm*Xyn10A_CM is evolved for another substrate arose. Endo-1,3-β-xylanase activity is found in GH10, 11 and 26 [29]. Docking of β-1,3-linked xylooligosaccharides suggest that the β-1,3 linkage is not permitted between subsite -1 and -2 due to steric hindrance (unpubl. data). However, mixed-linked β-1,4/1,3-linked xylan exist, e.g. in the red alga *Palmaria palmata* present in the Atlantic ocean around Iceland [89]. Activity on an extract from *P. palmata* have been observed (unpubl. data). Docking of various mixed-linked β-1,4/1,3-xylotetraoses suggested the acceptance of a β-1,3-linkage between subsites -1 and +1 as well as +1 and +2, see Figure 4.6. A β-1,3-linkage between subsites -1 and +1 changes the position of the Xyl*p* at subsite +2 in such a way that there is no steric hindrance from the α-helix on loop $\beta_6\alpha_6$ and stacking interaction from Tyr719 occurs. The Xyl*p* in subsite +2 makes stacking interaction with Phe754 on loop $\beta_6\alpha_6$ when there is a β-1,3-linkage between the Xyl*p* in subsites +1 and +2. The activity towards mixed-linked xylan is interesting in order to understand the structure-function relationship in *Rm*Xyn10A_CM, and also for future applications of dietary fibres from marine sources which are much less explored that their

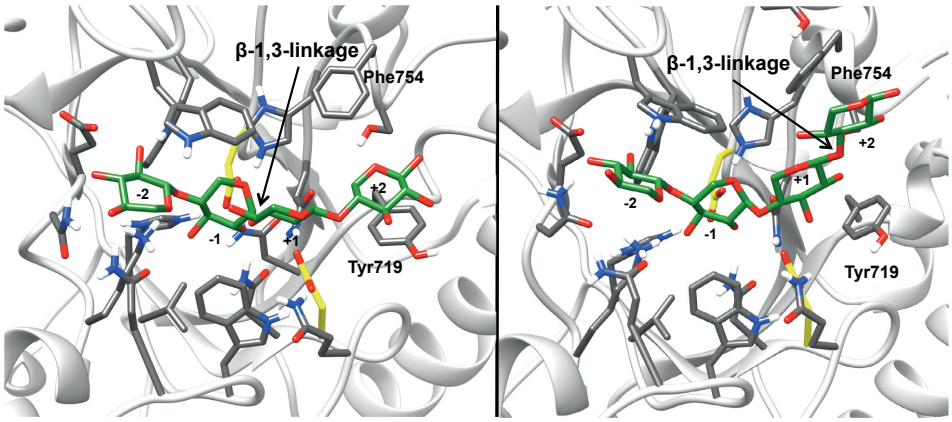

Figure 4.6: Illustrations of *Rm*Xyn10A_CM docked with mixed-linked xylan in subsites -2 to +2, with β-1,3-linkage between subsites -1 and +1 (left) and subsites +1 and +2 (right) and the rest being β-1,4-linkages (unpubl. data). Catalytic residues are coloured in yellow and interacting residues in grey.

terrestrial counterparts. The first report aiming at producing oligosaccharides for use in functional foods from *Palmaria* sp. by endo-β-xylanases was recently published [90].

4.3.3 Structural basis for Ara*f* substitutions in the aglycone region

Like the presence and conformation of subsites, Ara*f* substitution possibilities also varies in the aglycone region of GH10 endo-β-xylanases. Substitution in subsite +1 is common and in subsite +2 rare, concluded by the combination of product profiles and structural information, despite the lack of any structure-determined complex with Ara*f* substitutions in the aglycone subsites [31, 32, 66]. The length of loops $\beta_7\alpha_7$ and $\beta_8\alpha_8$ differs with different hydrolysis profiles regarding the hydrolysis product XA^{3}X, see Figure 4.7. *So*Xyn10A do not have extended loops $\beta_7\alpha_7$ and $\beta_8\alpha_8$ and can accommodate an Ara*f* at subsites -2, +1 and +2, as both A^{3}X and XA^{3}X is seen as hydrolysis products [91]. This is also the case for *Ta*Xyn10A from *Thermoascus aurantiacus* [85, 92]. However, both loops are extended in *Cm*Xyn10B, which therefore is concluded not to be able to accommodate an Ara*f* at +2 [31]. Another reason *Cm*Xyn10B cannot accommodate Ara*f* at +2 is believed to be the strong binding in subsite +3 which prevents conformational change of the Xyl*p* in subsite +2 which would be necessary [31, 66]. The strong binding of subsite +3 is build up from interactions from residues of the extended loops $\beta_7\alpha_7$ and $\beta_8\alpha_8$. Loops $\beta_7\alpha_7$ and $\beta_8\alpha_8$, thus, play a dual role in the specificity of GH10 endo-β-xylanases towards Ara*f* substitutions.

In Paper **IV**, Ara*f* substitutions were explored in *Rm*Xyn10A_CM and extracellular XynA from *G. stearothermophilus*, hereafter named *Gs*Xyn10A, by manual docking

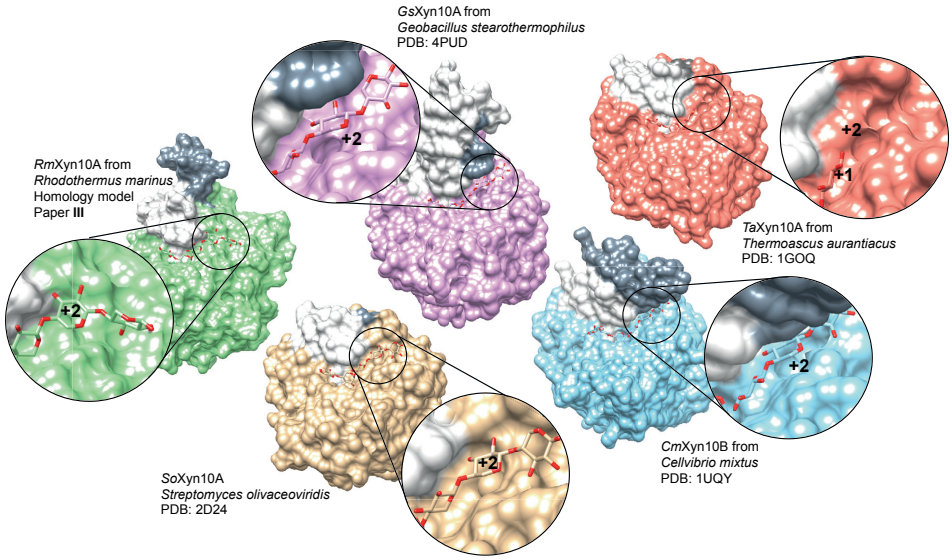

Figure 4.7: Surface representation of catalytic modules of GH10 endo-β-xylanases for comparison of structural elements affecting to possibility of an Ara*f* substitution in subsite +2, loop $\beta_7\alpha_7$ in dark grey and loop $\beta_8\alpha_8$ in light grey.

and energy minimisation. *Gs*Xyn10A have previously been structure-determined by others in complex with X_5 in subsite -2 to +3 (PDB: 4PUD). O3-bound Ara*f* were found possible in subsites -2 and +1 for both enzymes, however difference were observed for subsite +2 and +3, see Figure 4.8. *Rm*Xyn10A_CM could accommodate Ara*f*, both O2- and O3-bound, and double-substituted Xyl*p*, in subsite +2 while this was only possible in subsite +3 of *Gs*Xyn10A, see Figure 4.8.

Ara*f* substitution in subsite +1 was seen for both *Rm*Xyn10A_CM and *Gs*Xyn10A, however *Rm*Xyn10A_CM showed at least two hydrogen bond possibilities. One of them is from Gln671 on loop $\beta_4\alpha_4$, a loop which has an unconserved conformation. This residue is not found in *Gs*Xyn10A which only have one hydrogen bonding residue to the O3-bound Ara*f* in subsite +1.

Ara*f* substitution in subsite +2 of *Rm*Xyn10A_CM, which have short loops $\beta_7\alpha_7$ and $\beta_8\alpha_8$, is assisted by tilting of the Xyl*p* in subsite +2. The conformational change described necessary for Ara*f* substitution in subsite +2 of *So*Xyn10A [32] which positions the hydroxyl groups 2 and 3 in parallel to the protein surface, is facilitated by the non-conserved α-helix on loop $\beta_6\alpha_6$ by the cost of interactions in this subsite with Xyl*p*. The affinity of the second binding region of *Rm*Xyn10A_CM (see Figure 4.5) can attract both Ara*f* substituted and unsubstituted xylan. Among subsites -2 and +2 and +3 of the first binding region, subsite +2 was found to have the weakest binding of Xyl*p*, followed by +3. Thus, *Rm*Xyn10A_CM seems to have evolved to accommodate

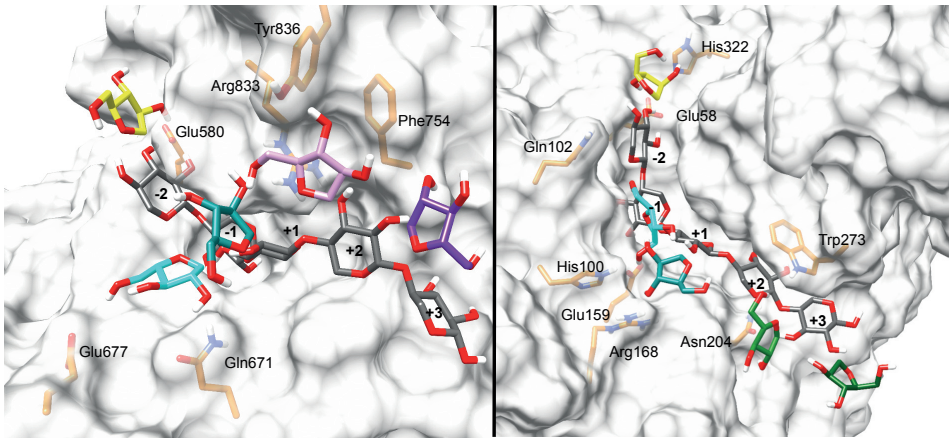

Figure 4.8: Possible Ara*f* substitutions in *Rm*Xyn10A_CM (left) and *Gs*Xyn10A (right) (Paper **IV**). Ara*f* are docked into subsites -2 (yellow), +1 (cyan), +2 (purple) and +3 (green). Ara*f* in O2 position are coloured in dark and O3 position in light. Ara*f* in subsite -2 is positioned at O3. Double substitutions are possible, with minor conformational change, in subsite +1 and +3 for *Gs*Xyn10A and in subsite +1 and +2 for *Rm*Xyn10A_CM. Residues for each enzyme interacting with the docked Ara*f* are coloured in orange.

highly-substituted xylan in the aglycone region while unsubstituted xylan will bind with low specificity.

Ara*f* substitutions in subsite +2 is not possible in *Gs*Xyn10A due to major steric hindrance from loops $\beta_7\alpha_7$ and $\beta_8\alpha_8$. However, there is space for substitutions in subsite +3. As a contrast to *Rm*Xyn10A_CM, subsite +2 was found to bind Xyl*p* the strongest. Isothermal titration calorimetry have shown that X_2 preferably occupies subsite -2 and -1, X_3 occupies subsite -2 to +1 and X_4 occupies subsite -2 to +2, suggesting subsite -2 to be stronger than +2 [87]. This enzyme seems to be evolved to accommodate lightly or non-substituted xylan with high specificity and strong binding in the aglycone region.

Hydrolysis profiles from *Rm*Xyn10A_CM and *Gs*Xyn10A acting on water-unextractable (WU) AX from wheat bran reveal differences in product formation which reflect the docking results, see Figure 4.9. The structural information of *Rm*Xyn10A_CM and *Gs*Xyn10A suggest possible arabinoxylooligosaccharides (AXOS) products from hydrolysis of AX. *Rm*Xyn10A_CM should be able to produce A^3X, XA^3X, A^2XX, XA^2XX, $A^{2+3}XX$ and $XA^{2+3}XX$. The same products can be expected by *Gs*Xyn10A except for XA^3X, XA^2XX and $XA^{2+3}XX$ which require Ara*f* substitution in subsite +2. This is in agreement with the AXOS products that could be identified by standards; A^3X, XA^3XX, A^2XX, XA^2XX and $A^{2+3}XX$. However, standards for XA^3X and $XA^{2+3}XX$ have not been available. In the analysis by high-performance anionic exchange chromatography coupled with pulsed amperiometric detection (HPAEC-PAD) of hydrolysate from *Rm*Xyn10A_CM, there is one

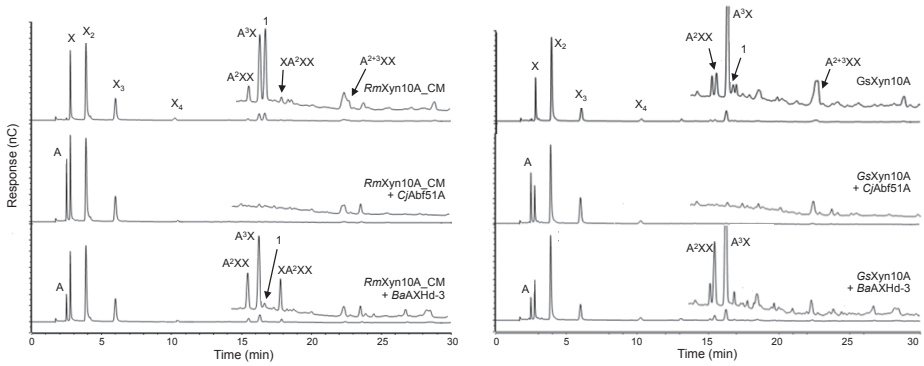

Figure 4.9: Analysis by HPAEC-PAD of water-unextractable AX from wheat bran hydrolysed by *Rm*Xyn10A_CM (top left) tailored with α-L-arabinofuranosidases *Cj*Abf51A (middle left) or *Ba*AXHd-3 (bottom left) and by *Gs*Xyn10A (top right) tailored with *Cj*Abf51A (middle right) or *Ba*AXHd-3 (bottom right) (Paper **IV**). The chromatograms are enlarged from 14 min and forward for a better resolution of AXOS products. Products identified by standards are named, while peak 1 is unidentified.

major unidentified peak (peak 1 in Figure 4.9). Based on the docking results, it is easy to believe peak 1 to correspond to XA^{3}X, but proper identification, e.g. by NMR, is necessary before the product is confirmed. There is however, some indications on its identity. The peak is removed by hydrolysis from GH51 α-L-arabinofuranosidase *Cj*Abf51A from *C. japonicus* which cleaves single O2- or O3-bound Ara*f* with only minor activity on double substitutions [93]. Peak 1 is also removed by the action of GH43 α-L-arabinofuranosidase *Ba*AXHd-3 from *Bifidobacterium adolescentis* which cleaves O3-bound Ara*f* from double-substituted Xyl*p* [47, 94, 95]. This is contradicting results, but interestingly XA^{3}XX was also cleaved by *Ba*AXHd-3, producing arabinose and X_4, thus revealing another specificity than previously have been described. In Paper **I**, the hydrolysate from rye bran AX treated with *Rm*Xyn10A_CM where further treated with a lower concentration of *Ba*AXHd-3. In this case, neither peak 1, nor XA^{3}XX was hydrolysed by *Ba*AXHd-3, which is in line with the previously described specificity. Thus, it seems like the concentration plays an important role in the specificity. One hypothesis is that, at high concentrations *Ba*AXHd-3 can cleave a single O3-bound Ara*f* if there is an additional Xyl*p* in the non-reducing end, like in the case of XA^{3}X and XA^{3}XX. If the substituted Xyl*p* in subsite +1 would turn face, the non-reducing terminal Xyl*p* would be positioned similar to the O2-bound Ara*f* believed to be necessary for hydrolysis. Contradicting data for the identification of peak 1 are also found; other groups have reported A^{3}X and XA^{3}X to co-elute or elute in the reverse order compare to what is seen for A^{3}X and peak 1 in Figure 4.9 during analysis with HPAEC-PAD [95–97].

4.4 GH11

GH11 belongs to clan C and shares the β-jelly roll fold which can be described as a partially closed hand with fingers, thumb and palm [98], see Figure 4.10. The overall structure consists of two anti-parallel β-sheets, A and B, and one α-helix [99]. β-Sheet A makes up the outside of the fingers while β-Sheet B makes up the inside of the fingers and the palm. The thumb is composted of a loop between two β-strands of β-sheet B consisting of eleven or twelve residues. The α-helix is situated next to β-sheet B on the outside of the thumb. The active site is situated inside the hand.

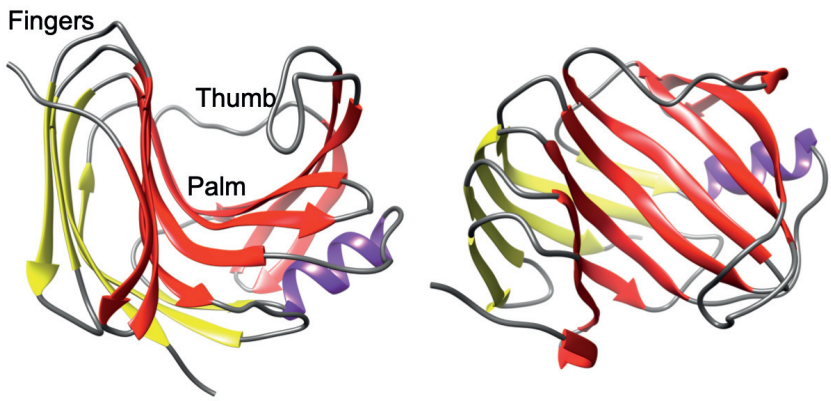

Figure 4.10: Typical 3D structure of GH11. XynA from *Thermomyces lanuginosus* (PDB: 1YNA) [100] illustrating a β-jelly roll with the α-helix in purple and β-sheet A and B in yellow and red, respectively (Paper **II**).

4.4.1 Active site

The active site of GH11 endo-β-xylanases consists of a deep and narrow cleft running along the palm of the hand. In the cleft, there is space for up to six subsites, three glycone and three aglycone [99]. The catalytic resides are situated in the middle of the hand, just below the thumb loop. A typical active site with five conserved subsites, -2 to +3, is illustrated in Figure 4.11 and is dominated by interactions from aromatic residues. The thumb loop provides hydrogen bonds from two residues, Arg122 and Pro126 [99], according to numbering in Xyn11A from *Trichoderma reesei*. The thumb loops is well conserved and plays an important role during the catalytic cycle. It is flexible and moves to open and close the active site cleft in the process of substrate binding, hydrolysis and product release. Conformational changes in the thumb loop have been observed both within crystal structures and during modeling [101–104].

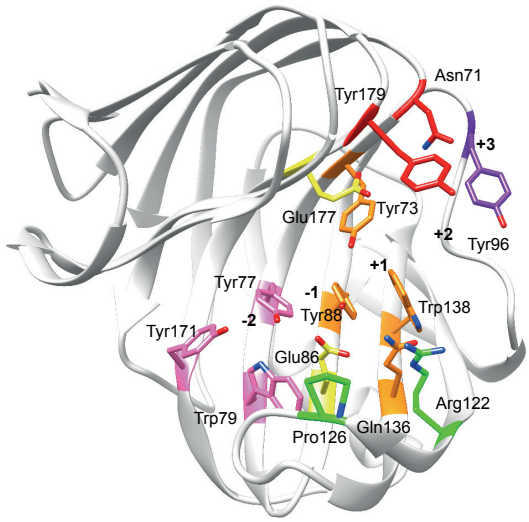

Figure 4.11: A typical active site of GH11 endo-β-xylanases, here illustrated by Xyn11A from *Trichoderma reesei* (PDB: 1XYO) [98]. The amino acids are coloured in accordance with subsite numbering; -2: pink, -1: green, +1: orange, +2: red and +3: purple. The catalytic residues are coloured in yellow (Paper **II**).

Due to the narrow cleft and the thumb loop, no Ara*f* substitutions can be accommodated in subsite -1 or +1 while substitutions in subsites +2 and -3 seems to be a common feature among GH11 endo-β-xylanases [99, 105]. Only one complex with an AXOS ligand have been structure-determined, *En*Xyn11A encoded from environmental DNA sample in complex with ferulated XA^3X in subsite +1 to +3 [105]. The Ara*f* bound to O3 of Xyl*p* in subsite +2 makes interactions with residues on the thumb loop, specifically one arginine (Arg122 in Figure 4.11).

4.4.2 Structural basis for Ara*f* substitutions in *Tl*Xyn11A and *Np*Xyn11A

Binding of AXOS in GH11 endo-β-xylanases was studied in Paper **IV** where two enzymes were explored; *Tl*Xyn11A from *Thermomyces lanuginosus* and *Np*Xyn11A from *Neocallimastix patriciarum* represented by the catalytic module only. Both enzymes have previously been structure-determined, but without any ligand in the active site [100, 105]. X_6 was docked into the active site of both enzymes by manual docking and MD, possible Ara*f* substitutions were subsequently explored by manual docking and EM, see Figure 4.12.

*Tl*Xyn11A and *Np*Xyn11A are similar in the proximal subsites and can, in accordance with the general pattern of GH11, accommodate Ara*f* in subsites -3 and +2. The active site cleft of *Tl*Xyn11A widens in the distal part around subsites -3 and +3 compared to *Np*Xyn11A. The tighter cleft of *Np*Xyn11A facilitates a hydrogen bond between the

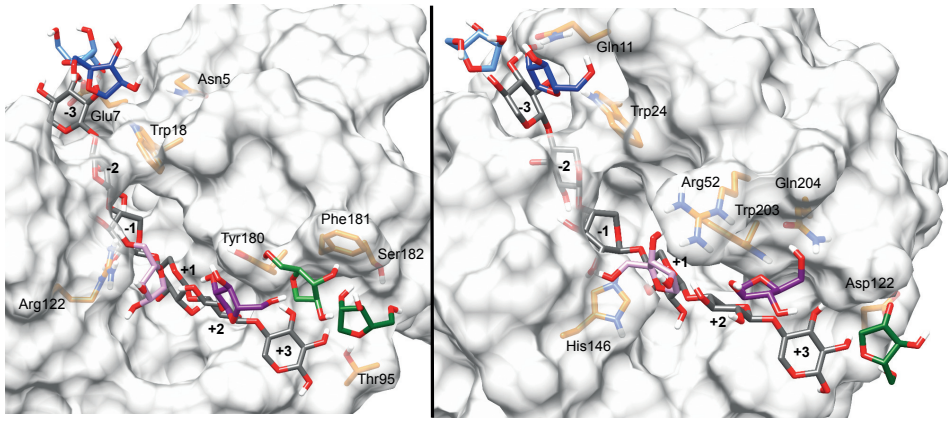

Figure 4.12: Possible Ara*f* substitutions in *Tl*Xyn11A (left) and *Np*Xyn11A (right) (Adapted from Paper **IV**). Ara*f* are docked into subsites -3 (blue), +2 (purple) and +3 (green). Ara*f* in O2 position are coloured in dark and O3 position in light. Double substitutions are possible, with minor conformational change, in subsite -3 and +2 for both enzymes and also in subsite +3 for *Tl*Xyn11A. Residues for each enzyme interacting with the docked Ara*f* are coloured in orange.

Xyl*p* in both -3 and +3 to the protein backbone. Also, an additional water-mediated hydrogen bond in subsite -3 was identified compared to the complex with *Tl*Xyn11A. This results in a stronger binding in subsite -3 and +3 of *Np*Xyn11A which initially produces more X_3 than X_2.

For both enzymes, O3-bound Ara*f* in subsite +2 is making hydrogen bond to the corresponding arginine seen in the structure-determined complex of *En*Xyn11A, which corresponds to Arg122 in *Tl*Xyn11A and His146 in *Np*Xyn11A, see Figure 4.12. In *Tl*Xyn11A, Tyr180 can make a hydrogen bond with an O2-bound Ara*f* in subsite +2, while there are several possible interacting residues to an Ara*f* in the same position in *Np*Xyn11A. In subsite -3, an O3-bound Ara*f* is mostly solvent exposed while the O2-bound Ara*f* can make hydrogen bonds to Trp12 and Asn5 in *Tl*Xyn11A and the corresponding Trp24 and Gln11 in *Np*Xyn11A. The binding of an Ara*f* in O2 position of *Np*Xyn11A requires some conformational change of the Xyl*p* in subsite -3. The narrower cleft of *Np*Xyn11A in the aglycone region results in less space for Ara*f* in subsite +3 which cannot accommodate any O3-bound Ara*f* unless there is conformation change in the complex. On the contrary, in *Tl*Xyn11A, there is space for an O3-bound Ara*f* in subsite +3 which makes stacking interaction with Phe181 and possible hydrogen bond with Tyr180. The two endo-β-xylanases seems to have been evolved to degrade AX with different average degree of substitution (avDS) where *Tl*Xyn11A can hydrolyse more heavily-substitutes AX than *Np*Xyn11A, and where *Np*Xyn11A shows higher binding energy for the less substituted substrate.

Hydrolysis of wheat bran WU-AX by the two studied GH11 endo-β-xylanases reflected the results observed by docking, see Figure 4.13. Pentopan Mono BG, hereafter

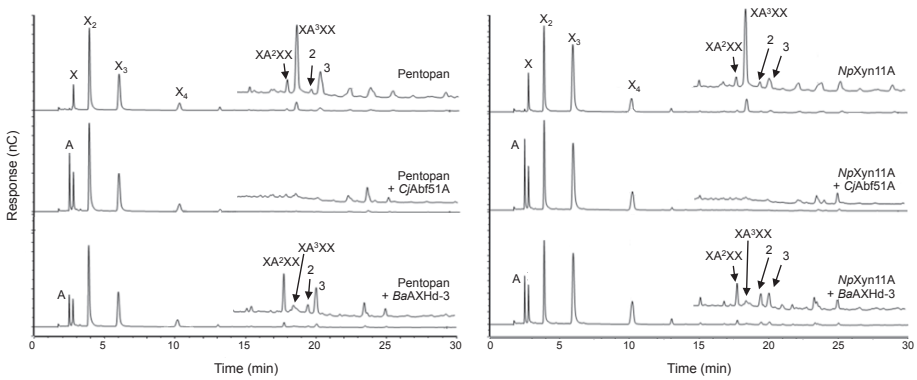

Figure 4.13: Analysis by HPAEC-PAD of water-unextractable AX from wheat bran hydrolysed by Pentopan (top left) tailored with α-L-arabinofuranosidases *Cj*Abf51A (middle left) or *Ba*AXHd-3 (bottom left) and by *Np*Xyn11A (top right) tailored with *Cj*Abf51A (middle right) or *Ba*AXHd-3 (bottom right) (Paper **IV**). The chromatograms are enlarged from 14 min and forward for a better resolution of AXOS products. Products identified by standards are named, while peak 2 and 3 are unidentified.

named Pentopan, is a commercial available variant of *Tl*Xyn11A used in the biochemical experiments. Connections between the structural studies of *Tl*Xyn11A and the biochemical studies of Pentopan should be done with caution as they might not be identical. The hydrolysates confirm the specificities of Ara*f* substitutions in subsites -3 and +2 by XA^3XX and XA^2XX as well as $XA^{2+3}XX$ identified by the increase of XA^2XX after treatment with *Ba*AXHd-3. Peaks 2 and 3 in Figure 4.13 are unidentified. Peak 2 increases after treatment with *Ba*AXHd-3, indicating an O2-bound Ara*f* in the AXOS. Peak 2 is believed to correspond to XXA^2XX, which would be in line with docking results, where both enzymes can accommodate an O2-bound Ara*f* in subsites -3 and +3. Peak 3 corresponds to a major AXOS product by Pentopan and a minor in *Np*Xyn11A. It is assumed to contain an O3-bound Ara*f* since this substitution is more common in wheat bran AX than O2-bound Ara*f* [106]. Peak 3 is believed to correspond to XXA^3XX as is would reflect the structural difference observed in subsite +3 where *Np*Xyn11A cannot accommodate O3-bound Ara*f* without structural change. XXA^3XX has been reported to elute after XA^3XX in HPAEC-PAD analysis, in line with current result [96]. As mention above, proper identification of the peaks needs to be done before conclusions are drawn.

4.5 Modularity

The catalytic module of GHs can be accompanied with other domains, both with other catalytic functions but often with another functionality. Carbohydrate-binding modules (CBMs) are common for GHs and have the role to bring the substrate and

active site in proximity for hydrolysis, target the enzyme to specific regions of the cell wall, and in some cases to disrupt polysaccharide structures [107]. CBMs do this by binding to a polysaccharide. The polysaccharide is often the same polysaccharide as the substrate, but CBMs binding to crystalline polysaccharides can accompany GHs hydrolysing another polysaccharide. Like GHs, CBMs are classified based on sequence similarity and 85 families can be found in the CAZy database [29]. CBMs are also classified based on which type of structure they bind: Type A binds to insoluble, crystalline surfaces of cellulose or chitin, Type B to polysaccharide chains and Type C to mono- or oligosaccharides.

4.5.1 CBMs of endo-β-xylanases

Different function of CBMs coupled with endo-β-xylanases from GH10 and GH11 have been identified. CBMs from GH10 have been shown to increase specific activity and thermostability [108], and they are often interacting with the catalytic domain as seen for the structure-determined *So*Xyn10A [109] and *Ct*Xyn10B from *Clostridium thermocellum* [110], but with one exception, *Cj*Xyn10C [82]. In some cases, the CBMs can interrupt the sequence of the catalytic module as found in GH10 endo-β-xylanases of the gut bacteria *Bacteroides intestinalis* and *Prevotella bryantii* [111]. Several CBMs from GH11 have been shown to introduce instability and decrease specific activity of the enzymes [108], indicating another function. The CBM module of GH11 endo-β-xylanase *Nf* Xyn11 from *Nonomuraea flexuosa* was shown to decrease adsorption of the enzyme to lignin during hydrolysis of wheat bran, thus improving the hydrolysis of the raw material by concentrating the enzyme to the substrate [112].

4.5.2 Modularity of *Rm*Xyn10A

*Rm*Xyn10A is modular enzyme containing five domains, two tandem CBM4 modules, one domain with unknown function (D3), the catalytic domain and a fifth domain with a putative cell-anchoring function (D5) [113, 114]. The two CBM4 modules binds to both insoluble and soluble xylan, amorphous cellulose as well as β-glucan and to some extent laminarin and lichenan [115]. No increase in activity on birchwood, oat spelt or rye AX have been seen for the full-length *Rm*Xyn10A compared to *Rm*Xyn10A_CM [24, 116], but decease in activity is seen when any of the two unknown domains are present. The two CBM4 modules seem to contribute to the stability of the full-length *Rm*Xyn10A [116]. *Rm*Xyn10A_CBM4-2 have been structure-determined by NMR and based on the structure, a homology model was built of *Rm*Xyn10A_CBM4-1 [117]. In Paper **III**, these structures together with the homology model of the catalytic module were used in the determination of the solution

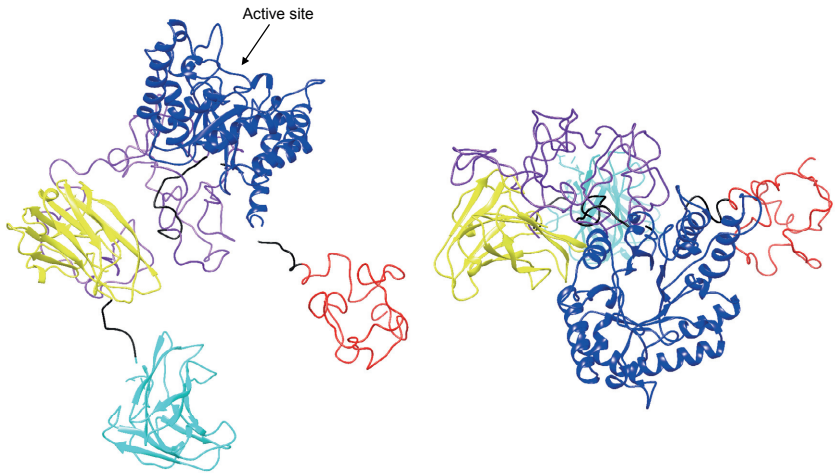

Figure 4.14: Model of the full-length *Rm*Xyn10A illustrating the spatial arrangement of its five domains; CBM4-1 (cyan), CBM4-2 (yellow), D3 (purple), catalytic module (blue) and D5 (red), where linkers are coloured in black (Paper **III**). CBM4-1, CBM4-2 and the catalytic module are represented by high-resolution structures while D3, D5 and linker regions are represented by backbone atoms. The right picture is rotated clockwise by 90°around the horizontal axis.

structure of the full-length version by Small-Angle X-ray Scattering (SAXS), see Figure 4.14. The active site is situated away from the rest of the domains and interaction with the catalytic domain is only likely for the unknown domain D3. The distance to the two CBM4 modules might explain why these domains do not contribute to the activity as they cannot affect the structure of the catalytic module. However, the two CBM4 modules seems to stabilise the domain organisation of the full-length enzyme. The functionality of the domain organisation remains to be further explored, but a hypothesis is that the D5 domain, as previously been described, anchors the enzyme to the cell surface, D3 facilitates the two CBM4 modules to reach out further from the cell to bind the substrate, and D3 has a role in bridging the substrate to the active site of the catalytic module.

5 Stimulation of health-promoting gut bacteria

The importance of the gut microbiota has led to the development of strategies to maintain a well-balanced gut microbiota and enhance its beneficial effect. Two ways to influence the composition and activity of the gut microbiota through diet are consumption of prebiotics and/or probiotics included in food items.

5.1 Probiotics

Direct addition of health-promoting microbes into the gut by ingestion is one strategy to maintain or modulate the gut microbiota in a health-promoting way. Probiotics is the term used for health-promoting microorganisms intended for this use. More strictly, probiotics are defined as live microorganisms that, when administrated in adequate amounts, confer a health benefit to the host [5]. In order to promote the health of the host as stated in the definition, safety, functional and technologial aspects need to be assessed. Important selection criteria suggested for probiotic bacteria aimed for human consumption are, but not limited to: being of human origin, having a history of being non-pathogenic and not associated with diseases, being tolerant to acid and bile salt, being able to adhere to epithelial surfaces and being persistent in the human gastrointestinal tract, being clinically validated and having documented health effects including dose-responses, having good sensory properties, being phage resistant, being viable during processing and being stable in the product and during storage [118, 119]. The documented health-promoting properties may include effect on cholesterol metabolism, bioavailability of vitamins and minerals, modulation of the intestinal epithelial barrier, faecal carcinogen and mutagen level, immune response, intestinal motility, production of anti-microbial substances and antimicrobial activity against pathogens.

Many well-documented probiotics are members of the genera *Lactobacillus* and *Bifidobacterium*. Numerous food products containing strains of these genera exist on the market, e.g. in the form of yoghurt and juices. *Lactobacillus* spp. have been shown to protect against pathogenic bacteria, lower the level of serum cholesterol, prolong induction of colon tumour and to reduce diarrhoea and symptoms of irritable bowel syndrome, ulcerative colitis, Crohn's disease and lactose intolerance [120, 121]. *Bifidobacterium* spp. have been shown to be effective against diarrhoea, ulcerative colitis and lactose intolerance as well as to lower levels of triglycerides and cholesterol, and reduce colon carcinogenesis. Other probiotics include strains belonging to *Saccharomyces*, *Lactococcus*, *Enterococcus*, *Streptococcus*, *Pediococcus*, *Leuconostoc*, *Bacillus* and *Escherichia* [122]. A few strains of commensal gut microbial bacteria associated with improved host functions has also been considered probiotic [5].

Fermented food has a long tradition in human history due to its preservative effect, long before the understanding about microorganisms arose. Fermented food contains microbial cultures that often are beneficial for human health and is therefore interesting as a source for exploring new probiotic taxa.

5.2 Prebiotics

Diet in general, and dietary fibres in particular, is one of the main influencers on both composition and activity of the gut microbiota [123]. Carbohydrates, from host diet but also in the mucus layer of the intestines, are the major energy source for the gut microbiota. The human genome harbours less than 20 hydrolytic enzymes acting on dietary carbohydrates. Besides monosaccharides, humans are only capable of digesting starch and some disaccharides, including lactose and sucrose [124]. The rest, collectively termed dietary fibres, will elude enzymatic degradation in the first part of the gastrointestinal tract and pass on to the microbial community of the intestines. The microbes in the distal gut have been estimated to contain around 150 times as many genes as in the human genome [125], and together, they can degrade and utilise a vast array of dietary fibres. Dietary fibre can promote health both by its physiochemical properties and through fermentation by the gut microbiota. When a dietary fibre is health-promoting by the fermentation in gut microbes, they are classified as prebiotics.

The latest definition of prebiotics is "a substrate that is selectively utilised by a host microorganism conferring a health benefit" [11]. Prebiotics aimed for the gut microflora must fulfil the following criteria; (1) resist gastric acidity, hydrolysis by mammalian enzymes and gastrointestinal absorption, (2) be fermented by the intestinal microflora and (3) selectively stimulate the growth/and or activity of intestinal bacteria associated

with health and well-being [126]. Like for probiotics, clinical studies including dose-response assessments are needed to confirm the prebiotic effect. According to the latest definition, a prebiotic must not be fermented in gut microbiota, but anywhere in the body, and the term is not limited to carbohydrates. However, most research is conducted on poly- and oligosaccharides originated from dietary fibre and its effect on the gut microbiota. Established prebiotics include galactooligosaccharides (GOS), fructooligosaccharides (FOS) and inulin, while xylooligosaccharides (XOS) and mannooligosaccharides (MOS) are prebiotic candidates lacking evidence for full acceptance [11].

Ingestion of prebiotic oligosaccharides increases the proportion of *Lactobacillus* and *Bifidobacterium* in the gut microbiota and its fermentation result in production of short-chain fatty acids (SCFAs) and lactate. SCFAs, including acetate, propionate and butyrate, and lactate lower the *p*H which creates a hostile environment for pathogens and improves mineral adsorption. They also stimulates the immune system and are an energy source in the host glucose, cholesterol and lipid metabolism [6–9]. Butyrate is especially beneficial due to its stimulation of the proliferation of normal colon epithelial cells and prevention of proliferation of colorectal cancer cells [127].

5.2.1 Arabinoxylan-oligosaccharides as prebiotics

Arabinoxylan-oligosaccharides ((A)XOS), including XOS and arabinoxylooligosaccharides (AXOS), have not yet acquired full acceptance as a prebiotic substrate. However, there is evidence for its prebiotic properties. According to Broekaert *et al.*, (A)XOS fulfil the three criteria for prebiotics outlined in the previous section. (A)XOS resist gastric acidity, hydrolysis by mammalian enzymes and gastrointestinal absorption, they are fermented by the intestinal bacterial, and they have a strong bifidogenic effect which has been shown by *in vitro*, animal, and human studies [12].

Health benefits associated with (A)XOS are normalisation of stool frequency and consistency by XOS and attenuation of increased levels of blood serum triglycerides, cholesterol and glucose levels during intake of certain diets by both AXOS and XOS [12]. It is speculated that especially AXOS but also XOS exhibit anti-carcinogenic effects due to stimulation of carbohydrate-degrading bacteria which leads to suppression of proteolytic fermentation in the distal colon. Fermentation of (A)XOS increases the concentration of SCFAs and lactate. Production of propionate is linked with presence of arabinose subsitutions in AXOS. (A)XOS has a butyrogenic effect, butyrate is produced in the colon upon fermentation of (A)XOS and arabinoxylan (AX) with simultaneous stimulation of butyrate producers, e.g. *Roseburia* spp. [127].

The fermentability of (A)XOS is affected by the degree of polymerisation (DP), any

substitutions to XOS, and presence of ferulic acid linked to the arabinose unit of AXOS. Slow fermentation is in general an advantage due to generation of SCFAs in the distal colon. Poor carbohydrate fermentation in the distal colon leads to protein fermentation which produces undesired metabolites such as ammonia. Branched SCFAs are an indicator of proteolytic fermentation since they are produced under these conditions as by-products. (A)XOS with a DP above 60 was seen to decrease branched SCFAs in rats. However, larger bifidogenic effect including production of acetate and butyrate was observed for (A)XOS with a DP below 15 [64]. (A)XOS with an average DP of 3.1 and 12.1 differed in fermentation rate, however, the production of SCFAs was similar [65]. Average degree of substitutions (avDS) does not seem to affect the fermentability unless it exceeds 1.0, in which case the fermentation is limited [64].

Ferulic acid linked to AXOS has antioxidant properties [12]. However, the ferulic acid affects the fermentability of these AXOS. Ferulated AXOS are poorly fermented *in vitro* compared to non-ferulated AXOS [65]. In a model of the human colon, ferulated AX induced extracellular feruloyl esterase and endo-β-xylanase activities releasing ferulic acids and hydrolysing the polysaccharides which enables fermentation by *Bifidobacterium* [128]. It is therefore likely that ferulated AXOS are fermented more in the distal part of the colon.

AX is also fermented by the human microbiota and generating SCFAs [129]. The time of fermentation of AX is related to the structure of AX including factors like type of branching and length of branches, as shown by different fermentation rates of AX from wheat bran, rice, corn and sorghum. The branching pattern affects the action of degradation and thus the possibility of fermentation [129, 130]. However, the bifidogenic effect of AX is weak as *Bifidobacterium* cannot ferment the polysaccharide unless it is hydrolysed into (A)XOS by other intestinal bacteria. Hence, AX does not fulfil the prebiotic criteria of selectively stimulating the growth/and or activity of intestinal bacteria associated with health and well-being.

5.3 Utilisation of AX and (A)XOS by gut bacteria

5.3.1 Degradation of AX

The probiotic bacteria do not degrade the polysaccharide AX, however, other gut bacteria do. Some species of the gut microbiota are specialised in degrading polysaccharides, the most well-studied example is *Bacteroides thetaiotaomicron* which alone harbours more than 300 genes encoding carbohydrate-degrading enzymes [29, 131]. For degradation of AX, endo-β-xylanase activity is needed, and this has been found

in the genera *Bacteroides*, *Prevotella* and *Roseburia* [132, 133].

Bacteroides and *Prevotella* are Gram-negative bacteria of the phylum Bacteroidetes. They have been found to utilise AX as well as other polysaccharides by the induction of polysaccharide utilisation loci (PULs) [133]. A PUL is a gene cluster including genes encoding glycoside hydrolases (GHs), the binding protein SusD, the outer membrane TonB-dependent transporter SusC and regulators [134]. Extracellular GHs degrade the polysaccharide, SusD binds the oligosaccharides and SusC transports the oligosaccharides through the outer membrane. In the periplasmic space, the oligosaccharides are further degraded by GHs to smaller oligosaccharides and monosaccharides which are transported into the intracellular space.

Roseburia are butyrate-producing Gram-positive bacteria of the phylum Firmicutes. The xylan utilisation by *Roseburia intestinalis* has recently been investigated [135]. A gene cluster including a modular GH family 10 (GH10) endo-β-xylanase active on AX, an ATP-binding cassette (ABC) transporter for (A)XOS and several intracellular GHs including an α-L-arabinofuranosidase and a β-xylosidase was identified and characterised.

5.3.2 *Bifidobacterium*

Bifidobacterium are Gram-positive bacteria of the phylum Actinobacteria. They are obligate anaerobes and are present in the distal colon. (A)XOS exhibit strong bifidogenic effects, however, the utilisation is strain specific, collaboration and avoidance of competition between strains during degradation of (A)XOS have been suggested [136]. For utilisation of (A)XOS, *Bifidobacterium* possess ABC transporters for transport of the oligosaccharides across the cell membrane, internal hydrolytic enzymes including β-xylosidases and α-L-arabinofuranosidases from GH43, endo-β-xylanases, esterases, and proteins for further metabolisation of D-xylose and L-arabinose [137, 138]. Specificity to XOS and AXOS with a DP up to 6 but preference for DP 3 to 4 has been shown for a binding protein associated with an ABC-transporter conserved within *Bifidobacterium* [139].

Bifidobacterium metabolise D-xylose and L-arabinose into acetate, ethanol and lactate via the phosphoketolase pathway. For hexose sugars, metabolism via the fructose-6-phosphate shunt, also known as the bifido shunt, occurs which yields more acetate and ATP but less lactate compared to what is produced by the metabolism in lactic acid bacteria [140].

5.3.3 *Lactobacillus*

Lactobacillus are Gram-positive facultative anaerobic bacteria of the phylum Firmicutes. XOS utilisation has only been seen in a few strains, most prominent for *L. brevis* [13, 22, 24, 141] (Paper **IV**), whereas AXOS utilisation has not been observed. In the genome of *L. brevis* ATCC 367, there are genes annotated for utilisation of XOS including a β-xyloside symporter, β-xylosidase and metabolising proteins for the conversion of D-xylose into D-xylulose-5-phosphate (Paper **V**). The β-xylosidase, LbX from GH43, has been characterised showing highest activity on X_2 [142].

Lactobacillus can be either homofermentative producing only lactate from carbohydrates, or heterofermentative, as in the case of *L. brevis*, which additionally can produce acetate and ethanol. The genome of *L. brevis* ATCC 367 possesses annotations of all proteins necessary for the conversion of D-xylose, through the phosphoketolase pathway as well as the pentose phosphate pathway, into lactate, acetate and ethanol (Paper **V**). Utilisation of pentose phosphate pathway produces lactate only.

5.3.4 Cross feeding

The microbial community in the colon cooperates and competes for utilisation of the nutrients. The degradation products and/or metabolites from one bacterium can be the substrate for another. As an example, AX can be hydrolysed extracellularly by *Bacteroides* or *Roseburia* into (A)XOS. (A)XOS are fermented by *Bifidobacterium* and some lactic acid bacteria producing lactate and acetate. Lactate and acetate are utilised by bacteria producing butyrate [127]. These mechanisms are called cross feeding which is one reason why it is important to study the whole microbial community in a continuation after studying individual strains. Exchange of nutrients also occurs between the microbial community and the host, e.g. SCFAs are absorbed into the blood stream and human intestinal epithelial cells produce glycans which are an important nutrient source for some microbes. To cover all these aspects, *in vivo* animal and human trials are necessary.

5.4 *Weissella cibaria* strain 92

To improve classification of probiotic bacteria into new taxa, the genus *Weissella* is an interesting candidate. *Weissella* was first described in 1993. After phylogenetic analysis of the genus *Leuconostoc* and some heterofermentative lactobacilli by 16S and 23S rRNA sequencing [143, 144], a subgroup consisting of *Leuconostoc paramesenteroides* and a few species of *Lactobacillus* was reclassified into the new genus *Weissella* [145].

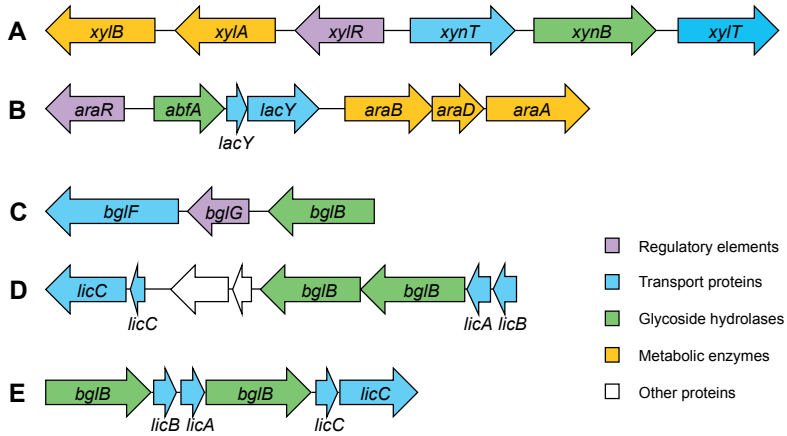

Figure 5.1: Organisation of gene clusters in *Weissella cibaria* strain 92 involved in regulation, transport, degradation and metabolism of β-xylosides (A), α-L-arabinosides (B) and β-glucosides (C-E) (Paper **V**). The genes are annotated to encode the following proteins; *xylB* – xylulose kinase, *xylA* – xylose isomerase, *xylR* – putative ROK family transcriptional regulator, *xynT* – xyloside transporter, *xynB* – β-xylosidase, *xylT* – D-xylose proton symporter, *araR* – transcriptional repressor of arabinoside utilization operon, GntR family, *abfA* – α-L-arabinofuranosidase II precursor, *lacY* – lactose permease, *araB* – ribulokinase, *araD* – L-ribulose-5-phosphate-4-epimerase, *araA* – L-arabinose isomerase, *bglF* – PTS, β-glucoside-specific II(A-C) component, *bglG* - β-glucoside bgl antiterminator bgl family, *bglB* – 6-phospho-β-glucosidase and *licA-C* – PTS, cellobiose-specific IIA-C component.

Weissella belongs to the phylum Firmicutes, class Bacilli, order Lactobacillales, family *Leuconostocaceae* and consists of Gram-positive, obligate heterofermentative bacteria that produces acetate, lactate and ethanol from fermentation of carbohydrates [10]. Strains of *Weissella* have been isolated from faeces, saliva, breast milk and vagina of humans as well as from fermented food.

W. cibaria strain 92 was previously isolated from Indian fermented food [146], and has shown production of lactate and acetate during fermentation of XOS [14, 22]. Among lactic acid bacteria, this ability has only been observed in *Leuconostoc lactis* [15] and a few strains of the established probiotics *Lactobacillus*. The XOS utilisation ability of *W. cibaria* strain 92 makes it an interesting prebiotic target and studies establishing the probiotic mechanisms and further investigation of other probiotic features are of interest. The genome of *W. cibaria* strain 92 was sequenced, annotated and analysed for utilisation of oligosaccharides originating from dietary fibres in Paper **V**.

The GH43 β-xylosidase, *W*Xyn43, was previously characterised and shows activity on XOS with a DP up to 4 [147]. *W*Xyn43 is included in a cluster containing genes annotated to a xylose-responsive transcriptor regulator, a xyloside symporter and metabolising genes for the conversion of D-xylose to D-xylulose-5-phosphate, see Figure 5.1 A (Paper **V**). The gene cluster enables the bacteria to transport XOS over the cell membrane, hydrolyse it to D-xylose and convert D-xylose to D-xylulose-5-phosphate which can enter the phosphoketolase pathway.

Growth of *W. cibaria* strain 92 on the arabinooligosaccharide (AOS) arabinobiose (A_2) has been detected (Paper **V**) which is in line with the presence of the previously characterised and structure-determined GH43 α-L-arabinofuranosidase, *W*Araf43, shown to hydrolyse both A_2 and A_3 [148]. The bacteria did not grow on A_3 indicating a limitation in the transportation over the cell membrane of AOS with a DP above 2. *W*Araf43 is present in a cluster containing genes annotated to a transcriptor regulator, a lactose permease and three genes for the conversion of L-arabinose to D-xylulose-5-phosphate, see Figure 5.1 B (Paper **V**). The gene cluster enables the bacteria to transport A_2 over the cell membrane, hydrolyse it to L-arabinose and convert it to D-xylulose-5-phosphate which can enter the phosphoketolase pathway.

Further screening of substrates for *W. cibaria* strain 92 detected growth on laminaribiose, a β-1,3-linked disaccharide of D-glucosyl units with prebiotic properties [149]. Laminaribiose can be derived from various sources including the brown seaweed polysaccharide laminarin [150], cereal mixed-linked β-glucan and microbially produced polysaccharides [151–153]. Several GHs potentially involved in the utilisation of laminaribiose were found annotated in the genome, including eight 6-phospho-β-glucosidases. Some 6-phospho-β-glucosidases were clustered with a phosphotransferase system (PTS), see Figure 5.1 C-E. PTS are common in *Lactobacillus* for transport of disaccharides of hexose sugars [154]. One 6-phospho-β-glucosidase clustered with a β-glucoside specific PTS, Figure 5.1 C, was found upregulated during growth on laminaribiose as only carbohydrate source compared to when glucose was the only carbohydrate source (Paper **V**), suggesting this gene cluster to be responsible for laminaribiose utilisation in *W. cibaria* strain 92. What substrate(s) the other 6-phospho-β-glucosidases and PTS target is not known, no growth was observed on either cellobiose (two β-1,4-linked glucosyl units), nor chitobiose (two β-1,4-linked *N*-acetylglucosylamine units). Possible candidates not tested are the glucose-based disaccharides sophorose (β-1,2 linked) and gentiobiose (β-1,6 linked). Besides 6-phospho-β-glucosidases, β-xylosidase and α-L-arabinofuranosidase, genes annotated to other GHs were annotated in the genome of *W. cibaria* strain 92, see Table 5.1.

W. cibaria strain 92 is heterofermentative and possesses all genes necessary for metabolising carbohydrates into lactate, acetate and ethanol through the phosphoketolase pathway (Paper **V**). Production of ethanol has only been observed during growth on hexose sugars (laminaribiose and glucose). Minor amounts of butyrate have been detected, however, only during fermentation of pentoses (A_2, arabinose and xylose). While grown on partly hydrolysed xylan, *W. cibaria* strain 92 produced around the same amounts of lactate and acetate [22]. This can be compared to *L. brevis* DSMZ 1269 which produced more lactate than acetate on the same material. Compared to *W. cibaria* strain 92, *L. brevis* ATCC 367 were found to harbour two additional metabolic genes in the genome, transketolase and transaldolase, enabling the use of both

Table 5.1: Glycoside hydrolases annotated within the genome of *W. cibaria* strain 92 (Paper **V**).

Enzyme	GH family	EC numbering	Gene number(s)	Signal peptide
β-xylosidase	GH43	3.2.1.37	362	No
α-L-arabinofuranosidase	GH43	3.2.1.55	636	No
6-phospho-β-glucosidase	GH1	3.2.1.86	302, 303, 379, 461, 905, 1258, 1261, 1679, 2328	No
β-glucosidase	GH1	3.2.1.21	197	No
α-xylosidase	GH31	3.2.1.177	216	No
β-galactosidase (small and large subunit)	GH2	3.2.1.23	1689, 1690	No
β-galactosidase	GH42	3.2.1.23	469	No
Endoglucanase[1]	GH8		661	Yes
Sucrose-6-phosphate hydrolase	GH32	3.2.1.26	1475	No
Neopullulanase	GH13	3.2.1.135	339	No
Family 13 glycoside hydrolase[2]	GH13		453	No

[1] 66 % coverage, 32 % identity to β-glucanase from *Bacillus circulans*, EC 3.2.1.73 (UniProtKB P19254). 85 % coverage, 27 % identity to endo-glucanase from *Bacillus* sp. (strain KSM-330), EC 3.2.1.4 (UniProtKB P29019).
[2] 97 % coverage, 39 % identity to oligo-1,6-glucosidase from *Geobacillus thermoglucosidasius*, EC 3.2.1.10 (UniProtKB P29094).

the phosphoketolase pathway and the pentose phosphate pathway, the latter resulting in lactose only (Paper **V**).

W. cibaria strain 92 is a probiotic candidate due to its ability to produce lactate and acetate by the utilisation of several types of indigestible oligosaccharides such as XOS, A_2 and laminaribiose [14, 22], (Paper **V**). Furthermore, it can survive in the *p*H present in the gut and in the presence of bile acid and it possesses some antimicrobial properties [146]. Several interesting features of *W. cibaria* strain 92 are worth investigate further; it produces exopolysaccharides (EPS) [146] but type, and hence, any potentially prebiotic properties are unknown, and also, growth on any additional indigestible fibre would improve the probiotic potential. The annotated GHs (Table 5.1) not assigned to any cellular function could potentially be involved in degradation of oligosaccharides derived from dietary fibres or synthesis and regeneration of EPS.

To gain probiotic status, *W. cibaria* strain 92 needs further evaluations. First, the safety of the strain needs to be assessed, despite it already being present in food and consequently also in the human gastrointestinal tract. Safety concerns within *Weissella* includes antibiotic resistance which is detected in *W. cibaria* strain 92 [146], presence in clinical samples (including *W. cibaria*) and classification of the closely related *W. confusa* as an opportunistic pathogen [10]. Furthermore, *W. cibaria* strain 92 needs to be tested in *in vivo* studies to investigate its behaviour within the gastrointestinal tract including the gut microbial community in order for any host health effects to be confirmed.

6 Bioinformatic methodology

The following section will describe the majority of the methods that has been used to acquire the data this thesis is based upon. The thesis has had a focus on using bioinformatics methods, i.e. interpreting biological data by computation software. However, to make these techniques valuable, they need to be combined with the more traditional wet-chemistry.

6.1 Structural bioinformatics

Structural bioinformatics deals with prediction and analysis of three-dimensional (3D) structures of macromolecules, e.g. proteins and DNA.

6.1.1 Protein 3D structure prediction by homology modeling

The gold standard for protein structure determination is X-ray analysis of protein crystals or nuclear magnetic resonance (NMR). The former technique requires crystallisation of the protein which can be a challenge due to different crystallisation conditions for different proteins, and the crystal structure do not give any information about the structure in solution. The latter requires a relative small protein and high protein concentration. Homology modeling (HM) can be used in cases where these methods cannot be applied. HM requires a template structure which has a sequence identity above 30 % to the protein to be structure-predicted. The model of the protein is created based on the template, and thus the quality of the model is closely connected to the quality of the template and the sequence identity between the two. In Paper**III**, HM was used to predict the structure of the catalytic module (CM) of glycoside hydrolase family 10 (GH10) endo-β-xylanase from *Rhodothermus marinus*.

The process of HM contains several steps: (1) template recognition and initial alignment, (2) alignment correction, (3) backbone generation, (4) loop modeling, (5) side-

chain modeling, (6) model optimisation and (7) model validation [155]. In this thesis the software YASARA [156] has been used which inhere a well-developed automatic HM process [157]. A few important aspects will be mentioned. First, identification of templates is based on related structures which are identified by Position-Specific Iterated Basic Local Alignment Search Tool (PSI-BLAST) [158] which utilises a position-specific scoring matrix (PSSM). Compared to the target sequence (which is used in a normal BLAST-search), the PSSM more accurately represents the evolution of the structure, i.e. which positions of the sequence that are conserved and can, thus, identify more distantly related structures. The PSSM is created and used by iteration of multiple sequence alignments. Second, alignment between target and template uses several type of information; sequence- and structure-based profile of target and template based on related structures, structural information in the template and predicted secondary structure of target [159, 160]. Finally, several templates are used and several alignments are created for each template, resulting in several created models. This enables the formation of a hybrid model where the most accurate part of the individual models are combined.

Validation of homology models is important. Software for validation of homology models covering different aspects is presented in Table 6.1. An additional validation parameter is overall RMSD (root mean square deviation) of C^{α} which is a measurements of how similar the backbones of two or more proteins are. A rule of thumb from the Critical Assessment of protein Structure Prediction (CASP) meetings is that an overall RMSD of C^{α} should be less than 1 Å if the sequence identity between target and template is over 60 %. A higher C^{α} would imply that the 3D structure is not as similar as expected base on sequence identity and the choice of template might need to be reconsidered [161]. The software USCF Chimera [162] was used to calculate RMSD of C^{α} atoms.

A few aspects of HM by YASARA needs specific attention including *cis* peptide bonds and ions. *Cis* peptide bonds in the template structures are altered to *trans* confirmation. Only a small fraction of the peptide bonds of proteins are in *cis* conformation. The *cis* conformation introduces steric hindrance between adjacent side groups of the amino acids which is not the case for a *trans* conformation [171]. The majority of the *cis* conformation occurs as X-Pro, where X is any amino acid. Importantly, some *cis* peptide bonds are conserved. This is especially relevant in the active site of enzymes where the conformation of the bond will affect the orientation of the side-chains interacting with the ligand and/or the hydrogen bonding network which is important for the binding. A *cis* peptide bond was identified in the GH10 endo-β-xylanase *Ta*Xyn10A from *Thermoascus aurantiacus* on β-strand 3 between a conserved histidine and the following residue [33]. The *cis* conformation enables a hydrogen bond between O3 of the xylopyranosyl unit (Xyl*p*) bound in subsite -1 and the histidine.

Table 6.1: Validation software for homology models.

Software	Description	Citation
Verify3D	Verify3D evaluates the compatibility of a protein's 3D structure with its amino acid sequence based on comparison with good-quality structures. Its purpose is to detect wrongly folded models rather than in principal correct folded models which is in need of refinement.	[163, 164]
PROCHECK	PROCHECK checks several stereochemical variables and generates the Ramachandran plot which illustrates the dihedral angles of the protein backbone.	[165, 166]
ProSA	ProSA (Protein Structure Analysis) indicates overall model quality based on the deviation of total energy of the structure compared to an energy distribution derived from random conformations. Total energy of a structure is calculated using C^{α} potentials of mean force including distance-based pairs and solvent exposure of residues.	[167]
WHAT_CHECK	WHAT_CHECK checks multiple variables against reference values and detects error like abnormally short distances and bumps.	[168]
ERRAT	ERRAT is an algorithm that calculates the error of the protein regarding non-bonded interactions between different kinds of atoms and is based on statistics from high-resolution crystal structures.	[169]
ANOLEA	ANOLEA (Atomic Non-Local Environmental Assessment) finds high energy zones by calculating non-local interactions based on knowledge-based mean force potential at an atomic level.	[170]

By reviewing the crystallographic structures available from GH10 in the Protein Data Bank (PDB) [172], the *cis* peptide bond was found to be conserved in the whole family. In *Rm*Xyn10A_CM these residues corresponds to His617 and Val618.

Ligands including ions present in the main template structure are included in the model. Except for conserved ions in e.g. active site, the presence of any ions in the created model needs to be confirmed. For GH10, ions are not common and the few present ion-binding sites are not conserved. For the homology model of *Rm*Xyn10A_CM, the presence of an added ion during the HM was investigated by molecular dynamics (MD) and the above-mentioned validation tools, as described below.

6.1.2 Molecular Dynamics

In MD, the conformational change of the protein in a solution is simulated over time [173]. However, standard MD cannot simulate electron transfers between atoms. The simulation is based on Newton's equation, $F = m \cdot a$, applied to every atom in the

system. Change in atom positions are simulated by integration of Newton's equation which is done stepwise where the forces are assumed to be constant. The time steps are in femtoseconds. To monitor the simulation, trajectories including atom positions and velocities are saved at regular intervals. The initial velocities of each atoms are acquired from a distribution of the temperature of the system. The energy is calculated based on a force field which includes equations for bonded atoms (stretching-, bending-, and torsion energies), non-bonding atoms (repulsion, van der Waals attraction and electrostatic interaction) and parameters describing properties of different atoms. The force field is a way of approximating atomic- or molecular interactions in a practical way and is thus a simplification of reality. There are numerous force fields and they have been developed targeting different applications.

In this thesis, MD has been used for several applications. The presence of a calcium ion in the homology model of *Rm*Xyn10A_CM was investigated in the force field YASARA2, which is developed for refinement of homology models by using knowledge from already determined structures [157] (Paper **III**). In the template structure, there is a calcium ion bound to the surface and thus, it was added to the model of *Rm*Xyn10A_CM. However, biochemical data suggests that no ions are bound to the protein [116]. By refining the homology model with and without the ion, several of the validation tools reported error in the refined model with the ion but not in the refined model where the ion had been removed. All software indicated a better quality without the ion. Furthermore, ERRAT, see Figure 6.1, and WHAT_CHECK found several abnormally short distances between non-bonding atoms in the ion-binding residues of the refined model including the ion, while this was not an issue in the refined model without the ion. Therefore, considering both biochemical and bioinformatic data, the ion could be removed from the model.

Stability of a homology model is an important aspect and can be simulated by MD for a relative long time, up to a microsecond. The stability of *Rm*Xyn10A_CM was simulated for 500 ns as part of the validation of the homology model (Paper **III**). The force field AMBER03 was used, which is developed from quantum mechanical calculations on short peptides for simulations of protein dynamics [174]. RMSD of C^{α} and root mean square fluctuation (RMSF) of each residue were monitored to identify any significant changes over time, and in that case, which part of the protein is affected. The GROMACS simulation software [175] was used for the simulations, mainly due to its speed since the simulations spanned a large time-interval. This type of simulation of MD was also used to study the impact of a His-tag. For production of proteins, a His-tag, consisting of six histidine residues, can be added to a protein sequence in either the N- or C-terminal to simplify the purification using metal-ion affinity chromatography with a HisTrap column. This has been done for *Rm*Xyn10A_CM in the C-terminus. It is important that the His-tag do not block the active site or inter-

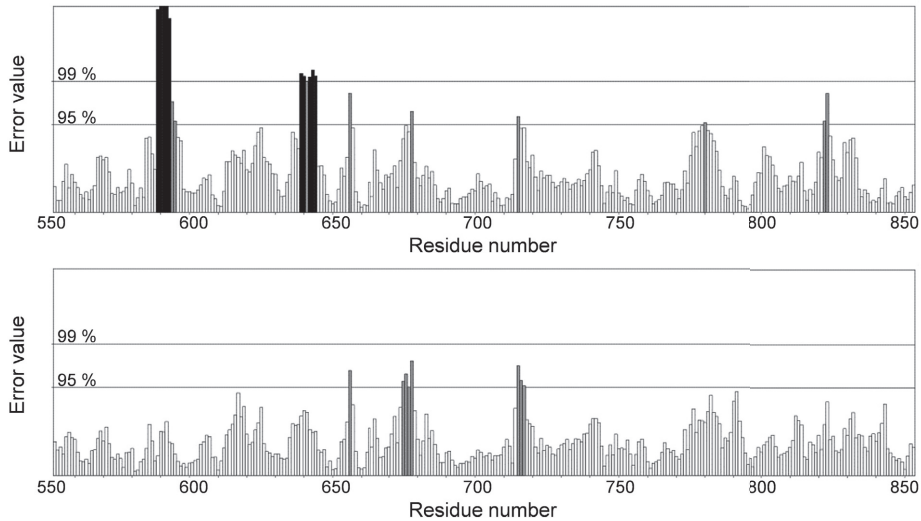

Figure 6.1: Error-value generated by ERRAT for each residue in the refined homology model of *Rm*Xyn10A_CM including the calcium ion (upper) and excluding the calcium ion (lower) (Paper **III**). The ion-binding residues are Glu589, Asp593, Glu640 and Glu643. The two lines in each graph indicate the confidence to which it is possible to reject regions that exceed the error value of the line.

fere with the integrity in such a way that the catalysing capacity is disrupted. MD simulation of the homology model of *Rm*Xyn10A_CM was done with and without the His-tag. The result showed that the RMSD of C^{α} increased, however, to a large extent due to fluctuations in the His-tag and some loop regions. The RMFS graph showed that the secondary structures were not affected. MD simulations were also used during docking of ligands in to the active site of several endo-β-xylanases, see below.

6.1.3 Substrate docking

Docking of oligosaccharides the active site of GHs is a difficult task, due to the manual preparation where knowledge about the complex is of high importance. Docking software such as AutoDock [176] and VINA [177] requires a very accurate starting complex. If the starting complex is not accurate, docking will generate unreasonable results. Hence, manual docking followed by energy minimisation (EM) and MD simulations was applied before introduction to docking software. EM is used to find local energy minimum conformation, i.e. a reasonable starting point for the simulations. In YASARA it is carried out by the steepest descent method and simulating annealing. Increased success in docking with MD was observed if the atoms of the

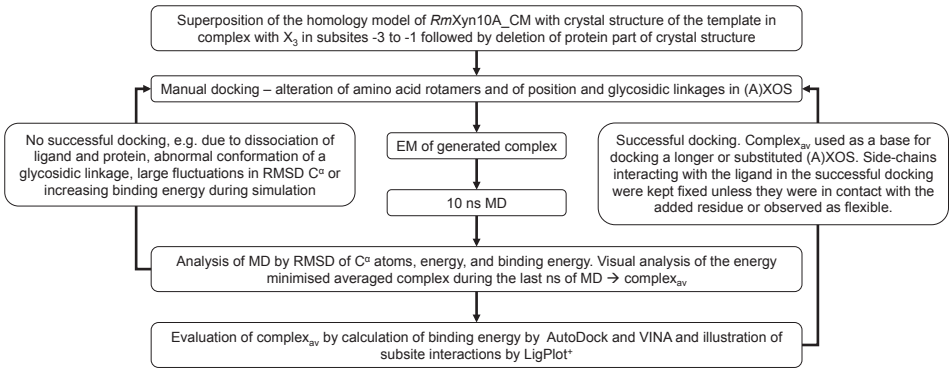

Figure 6.2: Docking scheme for docking of (A)XOS into the active site of *Rm*Xyn10A_CM starting from X_3 in subsite -3 to -1 following addition of one sugar unit at a time (Paper **III**).

catalytic residues were not allowed to move during the simulation. In reality, upon binding, electron transfer between the catalytic residues and the ligand would occur, but these events are not covered by the force field, instead the simulation results in dissociation. The results of MD is highly affected by the starting configuration which in turn is strongly influenced by the bioinformatician's idea about the how the ligand is supposed to dock given the structure, available structure-determined complexes, experience and continuous information obtain from simulations of the protein. To avoid bias from the bioinformatician, MD simulations must be applied several times with different start configurations.

During docking of arabinoxylan-oligosaccharides ((A)XOS) into the active site of *Rm*Xyn10A_CM (Paper **III**), manual docking followed by EM, MD simulation using the AMBER03 force field and finally docking by AutoDock and VINA was applied, see Figure 6.2. Modeling and simulation do not necessarily yield accurate data, it often adds a layer of insecurity. Therefore, during docking of xylooligosaccharides (XOS) on the endo-β-xylanases *Tl*Xyn11A from *Thermomyces lanuginosus* and *Np*Xyn11A from *Neocallimastix patriciarum* represented by the catalytic module only (Paper **IV**), elongation of the xylan chain was applied after the EM step rather than after MD in order to not induce large change in the protein structure which was determined by X-ray. To study possible arabinose-substitutions to the XOS docked in the active site of *Rm*Xyn10A_CM, *Gs*Xyn10A from *Geobacillus stearothermophilus*, *Tl*Xyn11A and *Np*Xyn11A, only EM was applied to detect if steric hindrance occurred or not. Increasing modeling generally yields higher insecurity to the output data. Thus, doing multiple docking on a structure predicted by homology modeling adds a lot of insecurity and results in hypothesis rather than conclusions. Accordingly, the simulation results need be complemented with experimental data before conclusions can be made.

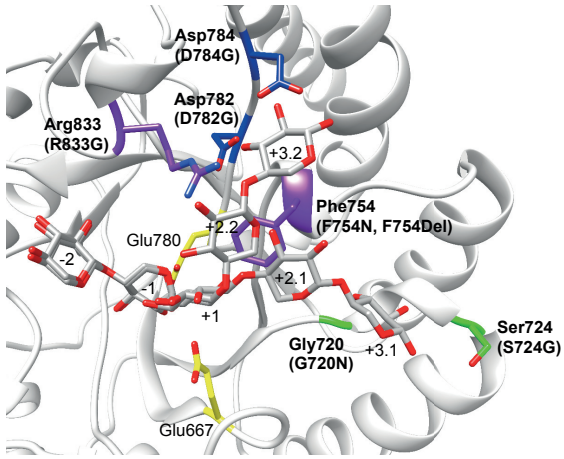

Figure 6.3: *Rm*Xyn10A_CM docked with X_5 in two positions illustrating the first and second alternative aglycone binding clefts (Paper III). Mutated residues in the first (green) and second (blue) cleft, mutated residues involved in arabinose binding in subsite +2.1 (purple) are marked as well as the catalytic residues (yellow).

During docking or XOS in *Rm*Xyn10A_CM (Paper **III**), two possible binding regions in the less conserved aglycone part of the active site were identified as several MD simulations moved the XOS ligand into one of the two regions, see Figure 6.3. To evaluate the two binding sites, parameters such as binding energy, overall RMSD of C^{α} to final model and the glycosidic bond angles were assessed as well as comparison to, by X-ray, structure-determined complex of similar proteins. The glycosidic bond angles were compared to observations of xylan and X_5 bound in the active site of *Cj*Xyn10A from *Cellvibrio japonicus* (former Xylanase A from *Pseudomonas fluorescens*) after soaking in substrate solution by X-ray [84], arabinoxylan (AX) from rice by X-ray [178] and xylan predicted by MD [179]. All parameters suggest a more favourable or conserved binding in the first region.

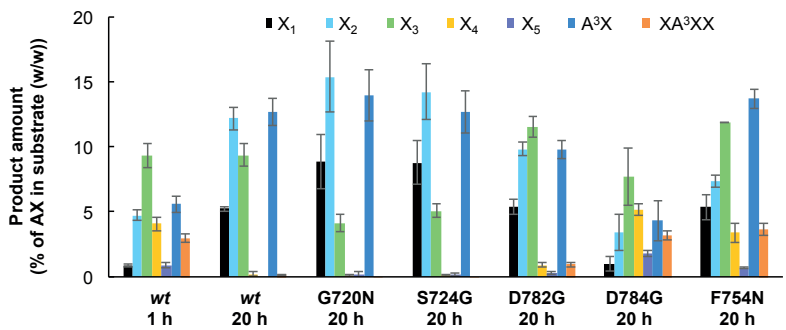

Figure 6.4: Product profiles of *wt* *Rm*Xyn10A_CM and mutants during hydrolysis of AX extracted from rye bran (Paper III).

To further study the two substrate binding regions in *Rm*Xyn10A_CM, mutants were designed to disturb or enhance binding in the regions found to be involved in the binding, see Figure 6.3 (Paper **III**). The wild-type (*wt*) *Rm*Xyn10A_CM and the mutants were experimentally produced and their activity tested by the DNS-assay [180] on birchwood xylan. The hydrolysis profiles were analysed from two time points during hydrolysis of AX isolated from rye bran (Paper **I**) by high-performance anionic exchange chromatography coupled with pulsed amperiometric detection (HPAEC-PAD), see Figure 6.4. The oligosaccharide products were separated by a CarboPac PA200 column and identified and quantified by oligosaccharide standards. The results indicate remained activity but altered product profile during mutations in the first region while a strong decrease in activity was seen for the mutants of the second binding region. Due to the low activity, it was not possible to resolve whether the product profile changed or not. The results indicate substrate binding in the first region, however, substrate binding in the second region cannot be confirmed nor excluded. The low activity from the mutations in the second region could, but does not necessarily, imply disruption of the binding affinity. Instead disruption of the structural integrity of the protein which destroys the catalytic efficiency may be the case.

6.2 Genomic bioinformatics

In Paper **V**, the genomes of four *Weissella* sp. strains were sequenced, assembled and annotated. A phylogenetic analysis was done to categorise the strains into a species. The genome of *W.* sp. strain 92 was used to find genes involved in carbohydrate degradation, uptake and metabolism.

6.2.1 Genome sequencing and assembly

Genomic DNA (gDNA) needs to be fragmented prior to sequencing. Sequenced fragments are called reads. The reads of a fragmented gDNA is called a pair end library. After sequencing, the genome is assembled based on overlapping sequences on the reads. It is rare that the assembly will fully complete the genome, instead a draft genome is generated which consists of several longer fragments called contigs. A method to improve the assembly is to create a mate pair library. In the preparation of a mate pair library, gDNA is fragmented into relatively long fragments of a specific length. These fragments are circularised by ligation of the ends. The circularised DNA fragments are further divided into smaller fragments. Some fragments will now contain the ligation point which is defined as a specific sequence detected during the assembly. The ligation point provides information that the sequences on each side of the point is as far apart in the genome as the size of the circularised gDNA fragment.

Table 6.2: Data from the genome assemblies of *Weissella* sp. strains (Paper **V**). The assembly of *W.* sp. strain 85 is based only on a paired end library while the other assemblies are based on both a pair end and a mate pair library.

	strain 85	**strain 92**	**strain 142**	**strain AV1**
Genome size (Mbp)	2.64	2.49	2.68	2.56
Contigs $\geq$ 1000 bp	47	18	27	12
Largest contig (bp)	226 575	702 551	931 233	931 688
L50[1]	8	2	2	2
L75[2]	17	4	4	3

[1] Minimum number of contigs needed for covering 50 % of the genome size.
[2] Minimum number of contigs needed for covering 75 % of the genome size.

In Paper **V**, both paired end and mate pair libraries were prepared for the sequencing of the *W.* sp. strains prior to assembly with the software SPAdes [181]. However, due to problems in cultivation of *W.* sp. strain 85, only a paired end library was prepared for this strain. This enabled the comparison of assembly with and without the mate pair library. Table 6.2 shows that the genome assemblies of *W.* sp. strains 92, 142 and AV1 based on both a paired end and a mate pair library resulted in fewer and longer contigs compared to the genome assembly of *W.* sp. strain 85 which was based only on a paired end library.

The contigs of the assembled genomes of were aligned to the complete genome of the closely related *W. cibaria* CH2 with the software Mauve (Paper **V**) [182]. The alignment revealed that the contigs were highly similar in the sequenced genomes in terms or size and position. A close up of the alignment showed minor gaps between the contigs. Gaps in the genome positioned in the same place for all four genomes suggest a common reason for the gaps. Gaps could be due to repetitive fragments in the gDNA sequence or a low coverage of reads in that area. However, this was not further explored.

6.2.2 Phylogenetic analysis

W. sp. strains 85, 92, 142 and AV1 have previously been classified to the species pair *W. cibaria*/*W. confusa* based on 16S rRNA phylogeny [14]. However, the two species cannot be separated by only 16S rRNA due to high similarity. Instead, the species have been separated based on a combination of different biochemical properties including DNA:DNA hybridisation, whole-cell protein patters, ribotyping patterns, interpeptide bridge formation and utilisation of L-arabinose [183]. In Paper **V**, after genome sequencing, several analyses were conducted in order to categorise the *W.* sp. strains into a species based on whole-genome phylogeny. Genomic data from all genome-sequenced strains of *W. cibaria* and *W. confusa* and one representative genome from all other genome-sequenced species of *Weissella* were downloaded from the

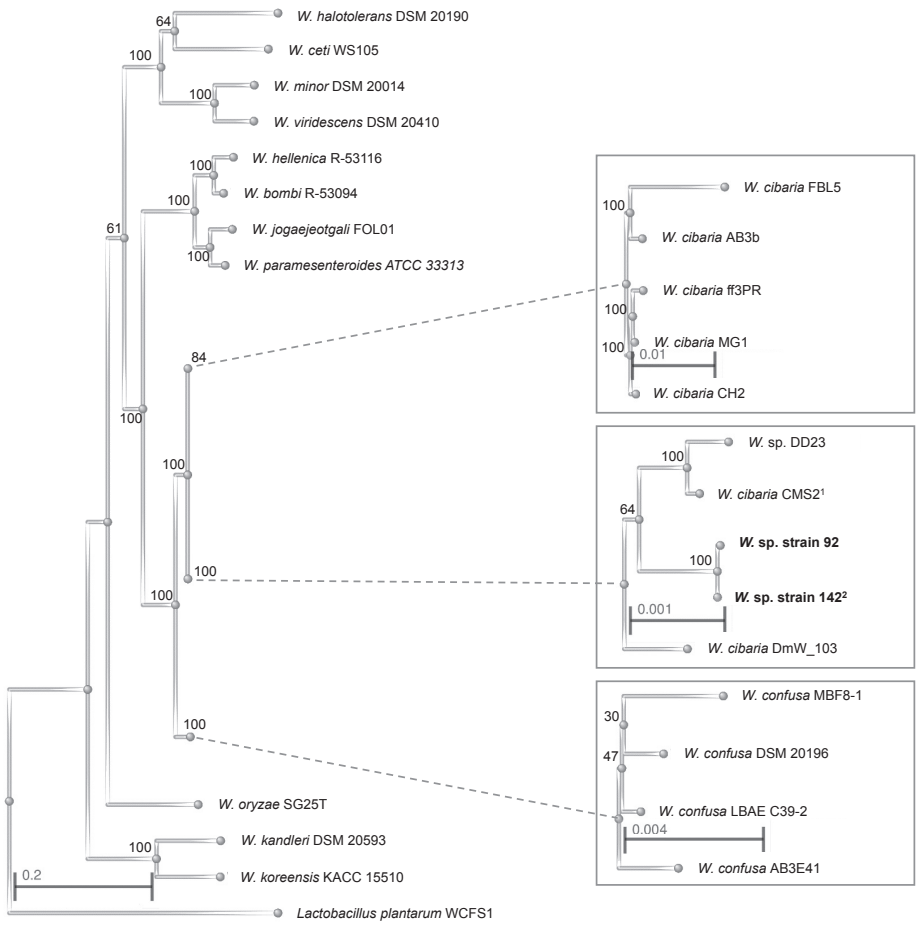

Figure 6.5: Phylogenetic tree of the genus *Weissella* based on 106 genes, constructed by the maximum likelihood approach (Paper V). The tree has a midpoint root and *Lactobacillus plantarum* WCFS1 as outgroup. The scales represent the genetic distance as number of substitutions divided by length of the sequences. The numbers adjacent to each branch node are the bootstrap support values expressed as percentages.
[1] The amino acid sequence of the 106 analysed genes of *W. cibaria* CMS2 were identical to the corresponding genes in *W. cibaria* CMS3, *W. cibaria* CMU and *W. cibaria* KACC 11862.
[2] The 106 analysed genes of *W.* sp. strain 142 were identical to *W.* sp. strains 85 and AV1.

National Centre for Biotechnology Information (NCBI) Genome database [184] and used in the analysis. The analysis included multiple sequence alignment of highly conserved genes of the entire *Weissella* genus, see in Figure 6.5, similarity of bidirectional gene pairs within *W. cibaria* and *W. confusa*, and comparison of core genome sizes of different groups within *Weissella*. All analyses supported the categorisation of the strains into the species *W. cibaria*.

Analysis of genes involved in the interpeptide bridge formation of the peptidoglycan layer as well as utilisation of L-arabinose was done since the original separation of

W. cibaria and *W. confusa* also was based on these specific traits. The genomes, both sequences in this work and the downloaded from NCBI, were added to the Rapid Annotation using Subsystem Technology (RAST) server [185] for annotation. The server categorise annotated genes into subsystem based on cellular functions. The annotation and categorisation is not always accurate. BLAST [186] has been used as a complement to the annotation from RAST during comparison of strains.

Composition of peptidoglycan has previously been an important aspect in the classification of Gram-positive bacteria, including *Weissella* and is conducted by biochemical means [145, 183, 187]. Non-ribosomal peptidyl transferases that use aminoacyl-tRNA as donor substrates catalyse the interpeptide bridge formation in the peptidoglycan layer [188]. Genomic analysis cannot conclude the sequence of the interpeptide bridge due to lack of characterised enzymes, however, the different set of genes for its synthesis between strains of *W. cibaria* and *W. confusa* suggests a different composition between the two species. *W.* sp. strains 85, 92, 142 and AV1 showed the same set of genes as found within the species *W. cibaria*.

Utilisation of L-arabinose for *W.* sp. strains 85, 92, 142 and AV1 has been observed [14]. An L-arabinose utilising cluster was found within the genomes of all strains belonging to *W. cibaria* including the four sequenced in this work. However, corresponding genes could not be found in any of the sequenced genomes of strains of *W. confusa*. By combining several phylogenetic analyses based on whole genomes and gene analysis connected to specific traits, substantial evidence for the classification of the *W.* sp. strains 85, 92, 142 and AV1 into *W. cibaria* has been gathered.

6.2.3 Annotation

Exploring possible oligosaccharide utilisation in *W. cibaria* strain 92 has been the main aim in Paper **V**. Identification of genes involved in oligosaccharide degradation, transport and metabolism was based on annotation from the RAST server. The main focus has been on the glycoside hydrolases. GHs were sometimes annotated to both GH family and activity (EC number) but in some cases the annotation was poor. In those cases BLAST was used.

Growth data for *W. cibaria* strain 92 has shown growth on XOS (X_2 - X_4) [14], arabinobiose (A_2) and laminaribiose (Paper **V**). Gene clusters for utilisation of XOS and arabinooligosaccharides (AOS) were identified in the genome including genes for degradation, transport and metabolism (Figure 5.1 A and B on p. 43). The GHs β-xylosidase and α-L-arabinofuranosidase were previously characterised [147, 148], supporting the mechanism for utilising XOS and A_2 to the identified clusters.

For laminaribiose, the mechanism for utilisation was unclear. Eight 6-phospho-β-glucosidases and one β-glucosidase were found annotated in the genome of *W. cibaria* strain 92. Based on the annotation, all could potentially hydrolyse laminaribiose or phosphated laminaribiose. Several phosphotransferase systems (PTS) which phosphorylate and transport disaccharides over the cell membrane were also annotated. Reverse transcriptase quantitative PCR (RT-qPCR) was performed after growth on glucose and laminaribiose as the sole carbohydrate source with primers designed for the putative laminaribiose degrading-enzymes. The result showed upregulation of two genes annotated to 6-phospho-β-glucosidases during growth on laminaribiose compared to glucose. One of the upregulated genes clustered with two genes annotated to a β-glucosidic-specific PTS and an antiterminator (Figure 5.1C on p. 43). Interestingly, two PTS clustered with 6-phospho-β-glucosidases were annotated as cellobiose-specific. However, growth studies on cellobiose as sole carbohydrate source in different concentrations during both microaerobic and anaerobic conditions did not yield any growth. Whether the right condition for growth on cellobiose has not been applied or over-annotation of the cellobiose-specific PTS is the case, is still unknown. According to Abou Hachem *et al.*, annotation of PTS in *Lactobacillus* is poor due to low sequence conservation and lack of experimental data [154]. The confusing results highlight the importance of combining bioinformatic data with biochemistry before any conclusion is made.

7 Concluding Remarks

The prebiotic candidates arabinoxylan-oligosaccharides ((A)XOS) can be produced from rye and wheat bran by a process involving washing, autohydrolysis, removal of starch and protein by enzymatic degradation, ethanol precipitation and hydrolysis by endo-β-xylanases. Both insoluble and soluble arabinoxylan (AX) can be hydrolysed into (A)XOS by endo-β-xylanases from glycoside hydrolase family 10 (GH10) and GH11. From insoluble AX, GH11 endo-β-xylanases perform the highest yield, while GH10 endo-β-xylanases perform the highest yield on soluble AX.

General differences in specificity between GH10 and GH11 endo-β-xylanases were observed; production of shorter (A)XOS by GH10 (accumulating mainly DP 2) than GH11 (accumulating mainly DP 2-4), a higher tolerance for arabinofuranosyl (Ara*f*) substitutions by GH10, as well as a higher accessibility to insoluble AX for GH11. This suggests the use of a GH10 endo-β-xylanase for hydrolysis of water-extractable AX with a higher A/X ratio, and a GH11 endo-β-xylanase for hydrolysis of water-unextractable AX and AX with a lower A/X ratio. However, a drawback with GH10 endo-β-xylanases is the accumulation of xylose which requires removal by a purification step.

The homology model of the catalytic module (CM) of thermostable GH10 endo-β-xylanase *Rm*Xyn10A revealed unconserved structures in the aglycone region of the active site resulting in unspecific binding of unsubstituted xylan and tolerance for highly substituted AX.

Docking studies and comparison with structural data and product profiles from GH10 endo-β-xylanases identified loops $\beta_7\alpha_7$ and $\beta_8\alpha_8$ being involved in the specificity towards accepting Ara*f* substitutions at subsite +2 for GH10 in general and also an α-helix on loop $\beta_6\alpha_6$ for *Rm*Xyn10A_CM in particular. In contrast to *Rm*Xyn10A_CM, *Gs*Xyn10A was found not to accommodate any Ara*f* at subsite +2 due to steric hindrance from loops $\beta_7\alpha_7$ and $\beta_8\alpha_8$, however, the affinity for the xylopyranosyl unit (Xyl*p*) was stronger in this subsite due to interaction form the above-mentioned loops.

While diversity within GH10 was mainly found in the aglycone subsites, the distal subsites on both side of the active site were found to be involved in different substrate specificities within GH11. Subsites -3 and +3 were structurally different in the two studied enzymes Pentopan derived from *Ta*Xyn11A and *Np*Xyn11A. More interactions between the protein and Xyl*p* and less space for Ara*f* substitutions were observed in *Np*Xyn11A compared to *Ta*Xyn11A. This results in relatively more X_3 than X_2 and less AXOS than XOS during hydrolysis with *Np*Xyn11A compared to with hydrolysis with Pentopan.

The lactic acid bacteria *Weissella* sp. strains 85, 92, 142 and AVI, isolated from Indian fermented foods, belongs to the species *W. cibaria*.

W. cibaria strain 92 can degrade X_2-X_4, A_2 and laminaribiose by the action of β-xylosidase, α-L-arabinofuranosidase and 6-phospho-β-glucosidases, respectively. Clusters including genes for transportation, degradation and conversion into the central metabolism for the oligosaccharides have been identified in the genome, as well as metabolic routes for production of the short-chain fatty acid acetate and lactate.

7.1 Future Perspectives

Production of (A)XOS from cereal bran rich in AX was demonstrated on a lab scale. The next step is to further scale up the process to a pilot scale and study how that affects the yield and purity of the (A)XOS as well as practical aspects in the process and the economy. One step to investigate further in an upscaled process is the purification. Ethanol precipitation is not suitable in a larger scale due to practical aspect and safety reason related to the use of large volumes of ethanol.

To further explore the mechanism behind the specificity of various endo-β-xylanases, protein-ligand structures are crucial. For GH10 endo-β-xylanases, much of the substrate specificity diversity is due to differences in the aglycone region, while most structure-determined complexes include a ligand in the glycone region. Accumulation of more structural data by both X-ray of crystals and bioinformatic techniques are important for an overall analysis of structure-function relationships within different GH family which will facilitate the choice of enzyme for different applications.

Weissella cibaria strain 92 possesses probiotic features. However, today no strains of *Weissella* are Generally Regarded as Safe (GRAS) by The U.S. Food and Drug Administration (FDA) which is necessary for the probiotic status, nor have they gained the status Qualified Presumption of Safety (QPS) by the European Food Safety Authority (EFSA) [189]. For *Weissella*, safety evaluation is necessary on a strain level to validate if these bacteria are safe for human consumption, despite their presence in food.

Despite extensive research on prebiotics and probiotics, the possibilities of making health claims on products containing these is very limited. Within the European Union, EFSA must approve any health claim to be made on food products or food supplements. To date, among prebiotics, only native chicory inulin from a specific producer can claim that it contributes to normal bowel function by increasing stool frequency [190], and among probiotics, only *Propinibacterium freudenreichii* from one producer can make health claims due to its high production of Vitamin B_{12} [191]. All other applications regarding health claims on prebiotics and probiotics has not been approved based on a lack of establishment between cause and effect, and thus, the terms 'probiotics' or 'prebiotics' are not allowed to be used. It is therefore important to continue the research, especially human and animal trials, in order to firmly establish the health effects of prebiotics and probiotics.

References

[1] R. Sender, S. Fuchs, and R. Milo, "Revised Estimates for the Number of Human and Bacteria Cells in the Body," *PLOS Biology*, vol. 14, no. 8, 2016.

[2] E. Thursby and N. Juge, "Introduction to the human gut microbiota," *Biochemical Journal*, vol. 474, no. 11, pp. 1823–1836, 2017.

[3] J. A. Foster and K.-A. M. Neufeld, "Gut-brain axis: how the microbiome influences anxiety and depression," *Trends in Neurosciences*, vol. 36, no. 5, pp. 305–312, 2013.

[4] P. D. Cani and W. M. de Vos, "Next-Generation Beneficial Microbes: The Case of *Akkermansia muciniphila*," *Frontiers in Microbiology*, vol. 8, no. 1765, 2017.

[5] C. Hill, F. Guarner, G. Reid, G. R. Gibson, D. J. Merenstein, B. Pot, L. Morelli, R. B. Canani, H. J. Flint, S. Salminen *et al.*, "The International Scientific Association for Probiotics and Prebiotics consensus statement on the scope and appropriate use of the term probiotic," *Nature Reviews Gastroenterology & Hepatology*, vol. 11, pp. 506 –514, 2014.

[6] J. H. Cummings, "Short chain fatty acids in the human colon," *Gut*, vol. 22, no. 9, pp. 763–779, 1981.

[7] T. P. Trinidad, T. M. Wolever, and L. U. Thompson, "Interactive effects of calcium and short chain fatty acids on absorption in the distal colon of man," *Nutrition Research*, vol. 13, no. 4, pp. 417–425, 1993.

[8] J. G. LeBlanc, F. Chain, R. Martín, L. G. Bermúdez-Humarán, S. Courau, and P. Langella, "Beneficial effects on host energy metabolism of short-chain fatty acids and vitamins produced by commensal and probiotic bacteria," *Microbial Cell Factories*, vol. 16, no. 79, 2017.

[9] A. Koh, F. De Vadder, P. Kovatcheva-Datchary, and F. Bäckhed, "From Dietary Fiber to Host Physiology: Short-Chain Fatty Acids as Key Bacterial Metabolites," *Cell*, vol. 165, no. 6, pp. 1332–1345, 2016.

[10] V. Fusco, G. M. Quero, G.-S. Cho, J. Kabisch, D. Meske, H. Neve, W. Bockelmann, and C. M. A. P. Franz, "The genus *Weissella*: taxonomy, ecology and biotechnological potential," *Frontiers in Microbiology*, vol. 6, no. 155, 2015.

[11] G. R. Gibson, R. Hutkins, M. E. Sanders, S. L. Prescott, R. A. Reimer, S. J. Salminen, K. Scott, C. Stanton, K. S. Swanson, P. D. Cani *et al.*, "Expert consensus document: The International Scientific Association for Probiotics and Prebiotics (ISAPP) consensus statement on the definition and scope of prebiotics," *Nature Reviews Gastroenterology & Hepatology*, vol. 14, pp. 491–502, 2017.

[12] W. F. Broekaert, C. M. Courtin, K. Verbeke, T. V. de Wiele, W. Verstraete, and J. A. Delcour, "Prebiotic and Other Health-Related Effects of Cereal-Derived Arabinoxylans, Arabinoxylan-Oligosaccharides, and Xylooligosaccharides," *Critical Reviews in Food Science and Nutrition*, vol. 51, no. 2, pp. 178–194, 2011.

[13] R. Crittenden, S. Karppinen, S. Ojanen, M. Tenkanen, R. Fagerström, J. Mättö, M. Saarela, T. Mattila-Sandholm, and K. Poutanen, "*In vitro* fermentation of cereal dietary fibre carbohydrates by probiotic and intestinal bacteria," *Journal of the Science of Food and Agriculture*, vol. 82, no. 8, pp. 781–789, 2002.

[14] A. Patel, P. Falck, N. Shah, P. Immerzeel, P. Adlercreutz, H. Stålbrand, J. B. Prajapati, O. Holst, and E. Nordberg Karlsson, "Evidence for xylooligosaccharide utilization in *Weissella* strains isolated from Indian fermented foods and vegetables," *FEMS Microbiology Letters*, vol. 346, no. 1, pp. 20–28, 2013.

[15] H. Ohara, M. Owaki, and K. Sonomoto, "Xylooligosaccharide fermentation with *Leuconostoc lactis*," *Journal of Bioscience and Bioengineering*, vol. 101, no. 5, pp. 415–420, 2006.

[16] J. L. Ward, K. Poutanen, K. Gebruers, V. Piironen, A.-M. Lampi, L. Nyström, A. A. M. Andersson, P. Å. , D. Boros, M. Rakszegi *et al.*, "The HEALTHGRAIN Cereal Diversity Screen: Concept, Results, and Prospects," *Journal of Agricultural and Food Chemistry*, vol. 56, no. 21, pp. 9699–9709, 2008.

[17] S. P. Chundawat, G. T. Beckham, M. E. Himmel, and B. E. Dale, "Deconstruction of Lignocellulosic Biomass to Fuels and Chemicals," *Annual Review of Chemical and Biomolecular Engineering*, vol. 2, no. 1, pp. 121–145, 2011.

[18] J.-G. Berrin and N. Juge, "Factors affecting xylanase functionality in the degradation of arabinoxylans," *Biotechnology Letters*, vol. 30, no. 7, pp. 1139–1150, 2008.

[19] G. A. Alfredsson, J. K. Kristjansson, S. Hjörleifsdottir, and K. O. Stetter, "*Rhodothermus marinus*, gen. nov., sp. nov., a Thermophilic, Halophilic Bacterium from Submarine Hot Springs in Iceland," *Microbiology*, vol. 134, no. 2, pp. 299–306, 1988.

[20] S. H. Bjornsdottir, T. Blondal, G. O. Hreggvidsson, G. Eggertsson, S. Petursdottir, S. Hjorleifsdottir, S. H. Thorbjarnardottir, and J. K. Kristjansson, "*Rhodothermus marinus*: physiology and molecular biology," *Extremophiles*, vol. 10, no. 1, pp. 1–16, 2006.

[21] L. Dahlberg, O. Holst, and J. K. Kristjansson, "Thermostable xylanolytic enzymes from *Rhodothermus marinus* grown on xylan," *Applied Microbiology and Biotechnology*, vol. 40, no. 1, pp. 63–68, 1993.

[22] P. Immerzeel, P. Falck, M. Galbe, P. Adlercreutz, E. Nordberg Karlsson, and H. Stålbrand, "Extraction of water-soluble xylan from wheat bran and utilization of enzymatically produced xylooligosaccharides by *Lactobacillus*, *Bifidobacterium* and *Weissella* spp." *LWT - Food Science and Technology*, vol. 56, no. 2, pp. 321–327, 2014.

[23] K. Berger, P. Falck, C. Linninge, U. Nilsson, U. Axling, C. Grey, H. Stålbrand, E. Nordberg Karlsson, M. Nyman, C. Holm, and P. Adlercreutz, "Cereal Byproducts Have Prebiotic Potential in Mice Fed a High-Fat Diet," *Journal of Agricultural and Food Chemistry*, vol. 62, no. 32, pp. 8169–8178, 2014.

[24] P. Falck, S. Precha-Atsawanan, C. Grey, P. Immerzeel, H. Stålbrand, P. Adlercreutz, and E. Nordberg Karlsson, "Xylooligosaccharides from Hardwood and Cereal Xylans Produced by a Thermostable Xylanase as Carbon Sources for *Lactobacillus brevis* and *Bifidobacterium adolescentis*," *Journal of Agricultural and Food Chemistry*, vol. 61, no. 30, pp. 7333–7340, 2013.

[25] D. M. Salas-Veizaga, R. Villagomez, J. A. Linares-Pastén, C. Carrasco, M. T. Álvarez, P. Adlercreutz, and E. Nordberg Karlsson, "Extraction of Glucuronoarabinoxylan from Quinoa Stalks (*Chenopodium quinoa* Willd.) and Evaluation of Xylooligosaccharides Produced by GH10 and GH11 Xylanases," *Journal of Agricultural and Food Chemistry*, vol. 65, no. 39, pp. 8663–8673, 2017.

[26] M. Sajib, P. Falck, R. R. R. Sardari, S. Mathew, C. Grey, E. Nordberg Karlsson, and P. Adlercreutz, "Valorization of Brewer's spent grain to prebiotic oligosaccharide: Production, xylanase catalyzed hydrolysis, *in-vitro* evaluation with

probiotic strains and in a batch human fecal fermentation model," *Journal of Biotechnology*, vol. 268, pp. 61–70, 2018.

[27] B. Henrissat, "A classification of glycosyl hydrolases based on amino acid sequence similarities," *Biochemical Journal*, vol. 280, no. 2, pp. 309–316, 1991.

[28] G. Davies and B. Henrissat, "Structures and mechanisms of glycosyl hydrolases," *Structure*, vol. 3, no. 9, pp. 853–859, 1995.

[29] "Carbohydrate-Active enZYmes Database," Online database, available at www.cazy.org.

[30] V. Lombard, H. Golaconda Ramulu, E. Drula, P. M. Coutinho, and B. Henrissat, "The carbohydrate-active enzymes database (CAZy) in 2013," *Nucleic Acids Research*, vol. 42, no. D1, pp. D490–D495, 2013.

[31] G. Pell, E. J. Taylor, T. M. Gloster, J. P. Turkenburg, C. M. Fontes, L. M. Ferreira, T. Nagy, S. J. Clark, G. J. Davies, and H. J. Gilbert, "The mechanisms by which family 10 glycoside hydrolases bind decorated substrates," *Journal of Biological Chemistry*, vol. 279, no. 10, pp. 9597–9605, 2004.

[32] Z. Fujimoto, S. Kaneko, A. Kuno, H. Kobayashi, I. Kusakabe, and H. Mizuno, "Crystal Structures of Decorated Xylooligosaccharides Bound to a Family 10 Xylanase from *Streptomyces olivaceoviridis* E-86," *Journal of Biological Chemistry*, vol. 279, no. 10, pp. 9606–9614, 2004.

[33] M. Vardakou, J. Flint, P. Christakopoulos, R. J. Lewis, H. J. Gilbert, and J. W. Murray, "A Family 10 *Thermoascus aurantiacus* Xylanase Utilizes Arabinose Decorations of Xylan as Significant Substrate Specificity Determinants," *Journal of Molecular Biology*, vol. 352, no. 5, pp. 1060–1067, 2005.

[34] H. Xie, J. Flint, M. Vardakou, J. H. Lakey, R. J. Lewis, H. J. Gilbert, and C. Dumon, "Probing the Structural Basis for the Difference in Thermostability Displayed by Family 10 Xylanases," *Journal of Molecular Biology*, vol. 360, no. 1, pp. 157–167, 2006.

[35] H. V. Scheller and P. Ulvskov, "Hemicelluloses," *Annual Review of Plant Biology*, vol. 61, pp. 263–289, 2010.

[36] R. Deutschmann and R. F. Dekker, "From plant biomass to bio-based chemicals: latest developments in xylan research," *Biotechnology Advances*, vol. 30, no. 6, pp. 1627–1640, 2012.

[37] M. S. Izydorczyk and C. G. Biliaderis, "Cereal arabinoxylans: advances in structure and physicochemical properties," *Carbohydrate Polymers*, vol. 28, no. 1, pp. 33–48, 1995.

[38] A. Ebringerová, "Structural Diversity and Application Potential of Hemicelluloses," in *Macromolecular Symposia*, vol. 232, no. 1. Wiley Online Library, 2005, pp. 1–12.

[39] C. J. A. Vinkx and J. A. Delcour, "Rye (*Secale cereale* L.) Arabinoxylans: A Critical Review," *Journal of Cereal Science*, vol. 24, no. 1, pp. 1–14, 1996.

[40] C. Maes and J. Delcour, "Structural Characterisation of Water-extractable and Water-unextractable Arabinoxylans in Wheat bran," *Journal of Cereal Science*, vol. 35, no. 3, pp. 315–326, 2002.

[41] S. Mathew, E. Nordberg Karlsson, and P. Adlercreutz, "Extraction of soluble arabinoxylan from enzymatically pretreated wheat bran and production of short xylo-oligosaccharides and arabinoxylo-oligosaccharides from arabinoxylan by glycoside hydrolase family 10 and 11 endoxylanases," *Journal of Biotechnology*, vol. 260, pp. 53–61, 2017.

[42] V. Van Craeyveld, U. Holopainen, E. Selinheimo, K. Poutanen, J. A. Delcour, and C. M. Courtin, "Extensive dry ball milling of wheat and rye bran leads to *in situ* production of arabinoxylan oligosaccharides through nanoscale fragmentation," *Journal of Agricultural and Food Chemistry*, vol. 57, no. 18, pp. 8467–8473, 2009.

[43] A. A. Andersson, R. Andersson, A. Jonsäll, J. Andersson, and H. Fredriksson, "Effect of different extrusion parameters on dietary fiber in wheat bran and rye bran," *Journal of Food Science*, vol. 82, no. 6, pp. 1344–1350, 2017.

[44] S. Karppinen, K. Kiiliäinen, K. Liukkonen, P. Forssell, and K. Poutanen, "Extraction and *in vitro* fermentation of rye bran fractions," *Journal of Cereal Science*, vol. 34, no. 3, pp. 269–278, 2001.

[45] H. J. Gilbert, H. Stålbrand, and H. Brumer, "How the walls come crumbling down: recent structural biochemistry of plant polysaccharide degradation," *Current Opinion in Plant Biology*, vol. 11, no. 3, pp. 338–348, 2008.

[46] J. A. Linares-Pastén, M. Andersson, and E. Nordberg Karlsson, "Thermostable Glycoside Hydrolases in Biorefinery Technologies," *Current Biotechnology*, vol. 3, no. 1, pp. 26–44, 2014.

[47] K. Van Laere, G. Beldman, and A. Voragen, "A new arabinofuranohydrolase from *Bifidobacterium adolescentis* able to remove arabinosyl residues from double-substituted xylose units in arabinoxylan," *Applied Microbiology and Biotechnology*, vol. 47, no. 3, pp. 231–235, 1997.

[48] R. Fauré, C. M. Courtin, J. A. Delcour, C. Dumon, C. B. Faulds, G. B. Fincher, S. Fort, S. C. Fry, S. Halila, M. A. Kabel *et al.*, "A brief and informationally rich naming system for oligosaccharide motifs of heteroxylans found in plant cell walls," *Australian Journal of Chemistry*, vol. 62, no. 6, pp. 533–537, 2009.

[49] E. de Jong, A. Higson, P. Walsh, M. Wellisch *et al.*, "Bio-based chemicals value added products from biorefineries," *IEA Bioenergy, Task42 Biorefinery*, 2012.

[50] M. Vazquez, J. Alonso, H. Domınguez, and J. Parajo, "Xylooligosaccharides: manufacture and applications," *Trends in Food Science & Technology*, vol. 11, no. 11, pp. 387–393, 2000.

[51] Z. Zhang, C. Smith, and W. Li, "Extraction and modification technology of arabinoxylans from cereal by-products: A critical review," *Food Research International*, vol. 65, pp. 423–436, 2014.

[52] J. S. Kim, Y. Lee, and T. H. Kim, "A review on alkaline pretreatment technology for bioconversion of lignocellulosic biomass," *Bioresource Technology*, vol. 199, pp. 42–48, 2016.

[53] M. Aguedo, C. Fougnies, M. Dermience, and A. Richel, "Extraction by three processes of arabinoxylans from wheat bran and characterization of the fractions obtained," *Carbohydrate Polymers*, vol. 105, pp. 317–324, 2014.

[54] G. Garrote, H. Dominguez, and J. Parajo, "Hydrothermal processing of lignocellulosic materials," *European Journal of Wood and Wood Products*, vol. 57, no. 3, pp. 191–202, 1999.

[55] D. J. Rose and G. E. Inglett, "Production of feruloylated arabinoxylo-oligosaccharides from maize (*Zea mays*) bran by microwave-assisted autohydrolysis," *Food Chemistry*, vol. 119, no. 4, pp. 1613 – 1618, 2010.

[56] M. Kataoka, J. Wiboonsirikul, Y. Kimura, and S. Adachi, "Properties of extracts from wheat bran by subcritical water treatment," *Food Science and Technology Research*, vol. 14, no. 6, pp. 553–556, 2008.

[57] A. A. Roos, T. Persson, H. Krawczyk, G. Zacchi, and H. Stålbrand, "Extraction of water-soluble hemicelluloses from barley husks," *Bioresource Technology*, vol. 100, no. 2, pp. 763–769, 2009.

[58] M.-C. Figueroa-Espinoza, C. Poulsen, J. Borch Søe, M. R. Zargahi, and X. Rouau, "Enzymatic solubilization of arabinoxylans from native, extruded, and high-shear-treated rye bran by different endo-xylanases and other hydrolyzing enzymes," *Journal of Agricultural and Food Chemistry*, vol. 52, no. 13, pp. 4240–4249, 2004.

[59] C. Maes, B. Vangeneugden, and J. Delcour, "Relative activity of two endoxylanases towards water-unextractable arabinoxylans in wheat bran," *Journal of Cereal Science*, vol. 39, no. 2, pp. 181–186, 2004.

[60] J. Beaugrand, G. Chambat, V. W. Wong, F. Goubet, C. Rémond, G. Paës, S. Benamrouche, P. Debeire, M. O'Donohue, and B. Chabbert, "Impact and efficiency of GH10 and GH11 thermostable endoxylanases on wheat bran and alkali-extractable arabinoxylans," *Carbohydrate Research*, vol. 339, no. 15, pp. 2529–2540, 2004.

[61] H. Goesaert, G. Elliott, P. A. Kroon, K. Gebruers, C. M. Courtin, J. Robben, J. A. Delcour, and N. Juge, "Occurrence of proteinaceous endoxylanase inhibitors in cereals," *Biochimica et Biophysica Acta (BBA)-Proteins and Proteomics*, vol. 1696, no. 2, pp. 193–202, 2004.

[62] F. Payan, P. Leone, S. Porciero, C. Furniss, T. Tahir, G. Williamson, A. Durand, P. Manzanares, H. J. Gilbert, N. Juge, and A. Roussel, "The Dual Nature of the Wheat Xylanase Protein Inhibitor XIP-I: Structural Basis for the Inhibition of Family 10 and Family 11 Xylanases," *Journal of Biological Chemistry*, vol. 279, no. 34, pp. 36 029–36 037, 2004.

[63] C. Courtin and J. Delcour, "Relative activity of endoxylanases towards water-extractable and water-unextractable arabinoxylan," *Journal of Cereal Science*, vol. 33, no. 3, pp. 301–312, 2001.

[64] V. Van Craeyveld, K. Swennen, E. Dornez, T. Van de Wiele, M. Marzorati, W. Verstraete, Y. Delaedt, O. Onagbesan, E. Decuypere, J. Buyse *et al.*, "Structurally Different Wheat-Derived Arabinoxylooligosaccharides have Different Prebiotic and Fermentation Rroperties in Rats," *The Journal of Nutrition*, vol. 138, no. 12, pp. 2348–2355, 2008.

[65] J. Snelders, H. Olaerts, E. Dornez, T. V. de Wiele, A.-M. Aura, L. Vanhaecke, J. A. Delcour, and C. M. Courtin, "Structural features and feruloylation modulate the fermentability and evolution of antioxidant properties of arabinoxylan-oligosaccharides during in vitro fermentation by human gut derived microbiota," *Journal of Functional Foods*, vol. 10, pp. 1–12, 2014.

[66] A. Pollet, J. A. Delcour, and C. M. Courtin, "Structural determinants of the substrate specificities of xylanases from different glycoside hydrolase families," *Critical Reviews in Biotechnology*, vol. 30, no. 3, pp. 176–191, 2010.

[67] M. A. S. Correia, K. Mazumder, J. L. A. Brás, S. J. Firbank, Y. Zhu, R. J. Lewis, W. S. York, C. M. G. A. Fontes, and H. J. Gilbert, "Structure and Function of

an Arabinoxylan-specific Xylanase," *Journal of Biological Chememistry*, vol. 286, no. 25, pp. 22 510–22 520, 2011.

[68] M. C. Gray, A. O. Converse, and C. E. Wyman, "Solubilities of Oligomer Mixtures Produced by the Hydrolysis of Xylans and Corn Stover in Water at 180 °C," *Industrial & Engineering Chemistry Research*, vol. 46, no. 8, pp. 2383–2391, 2007.

[69] L. Viikari, M. Alapuranen, T. Puranen, J. Vehmaanperä, and M. Siika-aho, *Thermostable Enzymes in Lignocellulose Hydrolysis*. Berlin, Heidelberg: Springer Berlin Heidelberg, 2007, pp. 121–145.

[70] C. Vieille and G. J. Zeikus, "Hyperthermophilic Enzymes: Sources, Uses, and Molecular Mechanisms for Thermostabilitys," *Microbiology and Molecular Biology Reviews*, vol. 65, no. 1, pp. 1–43, 2001.

[71] E. Nordberg Karlsson, L. Dahlberg, N. Torto, L. Gorton, and O. Holst, "Enzymatic specificity and hydrolysis pattern of the catalytic domain of the xylanase Xyn1 from *Rhodothermus marinus*," *Journal of Biotechnology*, vol. 60, no. 1, pp. 23–35, 1998.

[72] S. R. Andrews, E. J. Taylor, G. Pell, F. Vincent, V. M.-A. Ducros, G. J. Davies, J. H. Lakey, and H. J. Gilbert, "The Use of Forced Protein Evolution to Investigate and Improve Stability of Family 10 Xylanases: The Production of Ca^{2+}-independent Stable Xylanases," *Journal of Biological Chemistry*, vol. 279, no. 52, pp. 54 369–54 379, 2004.

[73] Ó. Gallardo, F. I. J. Pastor, J. Polaina, P. Diaz, R. Łysek, P. Vogel, P. Isorna, B. González, and J. Sanz-Aparicio, "Structural Insights into the Specificity of Xyn10B from *Paenibacillus barcinonensis* and Its Improved Stability by Forced Protein Evolution," *Journal of Biological Chemistry*, vol. 285, no. 4, pp. 2721–2733, 2010.

[74] D. L. Zechel and S. G. Withers, "Glycosidase mechanisms: anatomy of a finely tuned catalyst," *Accounts of Chemical Research*, vol. 33, no. 1, pp. 11–18, 2000.

[75] G. J. Davies, K. S. Wilson, and B. Henrissat, "Nomenclature for sugar-binding subsites in glycosyl hydrolases," *Biochemical Journal*, vol. 321, no. 2, pp. 557–559, 1997.

[76] H. Aspeborg, P. M. Coutinho, Y. Wang, H. Brumer, and B. Henrissat, "Evolution, substrate specificity and subfamily classification of glycoside hydrolase family 5 (GH5)," *BMC Evolutionary Biology*, vol. 12, no. 186, 2012.

[77] F. J. St John, J. M. González, and E. Pozharski, "Consolidation of glycosyl hydrolase family 30: A dual domain 4/7 hydrolase family consisting of two structurally distinct groups," *FEBS Letters*, vol. 584, no. 21, pp. 4435–4441, 2010.

[78] K. Mewis, N. Lenfant, V. Lombard, and B. Henrissat, "Dividing the Large Glycoside Hydrolase Family 43 into Subfamilies: a Motivation for Detailed Enzyme Characterization," *Applied and Environmental Microbiology*, vol. 82, no. 6, pp. 1686–1692, 2016.

[79] A. Canals, M. C. Vega, F. X. Gomis-Rüth, M. Díaz, R. o. I. Santamaria, and M. Coll, "Structure of xylanase Xys1Δ from *Streptomyces halstedii*," *Acta Crystallographica Section D: Biological Crystallography*, vol. 59, no. 8, pp. 1447–1453, 2003.

[80] Y. Chu, T. Tu, L. Penttinen, X. Xue, X. Wang, Z. Yi, L. Gong, J. Rouvinen, H. Luo, N. Hakulinen *et al.*, "Insights into the roles of non-catalytic residues in the active site of a GH10 xylanase with activity on cellulose," *Journal of Biological Chemistry*, vol. 292, no. 47, pp. 19 315–19 327, 2017.

[81] A. Schmidt, G. M. Gübitz, and C. Kratky, "Xylan binding subsite mapping in the xylanase from *Penicillium simplicissimum* using xylooligosaccharides as cryo-protectant," *Biochemistry*, vol. 38, no. 8, pp. 2403–2412, 1999.

[82] G. Pell, L. Szabo, S. J. Charnock, H. Xie, T. M. Gloster, G. J. Davies, and H. J. Gilbert, "Structural and biochemical analysis of *Cellvibrio japonicus* xylanase 10C how variation in substrate-binding cleft influences the catalytic profile of family GH-10 xylanases," *Journal of Biological Chemistry*, vol. 279, no. 12, pp. 11 777–11 788, 2004.

[83] A. White, D. Tull, K. Johns, S. G. Withers, and D. R. Rose, "Crystallographic observation of a covalent catalytic intermediate in a β-glycosidase," *Nature Structural Biology*, vol. 3, no. 2, pp. 149–154, 1996.

[84] L. Lo Leggio, J. Jenkins, G. Harris, and R. Pickersgill, "X-Ray Crystallographic Study of Xylopentaose Binding to *Pseudomonas fluorescens* Xylanase A," *Proteins: Structure, Function, and Bioinformatics*, vol. 41, no. 3, pp. 362–373, 2000.

[85] L. Lo Leggio, S. Kalogiannis, K. Eckert, S. C. Teixeira, M. K. Bhat, C. Andrei, R. W. Pickersgill, and S. Larsen, "Substrate specificity and subsite mobility in *T. aurantiacus* xylanase 10A," *FEBS Letters*, vol. 509, no. 2, pp. 303–308, 2001.

[86] K. Manikandan, A. Bhardwaj, N. Gupta, N. K. Lokanath, A. Ghosh, V. S. Reddy, and S. Ramakumar, "Crystal structures of native and xylosaccharide-bound alkali thermostable xylanase from an alkalophilic *Bacillus* sp. NG-27:

Structural insights into alkalophilicity and implications for adaptation to poly-extreme conditions," *Protein Science*, vol. 15, no. 8, pp. 1951–1960, 2006.

[87] G. Zolotnitsky, U. Cogan, N. Adir, V. Solomon, G. Shoham, and Y. Shoham, "Mapping glycoside hydrolase substrate subsites by isothermal titration calorimetry," *Proceedings of the National Academy of Sciences*, vol. 101, no. 31, pp. 11 275–11 280, 2004.

[88] C. R. Santos, Z. B. Hoffmam, V. P. de Matos Martins, L. M. Zanphorlin, L. H. de Paula Assis, R. V. Honorato, P. S. L. de Oliveira, R. Ruller, and M. T. Murakami, "Molecular Mechanisms Associated with Xylan Degradation by *Xanthomonas* Plant Pathogens," *Journal of Biological Chemistry*, vol. 289, no. 46, pp. 32 186–32 200, 2014.

[89] K. C. Morgan, J. L. Wright, and F. Simpson, "Review of Chemical Constituents of the Red Alga *Palmaria palmata* (Dulse)," *Economic Botany*, vol. 34, no. 1, pp. 27–50, 1980.

[90] Y. Yamamoto, H. Kishimura, Y. Kinoshita, W. Saburi, Y. Kumagai, H. Yasui, and T. Ojima, "Enzymatic production of xylooligosaccharides from red alga dulse (*Palmaria* sp.) wasted in Japan," *Process Biochemistry*, vol. 82, pp. 117–122, 2019.

[91] S. Yoshida, I. Kusakabe, N. Matsuo, K. Shimizu, T. Yasui, and K. Murakami, "Structure of rice-straw arabinoglucuronoxylan and specificity of *Streptomyces* xylanase toward the xylan," *Agricultural and Biological Chemistry*, vol. 54, no. 2, pp. 449–457, 1990.

[92] J. Zhang, M. Siika-aho, T. Puranen, M. Tang, M. Tenkanen, and L. Viikari, "Thermostable recombinant xylanases from *Nonomuraea flexuosa* and *Thermoascus aurantiacus* show distinct properties in the hydrolysis of xylans and pretreated wheat straw," *Biotechnology for Biofuels*, vol. 4, no. 12, 2011.

[93] M.-H. Beylot, V. A. McKie, A. G. Voragen, C. H. Doeswijk-Voragen, and H. J. Gilbert, "The *Pseudomonas cellulosa* glycoside hydrolase family 51 arabinofuranosidase exhibits wide substrate specificity," *Biochemical Journal*, vol. 358, no. 3, pp. 607–614, 2001.

[94] L. A. van den Broek, R. M. Lloyd, G. Beldman, J. C. Verdoes, B. V. McCleary, and A. G. Voragen, "Cloning and characterization of arabinoxylan arabinofuranohydrolase-D3 (AXHd3) from *Bifidobacterium adolescentis* DSM20083," *Applied Microbiology and Biotechnology*, vol. 67, no. 5, pp. 641–647, 2005.

[95] B. V. McCleary, V. A. McKie, A. Draga, E. Rooney, D. Mangan, and J. Larkin, "Hydrolysis of wheat flour arabinoxylan, acid-debranched wheat flour arabinoxylan and arabino-xylo-oligosaccharides by β-xylanase, α-L-arabinofuranosidase and β-xylosidase," *Carbohydrate Research*, vol. 407, pp. 79–96, 2015.

[96] F. J. Kormelink, H. Gruppen, R. J. Viëtor, and A. G. Voragen, "Mode of action of the xylan-degrading enzymes from *Aspergillus awamori* on alkali-extractable cereal arabinoxylans," *Carbohydrate Research*, vol. 249, no. 2, pp. 355–367, 1993.

[97] M. Kabel, F. Carvalheiro, G. Garrote, E. Avgerinos, E. Koukios, J. Parajó, F. Gírio, H. Schols, and A. Voragen, "Hydrothermally treated xylan rich by-products yield different classes of xylo-oligosaccharides," *Carbohydrate Polymers*, vol. 50, no. 1, pp. 47–56, 2002.

[98] A. Törrönen, A. Harkki, and J. Rouvinen, "Three-dimensional structure of endo-1, 4-beta-xylanase II from *Trichoderma reesei*: two conformational states in the active site," *The EMBO Journal*, vol. 13, no. 11, pp. 2493–2501, 1994.

[99] G. Paës, J.-G. Berrin, and J. Beaugrand, "GH11 xylanases: structure/function/properties relationships and applications," *Biotechnology Advances*, vol. 30, no. 3, pp. 564–592, 2012.

[100] K. Gruber, G. Klintschar, M. Hayn, A. Schlacher, W. Steiner, and C. Kratky, "Thermophilic xylanase from *Thermomyces lanuginosus*: High-resolution X-ray structure and modeling studies," *Biochemistry*, vol. 37, no. 39, pp. 13 475–13 485, 1998.

[101] A. Torronen and J. Rouvinen, "Structural comparison of two major endo-1, 4-xylanases from *Trichoderma reesei*," *Biochemistry*, vol. 34, no. 3, pp. 847–856, 1995.

[102] G. Paës, V. Tran, M. Takahashi, I. Boukari, and M. J. O'Donohue, "New insights into the role of the thumb-like loop in GH-11 xylanases," *Protein Engineering, Design & Selection*, vol. 20, no. 1, pp. 15–23, 2007.

[103] A. Pollet, E. Vandermarliere, J. Lammertyn, S. V. Strelkov, J. A. Delcour, and C. M. Courtin, "Crystallographic and activity-based evidence for thumb flexibility and its relevance in glycoside hydrolase family 11 xylanases," *Proteins: Structure, Function and Bioinformatics*, vol. 77, no. 2, pp. 395–403, 2009.

[104] G. Paës, J. Cortés, T. Siméon, M. J. O'Donohue, and V. Tran, "Thumb-loops up for catalysis: a structure/function investigation of a functional loop movement in a GH11 xylanase," *Computational and Structural Biotechnology Journal*, vol. 1, no. 2, 2012.

[105] M. Vardakou, C. Dumon, J. W. Murray, P. Christakopoulos, D. P. Weiner, N. Juge, R. J. Lewis, H. J. Gilbert, and J. E. Flint, "Understanding the structural basis for substrate and inhibitor recognition in eukaryotic GH11 xylanases," *Journal of Molecular Biology*, vol. 375, no. 5, pp. 1293–1305, 2008.

[106] M. Schooneveld-Bergmans, G. Beldman, and A. Voragen, "Structural features of (glucurono) arabinoxylans extracted from wheat bran by barium hydroxide," *Journal of Cereal Science*, vol. 29, no. 1, pp. 63–75, 1999.

[107] A. B. Boraston, D. N. Bolam, H. J. Gilbert, and G. J. Davies, "Carbohydrate-binding modules: fine-tuning polysaccharide recognition," *Biochemical Journal*, vol. 382, no. 3, pp. 769–781, 2004.

[108] D.-D. Meng, Y. Ying, X.-H. Chen, M. Lu, K. Ning, L.-S. Wang, and F.-L. Li, "Distinct roles for carbohydrate-binding modules of glycoside hydrolase 10 (GH10) and GH11 xylanases from *Caldicellulosiruptor* sp. strain F32 in thermostability and catalytic efficiency," *Applied Environmental Microbiology*, vol. 81, no. 6, pp. 2006–2014, 2015.

[109] Z. Fujimoto, A. Kuno, S. Kaneko, S. Yoshida, H. Kobayashi, I. Kusakabe, and H. Mizuno, "Crystal structure of *Streptomyces olivaceoviridis* E-86 β-xylanase containing xylan-binding domain," *Journal of Molecular Biology*, vol. 300, no. 3, pp. 575–585, 2000.

[110] S. Najmudin, B. A. Pinheiro, J. A. Prates, H. J. Gilbert, M. J. Romão, and C. M. Fontes, "Putting an N-terminal end to the *Clostridium thermocellum* xylanase Xyn10B story: Crystal structure of the CBM22-1–GH10 modules complexed with xylohexaose," *Journal of Structural Biology*, vol. 172, no. 3, pp. 353–362, 2010.

[111] M. Zhang, J. R. Chekan, D. Dodd, P.-Y. Hong, L. Radlinski, V. Revindran, S. K. Nair, R. I. Mackie, and I. Cann, "Xylan utilization in human gut commensal bacteria is orchestrated by unique modular organization of polysaccharide-degrading enzymes," *Proceedings of the National Academy of Sciences*, vol. 111, no. 35, pp. E3708–E3717, 2014.

[112] J. Zhang, U. Moilanen, M. Tang, and L. Viikari, "The carbohydrate-binding module of xylanase from *Nonomuraea flexuosa* decreases its non-productive adsorption on lignin," *Biotechnology for Biofuels*, vol. 6, no. 18, 2013.

[113] E. Nordberg Karlsson, E. Bartonek-Roxå, and O. Holst, "Cloning and sequence of a thermostable multidomain xylanase from the bacterium *Rhodothermus marinus*," *Biochimica et Biophysica Acta (BBA)-Gene Structure and Expression*, vol. 1353, no. 2, pp. 118–124, 1997.

[114] E. Nordberg Karlsson, M. Abou Hachem, S. Ramchuran, H. Costa, O. Holst, Å. F. Svenningsen, and G. O. Hreggvidsson, "The modular xylanase Xyn10A from *Rhodothermus marinus* is cell-attached, and its C-terminal domain has several putative homologues among cell-attached proteins within the phylum Bacteroidetes," *FEMS Microbiology Letters*, vol. 241, no. 2, pp. 233–242, 2004.

[115] M. Abou Hachem, E. Nordberg Karlsson, E. Bartonek-Roxå, S. Raghothama, P. J. Simpson, H. J. Gilbert, M. P. Williamson, and O. Holst, "Carbohydrate-binding modules from a thermostable *Rhodothermus marinus* xylanase: cloning, expression and binding studies," *Biochemical Journal*, vol. 345, no. 1, pp. 53–60, 2000.

[116] M. Abou Hachem, F. Olsson, and E. Nordberg Karlsson, "Probing the stability of the modular family 10 xylanase from *Rhodothermus marinus*," *Extremophiles*, vol. 7, no. 6, pp. 483–491, 2003.

[117] P. J. Simpson, S. J. Jamieson, M. Abou Hachem, E. Nordberg Karlsson, H. J. Gilbert, O. Holst, and M. P. Williamson, "The solution structure of the CBM4-2 carbohydrate binding module from a thermostable *Rhodothermus marinus* xylanase," *Biochemistry*, vol. 41, no. 18, pp. 5712–5719, 2002.

[118] A. C. Ouwehand, P. V. Kirjavainen, C. Shortt, and S. Salminen, "Probiotics: mechanisms and established effects," *International Dairy Journal*, vol. 9, no. 1, pp. 43–52, 1999.

[119] M. Saarela, G. Mogensen, R. Fondén, J. Mättö, and T. Mattila-Sandholm, "Probiotic bacteria: safety, functional and technological properties," *Journal of Biotechnology*, vol. 84, no. 3, pp. 197–215, 2000.

[120] K. R. Pandey, S. R. Naik, and B. V. Vakil, "Probiotics, prebiotics and synbiotics-a review," *Journal of Food Science and Technology*, vol. 52, no. 12, pp. 7577–7587, 2015.

[121] M. Kleerebezem and E. E. Vaughan, "Probiotic and Gut Lactobacilli and Bifidobacteria: Molecular Approaches to Study Diversity and Activity," *Annual Review of Microbiology*, vol. 63, pp. 269–290, 2009.

[122] S. Fijan, "Microorganisms with claimed probiotic properties: an overview of recent literature," *International Journal of Environmental Research and Public Health*, vol. 11, no. 5, pp. 4745–4767, 2014.

[123] H. D. Holscher, "Dietary fiber and prebiotics and the gastrointestinal microbiota," *Gut Microbes*, vol. 8, no. 2, pp. 172–184, 2017.

[124] B. L. Cantarel, V. Lombard, and B. Henrissat, "Complex Carbohydrate Utilization by the Healthy Human Microbiome," *PLOS ONE*, vol. 7, no. 6, 2012.

[125] J. Qin, R. Li, J. Raes, M. Arumugam, K. S. Burgdorf, C. Manichanh, T. Nielsen, N. Pons, F. Levenez, T. Yamada *et al.*, "A human gut microbial gene catalogue established by metagenomic sequencing," *Nature*, vol. 464, pp. 59–67, 2010.

[126] G. R. Gibson, H. M. Probert, J. V. Loo, R. A. Rastall, and M. B. Roberfroid, "Dietary modulation of the human colonic microbiota: updating the concept of prebiotics," *Nutrition Research Reviews*, vol. 17, no. 2, pp. 259–275, 2004.

[127] A. Rivière, M. Selak, D. Lantin, F. Leroy, and L. De Vuyst, "*Bifidobacteria* and Butyrate-Producing Colon Bacteria: Importance and Strategies for Their Stimulation in the Human Gut," *Frontiers in Microbiology*, vol. 7, no. 979, 2016.

[128] M. Vardakou, C. N. Palop, M. Gasson, A. Narbad, and P. Christakopoulos, "*In vitro* three-stage continuous fermentation of wheat arabinoxylan fractions and induction of hydrolase activity by the gut microflora," *International Journal of Biological Macromolecules*, vol. 41, no. 5, pp. 584–589, 2007.

[129] D. J. Rose, J. A. Patterson, and B. R. Hamaker, "Structural Differences among Alkali-Soluble Arabinoxylans from Maize (*Zea mays*), Rice (*Oryza sativa*), and Wheat (*Triticum aestivum*) Brans Influence Human Fecal Fermentation Profiles," *Journal of Agricultural and Food Chemistry*, vol. 58, no. 1, pp. 493–499, 2010.

[130] P. Rumpagaporn, B. L. Reuhs, A. Kaur, J. A. Patterson, A. Keshavarzian, and B. R. Hamaker, "Structural features of soluble cereal arabinoxylan fibers associated with a slow rate of *in vitro* fermentation by human fecal microbiota," *Carbohydrate Polymers*, vol. 130, pp. 191–197, 2015.

[131] J. Xu, M. K. Bjursell, J. Himrod, S. Deng, L. K. Carmichael, H. C. Chiang, L. V. Hooper, and J. I. Gordon, "A Genomic View of the Human-*Bacteroides thetaiotaomicron* Symbiosis," *Science*, vol. 299, no. 5615, pp. 2074–2076, 2003.

[132] C. Chassard, V. Goumy, M. Leclerc, C. Del'homme, and A. Bernalier-Donadille, "Characterization of the xylan-degrading microbial community from human faeces," *FEMS microbiology ecology*, vol. 61, no. 1, pp. 121–131, 2007.

[133] D. Dodd, R. I. Mackie, and I. K. Cann, "Xylan degradation, a metabolic property shared by rumen and human colonic Bacteroidetes," *Molecular Microbiology*, vol. 79, no. 2, pp. 292–304, 2011.

[134] E. C. Martens, N. M. Koropatkin, T. J. Smith, and J. I. Gordon, "Complex glycan catabolism by the human gut microbiota: the Bacteroidetes Sus-like paradigm," *Journal of Biological Chemistry*, vol. 284, no. 37, pp. 24 673–24 677, 2009.

[135] M. L. Leth, M. Ejby, C. Workman, D. A. Ewald, S. S. Pedersen, C. Sternberg, M. I. Bahl, T. R. Licht, F. L. Aachmann, B. Westereng, and M. Abou Hachem, "Differential bacterial capture and transport preferences facilitate co-growth on dietary xylan in the human gut," *Nature microbiology*, vol. 3, no. 5, pp. 570–580, 2018.

[136] A. Rivière, F. Moens, M. Selak, D. Maes, S. Weckx, and L. De Vuyst, "The Ability of Bifidobacteria To Degrade Arabinoxylan Oligosaccharide Constituents and Derived Oligosaccharides Is Strain Dependent," *Applied Environmental Microbiology*, vol. 80, no. 1, pp. 204–217, 2014.

[137] O. Gilad, S. Jacobsen, B. Stuer-Lauridsen, M. B. Pedersen, C. Garrigues, and B. Svensson, "Combined transcriptome and proteome analysis of *Bifidobacterium animalis* subsp. lactis BB-12 grown on xylo-oligosaccharides and a model of their utilization," *Applied and Environmental Microbiology*, vol. 76, no. 21, pp. 7285–7291, 2010.

[138] J. M. Andersen, R. Barrangou, M. Abou Hachem, S. J. Lahtinen, Y. J. Goh, B. Svensson, and T. R. Klaenhammer, "Transcriptional analysis of oligosaccharide utilization by *Bifidobacterium lactis* Bl-04," *BMC Genomics*, vol. 14, no. 312, 2013.

[139] M. Ejby, F. Fredslund, A. Vujicic-Zagar, B. Svensson, D. J. Slotboom, and M. Abou Hachem, "Structural basis for arabinoxylo-oligosaccharide capture by the probiotic *Bifidobacterium animalis* subsp. lactis Bl-04," *Molecular Microbiology*, vol. 90, no. 5, pp. 1100–1112, 2013.

[140] K. Pokusaeva, G. F. Fitzgerald, and D. van Sinderen, "Carbohydrate metabolism in Bifidobacteria," *Genes & Nutrition*, vol. 6, no. 3, pp. 285–306, 2011.

[141] K. M. J. Van Laere, R. Hartemink, M. Bosveld, H. A. Schols, and A. G. J. Voragen, "Fermentation of Plant Cell Wall Derived Polysaccharides and Their Corresponding Oligosaccharides by Intestinal Bacteria," *Journal of Agricultural and Food Chemistry*, vol. 48, no. 5, pp. 1644–1652, 2000.

[142] D. B. Jordan, K. Wagschal, A. A. Grigorescu, and J. D. Braker, "Highly active β-xylosidases of glycoside hydrolase family 43 operating on natural and artificial substrates," *Applied Microbiology and Biotechnology*, vol. 97, no. 10, pp. 4415–4428, 2013.

[143] A. Martinez-Murcia and M. Collins, "A phylogenetic analysis of the genus *Leuconostoc* based on reverse transcriptase sequencing of 16 S rRNA," *FEMS Microbiology Letters*, vol. 70, no. 1, pp. 73–83, 1990.

[144] A. Martinez-Murcia, N. Harland, and M. Collins, "Phylogenetic analysis of some leuconostocs and related organisms as determined from large-subunit rRNA gene sequences: assessment of congruence of small-and large-subunit rRNA derived trees," *The Journal of Applied Bacteriology*, vol. 74, no. 5, pp. 532–541, 1993.

[145] M. Collins, J. Samelis, J. Metaxopoulos, and S. Wallbanks, "Taxonomic studies on some leuconostoc-like organisms from fermented sausages: description of a new genus *Weissella* for the *Leuconostoc paramesenteroides* group of species," *Journal of Applied Bacteriology*, vol. 75, no. 6, pp. 595–603, 1993.

[146] A. Patel, C. Lindström, A. Patel, J. Prajapati, and O. Holst, "Probiotic properties of exopolysaccharide producing lactic acid bacteria isolated from vegetables and traditional Indian fermented foods," *International Journal of Fermented Foods*, vol. 1, no. 1, pp. 87–101, 2012.

[147] P. Falck, J. A. Linares-Pastén, P. Adlercreutz, and E. Nordberg Karlsson, "Characterization of a family 43 β-xylosidase from the xylooligosaccharide utilizing putative probiotic *Weissella* sp. strain 92." *Glycobiology*, vol. 26, no. 2, pp. 193–202, 2016.

[148] J. A. Linares-Pastén, P. Falck, K. Albasri, S. Kjellström, P. Adlercreutz, D. T. Logan, and E. Nordberg Karlsson, "Three-dimensional structures and functional studies of two GH43 arabinofuranosidases from *Weissella* sp. strain 142 and *Lactobacillus brevis*," *The FEBS Journal*, vol. 284, no. 13, pp. 2019–2036, 2017.

[149] Y. Shi, J. Liu, Q. Yan, X. You, S. Yang, and Z. Jiang, "*In vitro* digestibility and prebiotic potential of curdlan (1 → 3)-β-D-glucan oligosaccharides in *Lactobacillus* species," *Carbohydrate Polymers*, vol. 188, pp. 17–26, 2018.

[150] R. R. Sardari and E. Nordberg Karlsson, "Marine poly-and oligosaccharides as prebiotics," *Journal of Agricultural and Food Chemistry*, vol. 66, no. 44, pp. 11 544–11 549, 2018.

[151] T. Immerstrand, C. J. Paul, A. Rosenquist, S. Deraz, O. B. Mårtensson, Å. Ljungh, A. Blücher, R. Öste, O. Holst, and E. Nordberg Karlsson, "Characterization of the properties of *Pediococcus parvulus* for probiotic or protective culture use," *Journal of Food Protection*, vol. 73, no. 5, pp. 960–966, 2010.

[152] M. E. Fraunhofer, A. J. Geissler, D. Wefers, M. Bunzel, F. Jakob, and R. F. Vogel, "Characterization of β-glucan formation by *Lactobacillus brevis* TMW 1.2112 isolated from slimy spoiled beer," *International Journal of Biological Macromolecules*, vol. 107, pp. 874–881, 2018.

[153] M. Mcintosh, B. Stone, and V. Stanisich, "Curdlan and other bacterial (1 → 3)-β-D-glucans," *Applied Microbiology and Biotechnology*, vol. 68, no. 2, pp. 163–173, 2005.

[154] M. Abou Hachem, J. M. Andersen, R. Barrangou, M. S. Møller, F. Fredslund, A. Majumder, M. Ejby, S. J. Lahtinen, S. Jacobsen, L. Lo Leggio *et al.*, "Recent insight into oligosaccharide uptake and metabolism in probiotic bacteria," *Biocatalysis and Biotransformation*, vol. 31, no. 4, pp. 226–235, 2013.

[155] E. Krieger, S. B. Nabuurs, and G. Vriend, *Homology Modeling*. John Wiley & Sons, Ltd, 2005, ch. 25, pp. 509–523.

[156] E. Krieger and G. Vriend, "YASARA View—molecular graphics for all devices—from smartphones to workstations," *Bioinformatics*, vol. 30, no. 20, pp. 2981–2982, 2014.

[157] E. Krieger, K. Joo, J. Lee, J. Lee, S. Raman, J. Thompson, M. Tyka, D. Baker, and K. Karplus, "Improving physical realism, stereochemistry, and side-chain accuracy in homology modeling: four approaches that performed well in CASP8," *Proteins: Structure, Function, and Bioinformatics*, vol. 77, no. S9, pp. 114–122, 2009.

[158] S. F. Altschul, T. L. Madden, A. A. Schäffer, J. Zhang, Z. Zhang, W. Miller, and D. J. Lipman, "Gapped BLAST and PSI-BLAST: a new generation of protein database search programs," *Nucleic Acids Research*, vol. 25, no. 17, pp. 3389–3402, 1997.

[159] R. D. King and M. J. Sternberg, "Identification and application of the concepts important for accurate and reliable protein secondary structure prediction," *Protein Science*, vol. 5, no. 11, pp. 2298–2310, 1996.

[160] J. Qiu and R. Elber, "SSALN: An alignment algorithm using structure-dependent substitution matrices and gap penalties learned from structurally aligned protein pairs," *Proteins: Structure, Function, and Bioinformatics*, vol. 62, no. 4, pp. 881–891, 2006.

[161] Č. Venclovas, A. Zemla, K. Fidelis, and J. Moult, "Some measures of comparative performance in the three CASPs," *Proteins: Structure, Function, and Bioinformatics*, vol. 37, no. S3, pp. 231–237, 1999.

[162] E. F. Pettersen, T. D. Goddard, C. C. Huang, G. S. Couch, D. M. Greenblatt, E. C. Meng, and T. E. Ferrin, "UCSF Chimera - A visualization system for exploratory research and analysis," *Journal of Computational Chemistry*, vol. 25, no. 13, pp. 1605–1612, 2004.

[163] J. Bowie, R. Luthy, and D. Eisenberg, "A method to identify protein sequences that fold into a known three-dimensional structure," *Science*, vol. 253, no. 5016, pp. 164–170, 1991.

[164] R. Lüthy, J. U. Bowie, and D. Eisenberg, "Assessment of protein models with three-dimensional profiles," *Nature*, vol. 356, no. 6364, pp. 83–85, 1992.

[165] G. T. Ramachandran and V. Sasisekharan, "Conformation of polypeptides and proteins," in *Advances in Protein Chemistry*. Elsevier, 1968, vol. 23, pp. 283–437.

[166] R. A. Laskowski, M. W. MacArthur, D. S. Moss, and J. M. Thornton, "PROCHECK: a program to check the stereochemical quality of protein structures," *Journal of Applied Crystallography*, vol. 26, no. 2, pp. 283–291, 1993.

[167] M. Wiederstein and M. J. Sippl, "ProSA-web: interactive web service for the recognition of errors in three-dimensional structures of proteins," *Nucleic Acids Research*, vol. 35, no. suppl_2, pp. W407–W410, 2007.

[168] R. W. W. Hooft, G. Vriend, C. Sander, and E. E. Abola, "Errors in protein structures," *Nature*, vol. 381, no. 6580, pp. 272–272, 1996.

[169] C. Colovos and T. O. Yeates, "Verification of protein structures: patterns of nonbonded atomic interactions," *Protein Science*, vol. 2, no. 9, pp. 1511–1519, 1993.

[170] F. Melo, D. Devos, E. Depiereux, and E. Feytmans, "ANOLEA: a www server to assess protein structures," in *ISMB*, vol. 5, 1997, pp. 187–190.

[171] D. E. Stewart, A. Sarkar, and J. E. Wampler, "Occurrence and Role of *Cis* Peptide Bonds in Protein Structures," *Journal of Molecular Biology*, vol. 214, no. 1, pp. 253–260, 1990.

[172] H. M. Berman, P. E. Bourne, J. Westbrook, and C. Zardecki, "The Protein Data Bank," in *Protein Structure*. CRC Press, 2003, pp. 394–410.

[173] A. Saxena, D. Wong, K. Diraviyam, and D. Sept, "The Basic Concepts of Molecular Modeling," in *Computer Methods Part B*, ser. Methods in Enzymology, M. L. Johnson and L. Brand, Eds. Academic Press, 2009, vol. 467, ch. 12, pp. 307–334.

[174] Y. Duan, C. Wu, S. Chowdhury, M. C. Lee, G. Xiong, W. Zhang, R. Yang, P. Cieplak, R. Luo, T. Lee *et al.*, "A point-charge force field for molecular mechanics simulations of proteins based on condensed-phase quantum mechanical calculations," *Journal of Computational Chemistry*, vol. 24, no. 16, pp. 1999–2012, 2003.

[175] H. J. Berendsen, D. van der Spoel, and R. van Drunen, "GROMACS: a message-passing parallel molecular dynamics implementation," *Computer Physics Communications*, vol. 91, no. 1-3, pp. 43–56, 1995.

[176] G. M. Morris, D. S. Goodsell, R. S. Halliday, R. Huey, W. E. Hart, R. K. Belew, and A. J. Olson, "Automated docking using a Lamarckian genetic algorithm and an empirical binding free energy function," *Journal of Computational Chemistry*, vol. 19, no. 14, pp. 1639–1662, 1998.

[177] O. Trott and A. J. Olson, "AutoDock Vina: improving the speed and accuracy of docking with a new scoring function, efficient optimization, and multithreading," *Journal of Computational Chemistry*, vol. 31, no. 2, pp. 455–461, 2010.

[178] T. Yui, K. Imada, N. Shibuya, and K. Ogawa, "Conformation of an Arabinoxylan Isolated from the Rice Endosperm Cell Wall by X-ray Diffraction and a Conformational Analysis," *Bioscience, Biotechnology, and Biochemistry*, vol. 59, no. 6, pp. 965–968, 1995.

[179] K. Mazeau, C. Moine, P. Krausz, and V. Gloaguen, "Conformational analysis of xylan chains," *Carbohydrate Research*, vol. 340, no. 18, pp. 2752–2760, 2005.

[180] M. J. Bailey, P. Biely, and K. Poutanen, "Interlaboratory testing of methods for assay of xylanase activity," *Journal of Biotechnology*, vol. 23, no. 3, pp. 257–270, 1992.

[181] S. Nurk, A. Bankevich, D. Antipov, A. Gurevich, A. Korobeynikov, A. Lapidus, A. Prjibelsky, A. Pyshkin, A. Sirotkin, Y. Sirotkin *et al.*, "Assembling genomes and mini-metagenomes from highly chimeric reads," in *Annual International Conference on Research in Computational Molecular Biology*. Springer, 2013, pp. 158–170.

[182] A. I. Rissman, B. Mau, B. S. Biehl, A. E. Darling, J. D. Glasner, and N. T. Perna, "Reordering contigs of draft genomes using the Mauve aligner," *Bioinformatics*, vol. 25, no. 16, pp. 2071–2073, 2009.

[183] K. J. Björkroth, U. Schillinger, R. Geisen, N. Weiss, B. Hoste, W. H. Holzapfel, H. J. Korkeala, and P. Vandamme, "Taxonomic study of *Weissella confusa* and description of *Weissella cibaria* sp. nov., detected in food and clinical samples."

International Journal of Systematic and Evolutionary Microbiology, vol. 52, no. 1, pp. 141–148, 2002.

[184] N. R. Coordinators, "Database resources of the national center for biotechnology information," *Nucleic Acids Research*, vol. 45, no. D1, pp. D12–D17, 2017.

[185] R. K. Aziz, D. Bartels, A. A. Best, M. DeJongh, T. Disz, R. A. Edwards, K. Formsma, S. Gerdes, E. M. Glass, M. Kubal *et al.*, "The RAST Server: rapid annotations using subsystems technology," *BMC Genomics*, vol. 9, no. 75, 2008.

[186] S. F. Altschul, W. Gish, W. Miller, E. W. Myers, and D. J. Lipman, "Basic local alignment search tool," *Journal of Molecular Biology*, vol. 215, no. 3, pp. 403–410, 1990.

[187] K. H. Schleifer and O. Kandler, "Peptidoglycan types of bacterial cell walls and their taxonomic implications." *Microbiology and Molecular Biology Reviews*, vol. 36, no. 4, pp. 407–477, 1972.

[188] R. Plapp and J. L. Strominger, "Biosynthesis of the Peptidoglycan of Bacterial Cell Walls: XVII. Biosynthesis of Peptidoglycan and of Interpeptide Briges in *Lactobacillus viridescens*," *Journal of Biological Chemistry*, vol. 245, no. 14, pp. 3667–3674, 1970.

[189] H. Abriouel, L. L. Lerma, M. d. C. Casado Muñoz, B. P. Montoro, J. Kabisch, R. Pichner, G.-S. Cho, H. Neve, V. Fusco, C. M. Franz *et al.*, "The controversial nature of the *Weissella* genus: Technological and functional aspects versus whole genome analysis-based pathogenic potential for their application in food and health," *Frontiers in Microbiology*, vol. 6, no. 1197, 2015.

[190] EFSA Panel on Dietetic Products, Nutrition and Allergies (NDA), "Scientific Opinion on the substantiation of a health claim related to "native chicory inulin" and maintenance of normal defecation by increasing stool frequency pursuant to Article 13.5 of Regulation (EC) No 1924/2006," EFSA Journal, 2015.

[191] Winclove Probiotics, "First Probiotic with EU Health Claim," Press release, 03 2017.

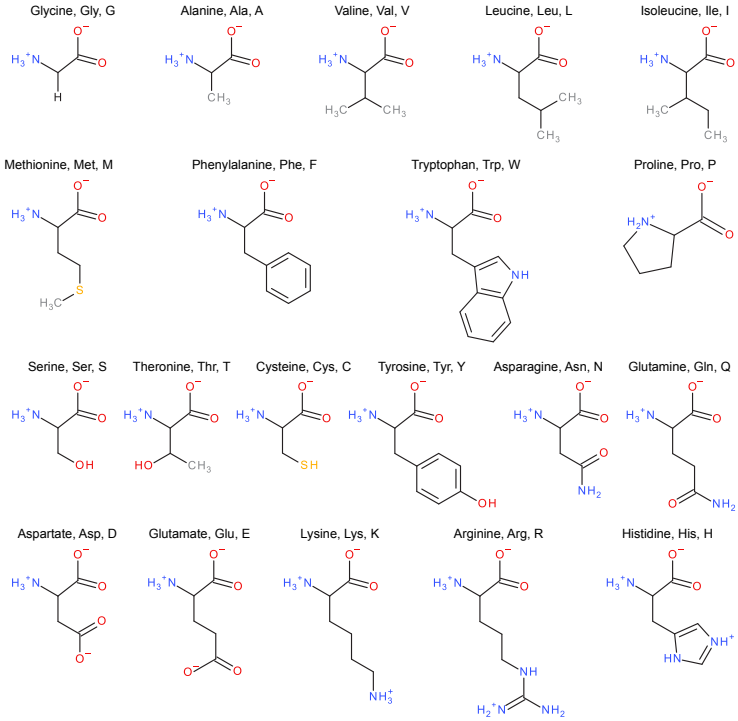

Printed by Media-Tryck, Lund 2019 NORDIC SWAN ECOLABEL 3041 0903

LUND UNIVERSITY

ISBN: 978-91-7422-690-4

ISRN: LUTKDH/TKBT-19/1176-SE
Division of Biotechnology
Faculty of Engineering, LTH
Lund University